AD-A113 381 INTERSPEC INC PHILADELPHIA PA F/G 20/14
APPLICATION OF SELF-ORGANIZING RANDOM ARRAYS TO COMMUNICATION S--ETC(U)
FEB 82 F HABER, Y BAR-NESS, B D STEINBERG F30602-80-C-0230
UNCLASSIFIED RADC-TR-81-248 NL

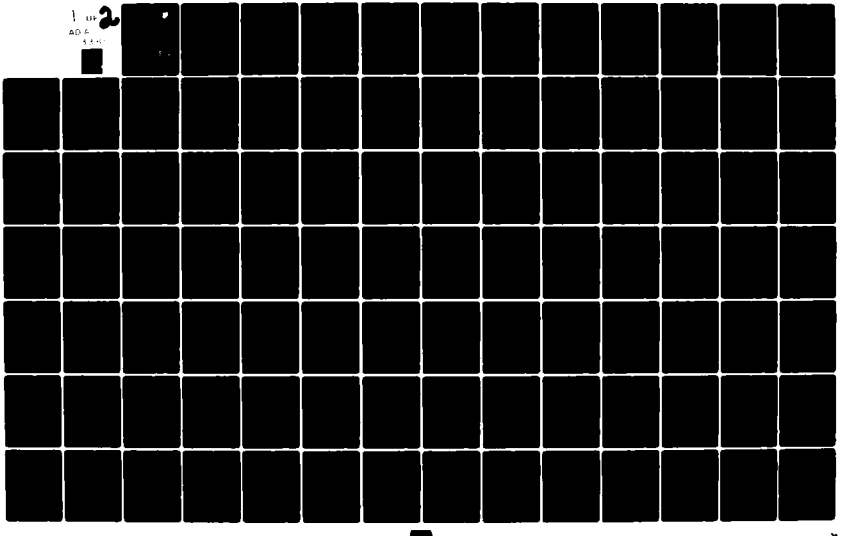

(12)

RADC-TR-81-248
Final Technical Report
February 1982

APPLICATION OF SELF-ORGANIZING RANDOM ARRAYS TO COMMUNICATION SATELLITES

Interspec, Inc.

Prof Fred Haber
Prof Yeheskel Bar-Ness
Prof Bernard D. Steinberg
Paul Chien-chang Yeh
Judy Herman

ROME AIR DEVELOPMENT CENTER
Air Force Systems Command
Griffiss Air Force Base, New York 13441

This report has been reviewed by the RADC Public Affairs Office (PA) and is releasable to the National Technical Information Service (NTIS). At NTIS it will be releasable to the general public, including foreign nations.

RADC-TR-81-248 has been reviewed and is approved for publication.

APPROVED: Walter J. Bushunow

WALTER J. BUSHUNOW
Project Engineer

APPROVED: Bruno Beek

BRUNO BEEK
Acting Technical Director
Communications and Control Division

FOR THE COMMANDER: John P. Huss

JOHN P. HUSS
Acting Chief, Plans Office

If your address has changed or if you wish to be removed from the RADC mailing list, or if the addressee is no longer employed by your organization, please notify RADC (DCCR) Griffiss AFB NY 13441. This will assist us in maintaining a current mailing list.

Do not return copies of this report unless contractual obligations or notices on a specific document requires that it be returned.

UNCLASSIFIED

SECURITY CLASSIFICATION OF THIS PAGE (When Data Entered)

REPORT DOCUMENTATION PAGE	READ INSTRUCTIONS BEFORE COMPLETING FORM
1. REPORT NUMBER: RADC-TR-81-248	2. GOVT ACCESSION NO.: AD A11 384
	3. RECIPIENT'S CATALOG NUMBER:
4. TITLE (and Subtitle): APPLICATION OF SELF-ORGANIZING RANDOM ARRAYS TO COMMUNICATION SATELLITES	5. TYPE OF REPORT & PERIOD COVERED: Final Technical Report 1 Jul 80 - 20 Feb 81
	6. PERFORMING ORG. REPORT NUMBER: N/A
7. AUTHOR(s): Prof Fred Haber, Paul Chien-chang Yeh, Prof Yeheskel Bar-Ness, Judy Herman, Prof Bernard D. Steinberg	8. CONTRACT OR GRANT NUMBER(s): F30602-80-C-0230
9. PERFORMING ORGANIZATION NAME AND ADDRESS: Interspec Inc., University City-Science Center, 3508 Market Street, Philadelphia PA 19118	10. PROGRAM ELEMENT, PROJECT, TASK AREA & WORK UNIT NUMBERS: 62702F, 45196311
11. CONTROLLING OFFICE NAME AND ADDRESS: Rome Air Development Center (DCCR), Griffiss AFB NY 13441	12. REPORT DATE: February 1982
	13. NUMBER OF PAGES: 123
14. MONITORING AGENCY NAME & ADDRESS(if different from Controlling Office): Same	15. SECURITY CLASS. (of this report): UNCLASSIFIED
	15a. DECLASSIFICATION/DOWNGRADING SCHEDULE: N/A

16. DISTRIBUTION STATEMENT (of this Report)

Approved for public release: distribution unlimited.

17. DISTRIBUTION STATEMENT (of the abstract entered in Block 20, if different from Report)

Same

18. SUPPLEMENTARY NOTES

RADC Project Engineer: Walter J. Bushunow (DCCR)

19. KEY WORDS (Continue on reverse side if necessary and identify by block number)

Random Arrays
Satellite Antennas
Spatial Filtering Algorithms
Ring Array
Interference Cancellation
Pointing Errors
Interference Cancellation Processor

20. ABSTRACT (Continue on reverse side if necessary and identify by block number)

The investigation of adaptive interference cancelling satellite-borne thinned arrays, capable of forming narrow beams in the direction of signal sources was performed. It was determined that an antenna configuration where the elements are placed in the form of a ring would be most appropriate for uniformity of the mainbeam pattern and for good beamwidth characteristics. However, satellite orientation and ground location uncertainty limit the pointing accuracy. Therefore,

DD FORM 1 JAN 73 1473 EDITION OF 1 NOV 65 IS OBSOLETE

UNCLASSIFIED

SECURITY CLASSIFICATION OF THIS PAGE (When Data Entered)

utilization of adaption algorithms which are able to work through these errors is required. It was concluded that by using this approach, the required performance can be achieved.

PREFACE

This final report was prepared by Interspec Inc., Philadelphia, PA, under Contract F30602-80-C-0230, Job Order 45196310, for Rome Air Development Center, Griffiss Air Force Base, New York. The major portion of the work was performed by Valley Forge Research Center, Moore School of Electrical Engineering, University of Pennsylvania, Philadelphia, PA, who was a subcontractor to Interspec Inc. The report describes work accomplished between 1 July 1980 through 20 February 1981.

TABLE OF CONTENTS

SECTION I

INTRODUCTION

Concern over the vulnerability to interference of the uplink of communication satellite relays has led to considering adaptive spatial filtering as a remedy. The subject of this study is the use of large, sparse, self-organizing satellite-borne arrays for this purpose. The specific application to which this research is directed is a time division multiple access (TDMA) relay for widely dispersed users. Reported here are the results of an initial 8-month study covering the interval July 1, 1980 through February 28, 1981.

The adaptive interference cancelling array may be viewed as a combination of a conventional non-adaptive beamforming array focused toward the desired signal, and a secondary array which adaptively provides cancelling signals to unwanted arrivals from other directions. It is well established that such cancelling is most effective if the interferers are sufficiently separated in angle from the desired signal to put them on the sidelobes of the non-adpative beamforming array pattern. Thus, to effectively withstand nearby interferers requires that the non-adaptive array main beam width be small - that is, that the array be of large size. Filled arrays of size require an unreasonably large number of elements so that sparse structures are indicated. With a sparse array, suppression of undesired signals will largely

depend on the adaptive nulling mechanism, since the sidelobe properties of such an array will not be adequate. The number of elements, which affects the nulling power, and the array structure, are system design issues to be faced. Large arrays suggest that array element locations will be difficult to control and that means for accepting element position variation will be required. Furthermore, there is the question whether or not the focusing quality will be regularly realizable, taking account of the propagation medium.

We further assume that for TOMA operation the array be required to rapidly beamswitch among ground sources, utilizing source location data supplied to it externally. This suggests the use of a directionally constrained array processing algorithm with capability for storing, recalling, and rapidly updating element weights. To assist in accurate pointing, we see the possibility for adapting the algorithm to utilize additional available *a priori information about the ground sources* - i.e., information on signal structure.

These considerations have led us to aim our work at the following problems.

(1) What is a preferred array configuration?

(2) Is atmospheric dispersion apt to affect beam quality adversely; is refraction significant?

(3) What can an adaptive spatial signal processing algorithm do?

(4) What means shall be used to organize the array assuming reasonable array element position tolerance?

At this stage of our work, all of these questions have been addressed with most of our results concentrated on item (3). In Section 2 we give a technical review of this work with references made to detailed technical reports given in Appendices. Section 3 gives the conclusions of our present study and recommendations for future work.

SECTION II

TECHNICAL REVIEW

a. Array structure

Appendix A on "The Ring Array," is a discussion of system ideas conceived for this application in the early stages of our work. The principal conclusion is that elements deployed with approximately equal spacing on a ring would be appropriate for its rotational uniformity of main beam pattern, and for its good beamwidth characteristics. The ring structure has the useful property of structural symmetry, allowing the elements to be fed by a common oscillator connected via equal length cables. Incidental non-uniformity in spacing would result in sidelobes typical of arrays with randomly deployed elements; that is, the sidelobes would be modeled by a complex spatial Gaussian process with mean value of the sidelobe power response relative to that of the main lobe equal to 1/N, where N is the number of elements. The number of elements will be chosen to provide (a) the requisite system gain, and (b) the necessary degrees of freedom to cope with a specified number of interferers. Practical limits on system complexity will also limit the number of elements. If we assume that individual elements are global coverage antennas with gain of 20 dB, a value of 20dB + 10log N will give the gain of the array. The average sidelobe response will not be too impressive; 10log (1/N) below the main lobe. The system will have to rely on adaptive interference nulling rather than sidelobe suppression. With N elements it is in principal possible to cope with (N-1) interferers. It should be pointed out that a large linear filled array would require an unreasonable number of elements.

If the method of self-organization described in Appendix G is used, a conventional antenna of about 1^{o} beamwidth (45dB gain) centered on the circular array structure will be suitable as a reference source. It would be advisable to provide for simultaneous mechanical steering of the reference antenna and array toward the ground beacon. This is suggested in order to minimize the range of delay differences across the array, hence to maximize the array bandwidth.

b. Medium characteristics

At this stage of our work a study on the subject of medium effects has been initiated with a literature research and a review of the most pertinent publications [1, 2, 3, 4, 5]. We are concerned with (1) refraction effects which may bend the beam as it enters the troposphere, thus complicating the steering, and (2) dispersion effects which will defocus the beam and possibly affect the array adaption process. The first of these is not viewed as a serious problem unless the refraction effect is severe. Satellite orientation, ground location uncertainty and other vagaries are apt to limit point accuracy.

We are therefore looking to adaption algorithms which will be able to work through these errors, as discussed in 2(c) below. Dispersion is potentially more serious if it is, in fact, found to occur to excess. The conventional adaption processes all are based on reception from point sources. It is known that highly correlated multiple arrivals from different directions confuse the array when it functions as a direction-finder [6]. It may pose similar problems as a receiver, and the question of how it will behave under such circumstances is proposed later for continued study.

A recent paper by Cox and Arnold [1] reports the results of propagation experiments using emissions from the COMSTAR satellite at 19 and 28 GHz. For our purposes it is important to know whether or not the phase front arriving at the array is planar over the extent of the array. The experiment reported measured instead the amplitude and phase as a function of frequency using a 7 meter dish as receiving antenna. Spatial and spectral measurements in a multipath medium are related, so that such an experiment should provide clues to the spatial integrity of the wavefront. However, making the measurements with a large dish has the effect of averaging over the wavefront; amplitudes at different frequencies would, as a result, not show great variation, though phase shift measurements should show a tendency to randomness with frequency if the phasefront is distorted. The results reported, however, that no significant phase distortion was observed over a band of 500 MHz, suggest no corresponding wavefront distortion over the extent of the antenna. Difficulties with the phase measurement, conceded by the authors, leave questions about this conclusion. Also, other papers, such as that by Harris and Hyde [2], though not explicit

about the mechanisms, lead one to believe that phenomena, other than merely rain attenuation, play roles. Because of the importance of this matter to the functioning of the adaption process, we believe it essential to carry out a definitive experiment to determine the spatial integrity of the wavefront, preferably by direct simultaneous measurement at a number of spatially distributed points.

c. The Spatial Filtering Algorithm

The preliminary candidates for the processing algorithm were (1) the Widrow-Compson scheme using an internally generated reference [8, 9], and (2) the Applebaum directionally-constrained scheme [7]. The former depends on a knowledge of some unique signal property; in this case, the signal is assumed sent using a spectrum spreading code known to the receiver. The latter depends on a knowledge of the direction of arrival of the wanted signal. In our application, the directionally-constrained array appeared to be a natural choice since knowledge of source location, perhaps to within some tolerance, is known. As a first step, we developed an analysis of a version of the Widrow-Compton scheme (using a reference-generating loop without limiter and with one element unweighted), as discussed in detail in Appendix B, and a comparison analysis of this scheme with the Applebaum directionally-constrained approach, as discussed in detail in Appendix C. Both analyses were done for a 2-element array in order to obtain the properties without undue complication. Briefly, the comparison showed that under ideal conditions (reference perfectly produced in the first and zero pointing error in the second), the first does a better job against interference close to the desired signal, and the latter

does a better job away from the desired signal. The effects of potential errors in either the reference or the pointing direction remained to be accounted for. The particular concerns are (1) uncompensated phase shift in the reference loop in the first scheme, and (2) simply not pointing accurately in the second scheme.

In connection with the effect of pointing error in the directionally-constrained array, we carried out calculations of Signal-to-Interference plus noise ratio (SINR) vs. pointing error for a variety of conditions: numbers of elements, numbers of interferers, and interference arrival directions. The sensitivity to pointing error turned out to be substantial; in the worst case, 0.1° pointing error resulted in about 3 dB loss of SINR. The detailed results are presented below in Appendix D.

This work was carried out with one realization of a linear array with arbitrarily placed elements. We digressed to carry out a simulation with various array element layouts randomly chosen to determine the effect of layout variation on the SINR with zero pointing error. These results are presented below in Appendix E.

Generally, for interference away from the main beam, the SINR (for the 7-element array simulated) varied about 3 dB, though we believe that the variation will be less for arrays with larger numbers of elements.

The conclusion that pointing error of relatively small magnitude causes significant loss of signal, suggests the need for methods which overcome the loss. In Appendix F, a brief report is presented of our first attempts in this direction. Two alternatives are

proposed. The first is a hybrid of the Applebaum and Widrow-Compton approaches. The second approach adds phase compensation to the reference loop and, more to the point, corrects the steering vector. Since the preparation of this report, additional analysis has been carried out on the hybrid (the first approach) which does in fact show that the sensitivity to pointing error is diminished. Qualitatively, we view the operation of this scheme as follows: The approximate steering vector puts the quiescent beam close to desired signal, giving a fair SINR quickly. The reference generator loop then has an adequate signal to function rapidly to raise the SINR to optimum. Though Appendix F shows two-element arrays, we see no problem in extending the scheme to multi-element arrays. In particular, one can imagine the constrained array shown in Figure 2 of [7] with the output going to the input of the reference loop (as shown in Figure 1 of Appendix F), and the output error signal of the reference loop used as the residue feedback in Figure 2 of [7].

Work on compensation of the reference loop for incidental phase shift has been carried out in connection with another study done here [10]. This work, done for a loop with limiter, is now being continued for a loop without limiter.

d. Array organization

If one is to use a directional constraint to form a quiescent beam, as discussed in 2(c) above, one requires (1) either element position information, or (2) a reference beacon on which to focus the array. Both of these approaches have long been subjects of analysis at this laboratory in connection with other studies. In this application, it may be advisable

to incorporate both schemes as protection against failure of either one. Self-contained systems based on distance-measuring infrared lasers appear to be feasible. We have not pursued the details of such a scheme during this phase of our study. We have, however, given consideration to the technique of focusing the array on a beacon and steering the beam so formed toward the desired source. The problem we see is that the initial beamforming, if done by conventional methods [11] in the face of strong interference, will be imperfect. This suggests that the initial beamforming should itself be done using an interference-cancelling algorithm. An approach of this kind with its theoretical basis is given in Appendix G below. It is based on a reference signal obtained from the beacon (which is assumed located far from interfering sources), through a separate conventional antenna, focusing the array using the Widrow algorithm. The element weights developed contain the steering information and this is isolated by appropriate processing. Once this is known, the beam may be further steered toward the desired source. The concept remains to be analyzed for its sensitivity to measurement errors and for the complexity which it will add.

We point out that the use of a separate reference link to the beacon may also be useful for the purpose of transmitting spread spectrum codes, timing signals, control information, etc., to the satellite.

3. CONCLUSIONS AND RECOMMENDATIONS

During this initial study, we have examined the large, sparse, self-organizing array for its potential as a spatial filter to be used on a

communication satellite uplink. We have focused on several problem areas - array structure, effect of propagation medium, processing algorithms, and array self-organization. As a consequence of this work, we conclude that

(a) a system with a ring structure of small earth coverage elements centered on reference antenna of conventional form,

(b) a Widrow interference-resistant processor for beamforming on a beacon, and

(c) a hybrid interference-cancelling processor (see 2(c)) tolerant to pointing error for focusing on the desired source,

can be expected to serve the intended purpose.

Our work has proceeded to a point of reasonable confidence in the approach, though certain problems, as enumerated below, require attention. Accordingly, we recommend the following steps be carried out in a continuing study.

(a) Obtain definitive information on the behavior of the propagation medium, preferably by direct experiment using spatially-distributed sensors receiving from a spaceborne point source, and translate the result into effect on the adaption process.

(b) Continue to pursue the hybrid and the self-correcting interference-cancelling processors described here, to establish their SINR properties and their convergence characteristics. Develop results for multi-element, multi-interference cases.

(c) Analyze the method described here of beamforming on a beacon in the presence of interference, assessing its complexity and determining the accuracy with which it generates the steering vector.

(d) Continue to study the effects of a non-ideal reference-generating loop, and seek means for overcoming these effects.

(e) Study the stability problems of the various feedback loops used.

(f) Investigate the problems arising from the multiple access feature of the system. Consider the alternatives of beam switching among users and the use of continuous multiple directional constraints which allows simultaneous beams to be formed on several users.

(g) Examine the alternative spread spectrum techniques - frequency hopping and PN code modulation for their respective advantages in the systems proposed.

REFERENCES

[1] Donald C. Cox and H. W. Arnold, "Phase and Amplitude Dispersion for Earth-Satellite Propagation in the 20- to 30- GHz Frequency Range," IEEE Trans. on Antennas and Propagation, Vol. AP-28, No. 3, May 1980, pp. 359-366.

[2] J. M. Harris and G. Hyde, "Preliminary Results of COMSTAR 19/29 GHz Beacon Measurements at Clarksburg, Maryland," COMSAT Technical Review, Vol. 7, No. 2, Fall 1977, pp. 599-623.

[3] D. C. Cox, "An Overview of the Bell Laboratories 19- and 28- GHz COMSTAR Beacon Propagation Experiments," BSTJ Vol. 57, No. 5, May-June 1978, pp. 1231-1255.

[4] Martin P. M. Hall, Effects of the Troposphere on Radio Communication, Peregrinus, England, 1979.

[5] R. K. Crane, "Propagation Phenomena Affecting Satellite Communication Systems Operating in the Centimeter and Millimeter Wavelength Bands," Proc. IEEE, Vol. 59, February 1971, pp. 173-188.

[6] W. F. Gabriel, "Spectral Analysis and Adaptive Array Superresolution Techniques," Proc. IEEE, Vol. 68, June 1980, pp. 654-666.

[7] S. P. Applebaum and D. J. Chapman, "Adaptive Arrays with Main Beam Constraints," IEEE Trans. on Antennas and Propagation, Vol. AP-24, September 1976, pp. 650-662.

[8] B. Widrow, J. McCool and J. Ball, "The Complex LMS Algorithm," Proc. IEEE, Vol. 63, April 1975, pp. 719-720.

[9] R. T. Compton, Jr., "An Adaptive Array in Spread-Spectrum Communication," Proc. IEEE, Vol. 66, March 1978, pp. 289-298.

[10] Y. Bar-Ness, "On the Problem of the Reference Loop Phase Shift in an N-Element Adaptive Array," VFRC-11-80, July 1980.

[11] B. D. Steinberg, Principles of Aperture and Array System Design, John Wiley & Sons, Inc., 1976, Chapter 11.

APPENDIX A

THE RING ARRAY

Bernard D. Steinberg

Interspec Inc.
University City Science Center
3508 Market Street
Philadelphia, Pennsylvania

THE RING ARRAY

Let the largest dimension of the two-dimensional aperture be called L, let the wave-length be λ, and let the following three assumptions be made: First, the shape of the radiation pattern must be independent of steering direction throughout the field of view that encompasses the earth. Second, jamming protection from as close to the beam axis as possible must be obtained. Third, the array is to be sufficiently large so that rigidity in its structure may not be assumed.

A concomitant of the first assumption is a requirement for rotational symmetry of the array. The second assumption places two requirements upon array design, one with respect to the cross-section of the main lobe and one with respect to the side radiation pattern--since these two requirements are uniquely associated with the second assumption. The first requirement is that the main lobe have as small a beamwidth as possible while the second requirement is that all side lobes be adequately low to reject jamming or that interference cancellation techniques be used against the jammers, or both.

A circular array with a central reference element is an attractive candidate. This array satisfies the circular symmetry requirement while also providing the smallest beam cross section consistent with a symmetrical design. While the side-lobe pattern of a circular array normally is not particularly attractive relative to what is obtainable from a carefully designed, tapered aperture, the third assumption (of nonrigidity) precludes such control of sidelobes irrespective of aperture design. Thus, the side radiation properties *may* degenerate into those of the random array regardless of the designers' wishes. Since the random array sidelobe properties are inadequate for this purpose (average sidelobe power level is 1/N relative to main lobe), interference cancellation techniques must be applied. In addition, because of the nonrigidity assumption, some form of self-cohering using one or more pilot signals from earth is proposed. The central element in the array will be the reference element both for adaptive beamforming and for interference cancellation.

The beamwidth of a continuous ring aperture is approximately $0.71\lambda/L$. By way of comparison the beamwidth of a uniformly excited rectangular aperture of length L is $0.88\lambda/L$. The beamwidth of a triangularly weighted aperture of the same length is $1.27\lambda/L$.

The ring array appears to have an additional virtue with respect to the interference cancellation function of the system. Interference cancellation is a nulling process whereby a null is formed in the radiation pattern in the direction of each jammer. The width of the null, or the local extent of the effect upon the radiation pattern of the null, is determined by the separation of the antenna elements from which the signals are derived that form the null. By placing all elements on the circumference of a circle the maximum number of pairs of elements having the maximum separation is obtained.

Since the array is assumed to be nonrigid the statistics of the side radiation pattern will be independent of the exact locations of the elements, provided that the element density is approximately uniform around the ring. Nevertheless, the designer has the choice of equal angular spacing between elements or some statistical distribution about equal angular spacing. The former appears more desirable from the point of view of practicality: given a random distribution of locations the signal processor must compute phase shifts for beam steering for each of the elements. On the other hand, with equal angular spacing between elements a much smaller set of calculations is required, making use of angular symmetry within the array. The value of angular symmetry is weakened, however, by the nonrigid frame of the array; nevertheless, the array at worst will be only somewhat distorted, relative positions of adjacent elements being at most slightly perturbed, and therefore the underlying angular symmetry may still be useful.

Two generally different approaches may be considered for the use of the element signals for interference cancellation. The first is a fully adaptive mode in which the array output (or an error signal derived from it) is correlated with each of the element signals, and the correlation products applied as gain controls to the element weights. This fully automatic technique has the advantage of distributing the available nulls of the array in their optimum locations so as to minimize the overall interference field. In one simple scheme successfully used in radar, called coherent sidelobe suppression, the signal from a single element is (complex) gain-controlled and added to the array output to remove the interference from a single jammer. However, the

technique has certain limitations when the desired signals and the interference signals occupy a wide dynamic range and when the interferers are amplitude modulated. This suggests that an alternative approach involving human interaction from the ground via a data link may be appropriate. Both approaches bear examination. Thus, it is possible that resilient automatic techniques can be designed for element selection, based upon array, earth station, and earth jammer geometry, as well as on automatic complex gain control. It is also possible that operator interaction in the selection of the element for the jammer suppression and/or the adjustment of the complex weight might be more satisfactory under conditions of severe jamming. A fully automatic system with an operator override capability is likely to be the most desirable.

The nonrigidity of the array requires that it be self-adaptively organized. One likely means is to self-cohere it retrodirectively upon the signal source on the ground. The same techniques can be applied with a separate set of phase shifters to a jamming source. The output of the second beam is that of the high gain array pointed at the jammer. If this signal is now added through a complex weight to the main array output, the result multiplied with the jammer signal beam output and sent back via LMS control to the complex weight, the system output becomes deprived of the jamming signal. In effect the system radiation pattern is that of the adaptively formed beam upon the signal source plus the complex weighted adaptively formed beam upon the jammer, where the complex weight causes the sum to be zero in the direction of the jammer. This technique uses all the resources of the array both for main beam formation for the signal as well as for jammer suppression.

In summary, one contemplated array design is a ring of diameter L of N uniformly spaced elements, plus a central reference element used for adaptive beamforming and nulling. The beamwidth is approximately $\lambda/0.7L$. A pilot signal from the ground station will phase synchronize the array so as to form a retrodirective beam on the source. Automatic or semi-automatic interference cancellation circuits will suppress jammers.

APPENDIX B

PERFORMANCE ANALYSIS OF INTERFERENCE CANCELER WITH REFERENCE SIGNAL LOOP

Yeheskel Bar-Ness*

Valley Forge Research Center
The Moore School of Electrical Engineering
University of Pennsylvania
Philadelphia, Pennsylvania

*On leave of absence from the School of Engineering, Tel Aviv University.

INTRODUCTION

The adaptive array processing has become a way of life in the design of advanced communication systems, particularly for automatic beam steering and interference cancellation. The Widrow LMS [1] algorithm is widely used. To obtain the "reference signal" required for the realization of this algorithm, Compton [2] suggested processing the array output using what is called a reference signal loop (Figure 1). This processing is intended to extract a good version of the desired signal while altering or suppressing the interference. For this to be possible the desired signal and the interference must differ in some way. For example, if the signal is of the spread spectrum type, then multiplying the array output by the right code will spread the interference bandwidth, collapse the desired signal spectrum, and reveal the condition of narrowband signal and broadband interference. This is obviously the case if the local code generator is in synchronization with the code of the incoming desired signal.

However, code acquisition can not be obtained when the interference-to-desired signal ratio is large. In this case the reference signal loop is ineffective (produces zero output) and the array might shut itself off by

[1] B. Widrow, J. McCool and J. Ball, "The Complex LMS Algorithm," Proc. IEEE, Vol. 63, April 1975, pp. 719-720.

[2] R.T. Compton, Jr., "An Adaptive Array in Spread-Spectrum Communication," Proc. IEEE, Vol. 66, March 1978, p. 289.

turning the weights down to zero. Therefore, for such a condition of interference-to-desired signal ratio, it might be preferable to use one of the power inversion schemes of interference cancelling such as, for example, the Widrow-based power-inversion scheme (one array element unweighted). As a result (even though the reference loop is initially ineffective) the interference will be suppressed below the desired signal level (power inversion), enabling code synchronization and finally the effective reference signal loop operation. Making the array control loop slower than the code acquisition time will assure that the array will not suppress the desired signal when its power at the input is larger than the interference.

Based on this argument it is plausible to assume that the array arrangement of a Widrow-based power inversion scheme with reference signal loop will better handle the ease of spread spectrum desired signal than would the regular LMS arrangement, particularly when both the interference and the signal have large dynamic range. It might be important to emphasize that this array arrangement does not require the limiter which is very crucial in Compton's arrangement of Figure 1.

The purpose of this work is to analyze this new interference canceler arrangement and consider its performance with different system conditions; namely, when the system is in the code acquisition or the tracking mode. This will be done by using the different bandwidth relations of the desired signal and interference in comparision to the reference loop filter bandwidth obtained when the local spread spectrum code is or is not in synchronism with the incoming code.. Obviously, when the system is in the acquisition mode (the local code is not in synchronism), both desired and interference signals will be spread in bandwidth and will be rejected by the comparably

smaller reference signal loop filter bandwidth, making this loop ineffective. The desired signal, however, will benefit from the resulting power inversion scheme, pushing the system toward synchronism. On the other hand, when the system is in the tracking mode, the desired signal bandwidth becomes smaller--and the interference signal bandwidth larger--than the reference signal loop filter bandwidth, so that a moderately clean replica of the desired signal will be extracted. In this mode the array arrangement operates as a regular LMS array. Rather than assuming only an ideal filter in the reference signal loop, in our analysis we will utilize the filter responses to the desired and interference signals. Depending on the relative bandwidth conditions, we will apply reasonable practical approximations to these responses and obtain the effect of filter design on the array performance.

SYSTEM REPRESENTATION AND ANALYSIS

The array arrangement is depicted in Figure 2. Here, for the sake of simplicity, we use a two element array (one unweighted). Generalization to a multielement case seems easy. The signals at the two elements are summed after being weighted by a complex gain, W. The reference-signal loop composed of a multiplier (spread-spectrum decoder), a narrowband bandpass filter and a second multiplier (encoder). The purpose of the first multiplier is to decode the spread-spectrum signal at the output of the array, resulting in a narrowband desired signal (bandwidth of the data), and a bandwidth spread interference. In this case the loop filter will sufficiently suppress the interference, leaving an output which is a sufficiently clean replica of the desired signal. Since the reference must carry the same code as the desired input signal, a second multiplier recoding the information signal

is needed. Notice that as a result of having one element unweighted there is no need, in this array processor, for a limiter in the reference signal loop as was needed in Compton's processor.

To simplify the analysis we will consider two modes of processor operation. In the first we assume that throughout the reference loop the interference signal bandwidth is very wide compared to the desired signal bandwidth (data bandwidth). This corresponds to the case when the local spread spectrum code is in synchronism with the incoming code. Obviously, we will choose the filter of the reference signal loop to be wider than the desired signal bandwidth, but narrower than the interference signal bandwidth. In the second mode we will assume that the bandwidths of both the desired and the interference signals are much wider than that of the reference loop filter bandwidth. This corresponds to the case when the local spread-spectrum code is not in synchronism and the code synchronization system is in the acquisition mode.

Let the complex envelope of the input signals at the main (unweighted) elements of the array be designated by $X_0(t)$ and $S_1(t)$ respectively. Also let

$$X_i(t) = I_i(t)+S_i(t)+N_i(t), \qquad 2 = 1,2, \tag{1}$$

where the interference signal I and the desired signal S are uncorrelated plane waveform signals (If they are CW signals then we assume that their frequency difference is larger than the array weight control loop bandwidth). The noises processes are white and independent. That is,

$$I_i(t) = |I_i(t)|e^{j\theta_{I_i}}$$

$$S_i(t) = |S_i(t)|e^{j\theta_{S_i}}$$

$$\overline{|N_i(t)|^2} = \sigma_N^2 \tag{2}$$

where $\Theta_{S_1} - \Theta_{S_0} \triangleq \Theta_{S_{10}} \simeq \frac{w_s d}{c} \sin\psi_s$, d is the distance between the array elements, w_s is the radian frequency of the desired signal, c is the speed of electromagnetic waves, and ψ_s is the direction of arrival of this signal with respect to the array broadside direction. Similar definitions apply for Θ_{I_i}. Obviously, depending on the signal's information contents, Θ_{I_i} and Θ_{S_i} are functions of time. Only when they are CW signals they turn out to be constants.

In complex notation the output of the array

$$V(t) = X_1(t)W_1(t) + X_0(t) \tag{3}$$

The output of the reference loop is termed $X_r(t)$ and the error signal becomes

$$e(t) = V(t) - X_r(t)$$

$$= X_1(t)W_1(t) + X_0(t) - X_r(t)$$

For the LMS processing $\overline{|e(t)|^2}$ is minimized by changing the complex weight $W_1(t)$. Using the steepest descent algorithm this leads to the Widrow-Hopf algorithm for controlling $W_1(t)$. That is,

$$dW_1(t)/dt = KX_1^*(t)[X_1(t)W_1(t)+X_0(t)-X_r(t)] \tag{4}$$

where K is the system gain and * stands for complex conjugate. In a practical system we may realize this by using a low pass filter instead of the ideal integration required by (4). That is, the weight is determined from

$$IdW_1(t)/dt+[1+K|X_1(t)|^2]W_1(t) = -KX_1^*(t)[X_0(t)-X_r(t)] \tag{5}$$

In the steady state (5) gives

$$W_1(t) = \overline{-KX_1^*(t)[X_0(t)-X_r(t)]}/[1+K\overline{|X_1(t)|^2}] \tag{6}$$

where the bar stands for the time average of the corresponding terms. That is, for example, using (1) and (2) we get

$$|X_1(t)|^2 = |I_1|^2 + |S_1|^2 + \sigma_N^2 \tag{7}$$

$$X_1^*(t)(X_0(t)-X_r(t)) = I_0I_1^* - I_rI_1^* + S_0S_1^* - S_rS_1^* \tag{8}$$

where we define $X_r(t) = I_r(t)+S_r(t)+N_r(t)$, the subscript r signifying the reference loop output, and where we used the uncorrelation property between pairs of interference signal, desired signal, and noise. We also assumed that the noise at the output of the reference loop $N_r(t)$ is uncorrelated with $N_1(t)$. Notice that in (7) and (8) in our notation we drop the dependence on t. We will also do so in the sequel whenever it is clear. However, even though I_i and S_i are time dependent due to their zero bandwidth, the terms $I_0I_1^*$ and $S_0S_1^*$ are time independent. They are complex numbers whose phases are constant depending on the direction of arrival of these signals. This is true if the distance between elements is small enough for the given rate of information these signals bear. Similarly, we will also assume that the reference signal loop group delay is sufficiently small so that $I_rI_1^*$ and $S_rS_1^*$ are constant complex numbers.

Using (7) and (8) in (6) we have for the steady state weight

$$W_1(t) = \frac{K(I_0I_1^* - I_rI_1^* + S_0S_1^* - S_rS_1^*}{1+K(|I_1|^2+|S_1|^2+\sigma_N^2)} \tag{9}$$

Substituting in (3) and using (1) we obtain the following for the output of the array (as derived in the appendix B-1, (P-3));

$$V(t) = \frac{I_0(1+g|S_1|^2)-gI_1(S_0S_1^*)+g(I_r|I_1|^2+I_1S_rS_1^*)}{1+g(|I_1|^2+|S_1|^2)}$$

$$+ \frac{S_0(1+g|I_1|^2)-gS_1(I_0I_1^*)+g(S_r|S_1|^2+S_1I_rI_1^*)}{1+g(|I_1|^2+|S_1|^2}$$

$$+ N_0 - \frac{gN_1(I_0I_1^* - I_rI_1^* + S_0S_1^* - S_rS_1^*}{1+g(|I_1|^2+|S_1|^2)} \qquad (10)$$

where we defined

$$(1+K\sigma_N^2)/K = 1/g \triangleq P_{th} \qquad (11)$$

P_{th} stands for the system threshold power. The first term of (11) represents the contribution of the interference signal I at the output, while the second is that of the desired signal S and the last terms represent the contribution of the white noise at the input to the output of the array.

The Reference Signal Loop Output

The output of the reference signal loop can be obtained by convoluting V(t) with the impulse response of the loop filter. Therefore, the contibution of the desired signal at this output can be written as

$$S_r = F_s \frac{S_0(1+g|I_1|^2)-gS_1(I_0I_1^*)+gS_r(|S_1|^2)+gS_1(I_rI_1^*)}{1+g(|I_1|^2+|S_1|^2)} \qquad (12)$$

where F_s is a linear operator representing the effect of the reference loop filter on the desired signal spectral content. When, for example, the local code is in synchronism with the incoming desired signal code, so that the desired signal has a very narrow band, then F_s can be approximately

represented as a constant complex number

$$F_s = \gamma e^{j\theta_{sr}} \tag{13}$$

where γ and θ_{sr} are the gain and phase shift of the loop filter at the desired signal center frequency. Combining terms we can write (12) as

$$[1+g(|I_1|^2+|S_1|^2(1-F_s))]S_r = F_s[S_0(1+g|I_1|^2)-gS_1(I_0I_1^*)+gS_1(I_rI_1^*)] \tag{14}$$

Similarly, for the interference signal we get

$$[1+g(|S_1|^2+|I_1|^2(1-F_I))]I_r = F_I[I_0(1+g\,S_1{}^2)-gI_1(S_0S_1^*)+gI_1(S_rS_1^*)] \tag{15}$$

Equations (14) and (15) can be written in matrix notation as

$$\begin{bmatrix} 1+g(|I_1|^2+|S_1|^2(1-F_s)) & -gF_sS_1I_1^* \\ -gF_II_LS_1^* & 1+g(|S_1|^2+|I_1|^2(1-F_I)) \end{bmatrix} \begin{bmatrix} S_r \\ I_r \end{bmatrix}$$

$$= \begin{bmatrix} F_s[S_0(1+g|I_1|^2)-gS_1(I_0I_1^*)] \\ F_I[I_0(1+g|S_1|^2)-gI_1(S_0S_1^*)] \end{bmatrix} \tag{16}$$

Therefore, the output of the reference loop is given by

$$\begin{bmatrix} S_r \\ I_r \end{bmatrix} = \underset{\sim}{A}^{-1}\,\underset{\sim}{B} \begin{bmatrix} S_{NOR} \\ I_{NOR} \end{bmatrix} \tag{17}$$

where,

$$\underset{\sim}{A}^{-1} = \frac{1}{\Delta} \begin{bmatrix} 1+g(|S_1|^2+|I_1|^2(1-F_I)) & gF_sS_1I_1^* \\ gF_II_1S_1^* & 1+g(|I_1|^2+|S_1|^2(1-F_s)) \end{bmatrix} \tag{18}$$

$$I_{NOR} = I_0(1+g|S_1|^2) - gI_1(S_0S_1^*), \tag{19}$$

$$S_{NOR} = S_0(1+g|I_1|^2) - gS_1(I_0I_1^*), \tag{20}$$

$$\underset{\sim}{B} = \begin{matrix} F_s & 0 \\ 0 & F_I \end{matrix}, \tag{21}$$

and from (P-6)

$$\Delta = [1+g(|I_1|^2+|S_1|^2)]\ [1+g(|S_1|^2(1-F_s)+|I_1|^2(1-F_I)] \tag{22}$$

Notice that when $\underset{\sim}{B} = \underset{\sim}{0}$ the reference signal loop output becomes zero. That is to say, the loop filter is such that no output is produced. This is obviously the case when the filter bandwidth is small in comparison to both the desired signal and interference signal bandwidths.

The Steady State Complex Weight

Using (9) and (11) the steady complex weight can be written as

$$W_1(t) = \frac{-g(I_0I_1^* - I_rI_1 + S_0S_1^* - S_rS_1^*)}{1+g(|I_1|^2+|S_1|^2)}$$

$$= \frac{-g}{1+g(|I_1|^2+|S_1|^2)}\left(I_0I_1^* + S_0S_1^* - [S_1^* \mid I_1^*]\left[\begin{matrix} S_r \\ \hline I_r \end{matrix}\right]\right)$$

By substituting (17) we get

$$W_1(t) = \frac{-g(I_0I_1^* + S_0S_1^* - [S_1^* \mid I_1^*]\underset{\sim}{A}^{-1}\underset{\sim}{B}}{1+g(|I_1|^2+|S_1|^2)} \left[\begin{matrix} S_{NOR} \\ I_{NOR} \end{matrix}\right]) \tag{23}$$

and together with (P-7), (App. B2), (23) becomes

$$W_1(t) = -g\left(\frac{I_0 I_1^* + S_0 S_1^*}{1+g(|I_1|^2+|S_1|^2)} - \frac{1}{\Delta}\,[S_1^*\ \ I_1^*]\ B \begin{matrix} S_{NOR} \\ I_{NOR} \end{matrix}\right) \quad (24)$$

where S_{NOR} and I_{NOR} are defined in (19) and (20) respectively. When the reference loop is ineffective ($B = 0$) then

$$W_{1NOR}(t) = \frac{-g\,(I_0 I_1^* + S_0 S_1^*)}{1+g(|I_1|^2+|S_1|^2} \quad (25)$$

which is proportional to the input's cross correlation. However, for the general case, the steady state of the complex weight becomes (see the derivation of P-8 in Appendix B-4).

$$W_1(t) = \frac{-g[I_0 I_1^* (1-F_I)+S_0 S_1^* (1-F_s)]}{1+g[|S_1|^2(1-F_s)+|I_1|^2(1-F_I)]} \quad (26)$$

where we notice the effect of the reference loop filter responses (F_I and F_s) to the interference and desired signal respectively. Particularly, we notice the case when this filter has perfect response to the desired signal ($F_s = 1$); then the weight depends on the cross correlation and power of the interference signal only and hence the array processor will produce a better null in the direction of this signal.

Desired and Interference Signals at the Array Output

To obtain the signal terms at the output of the array we can use (10), in which we substitute the expression for I_r and S_r as they were obtained in (17). However, we can directly use (3) to get

$$V_s(t) = S_0 + S_1 W_1(t) \quad (27)$$

$$V_I(t) = I_0 + S_1 W_1(t), \quad (28)$$

for the desired signal and the interference signal, respectively, at the output of the array. $W_1(t)$ is given by (25). In appendix B-5 we derived the final expression for these signals.

$$V_s(t) = \frac{S_0+g(1-F_I)[S_0|I_1|^2-S_1(I_0I_1^*)]}{1+g(|S_1|^2(1-F_s)+|I_1|^2(1-F_I))} \tag{29}$$

$$V_I(t) = \frac{I_0+g(1-F_s)[I_0|S_1|^2-I_1(S_0S_1^*)]}{1+g(|S_1|^2(1-F_s)+|I_1|^2(1-F_I))} \tag{30}$$

In fact, (29) and (30) represent the complex envelopes of the desired signal and the interference signal, respectively, at the output of the array as a function of the complex envelopes of these signals at the inputs to the two elements as well as the reference loop filter's responses to these signals, F_s and F_I, respectively. In particular, we notice that when these responses are small ($F_s \simeq 0$, $F_I \simeq 0$), the corresponding array output signals are

$$V_{SNOR}(t) = \frac{S_{NOR}}{1+g(|S_1|^2+|I_1|^2} \tag{31}$$

$$V_{INOR}(t) = \frac{I_{NOR}}{1+g(|S_1|^2+|I_1|^2} \tag{32}$$

We will further assume, without loss of generality, that the two array elements are sufficiently close so that $|I_1| = |I_0| = I$ and $|S_1| = |S_0| = S$. Together with the definition made in (2) we can write (29) and (30) as

$$V_s(t) = \frac{S[1+g(1-F_I)|I|^2(1-e^{j(\theta_{s10}-\theta_{I10})})]}{1+g(|S|^2(1-F_s)+|I|^2(1-F_I))} \tag{33}$$

$$V_I(t) = \frac{I[1+g(1-F_s)|S|^2(1-e^{j(\theta_{I10}-\theta_{S10})})]}{1+g(|S|^2(1-F_s)+|I|^2(1-F_I))} \tag{34}$$

where $\theta_{s10} = \theta_{s1} - \theta_{s0}$, and $\theta_{I10} = \theta_{I_1} - \theta_{I_0}$. Using the assumption of nearly stationary of the desired and interference signal (as is the case when the distance between the elements is small), $\theta_{s_{10}}$ and $\theta_{I_{10}}$ are constant phases which depend on the direction of arrival of these signals.

The Noise Term at the Array Output

Using (26) we can write

$$V_N(t) = N_0 - N_1 \frac{g[I_0 I_1^* (1-F_I)+S_0 S_1^* (1-F_s)]}{1+g(|S_1|^2(1-F_s)+|I_1|^2(1-F_I))} \tag{35}$$

where N_0 and N_1 are two independent processes.

DESIRED SIGNAL-TO-INTERFERENCE RATIO AT ARRAY OUTPUT

Since the different terms at the array output, (namely, $V_s(t)$, $V_I(t)$ and $V_N(t)$) are uncorrelated, the power output is composed of the sum of the powers included in these terms. To find the power ratios of these different terms we will distinguish between different processor modes of operation by using the different ratios of the bandwidths of desired signal and interference signal (at the input of reference loop filter) to the bandwidth of this filter, respectively. Ideally, the reference loop

filter bandwidth should be much greater than the desired information bandwidth and much smaller than the spread signal bandwidth.

Acquisition Mode

Due to the fact that the local spread spectrum code is not in synchronism with the incoming desired signal code, the bandwidth of both the desired signal and the interference signal are larger than the loop filter bandwidth. Therefore, we can reasonably assume that both F_I and F_s are approximately zero. Using this in (33) and (34) we get

$$\frac{|S|^2_{out}}{|I|^2_{out}} = \frac{|S|^2\left|1+g|I|^2(1-e^{j(\theta_{s_{10}}-\theta_{s_{10}})}\right|^2}{|I|^2\left|1+g|S|^2(1-e^{j(\theta_{I_{10}}-\theta_{s_{10}})}\right|^2} \tag{36}$$

Computing the absolute value in (36) we have

$$\frac{|S|^2_{out}}{|I|^2_{out}} = \frac{|S|^2}{|I|^2}\,\frac{1+2g|I|^2(1+g|I|^2)[1-\cos(\theta_{s_{10}}-\theta_{I_{10}})]}{1+2g|S|^2(1+g|S|^2)[1-\cos(\theta_{I_{10}}-\theta_{s_{10}})]} \tag{37}$$

Notice that if the directions of the two signals are close ($\cos(\theta_{s_{10}}-\theta_{I_{10}}) \approx 1$), of if the desired signal and the interference signal powers (namely, $|S|^2$ and $|I|^2$, respectively) are small compared to the threshold power Pth (Pth = 1/g), then

$$\frac{|S|^2_{out}}{|I|^2_{out}} = \frac{|S|^2}{|I|^2} \tag{38}$$

and the array has no effect on the output signal-to-interference ratio. On the other hand, if the relative directions and the powers of the two signals are such that the second terms of both numerator and denominator of (37) are much

larger than one, then

$$\frac{|S|^2_{out}}{|I|^2_{out}} = \frac{|S|^2}{|I|^2} \cdot \frac{|I|^2(1+g|I|^2)}{|S|^2(1+g|S|^2)}$$

$$\cong \frac{|I|^2}{|S|^2} \qquad (39)$$

This is, in fact, the power inversion formula.

Thus, the array will gradually reduce the power of the larger signal which is necessarily being the interference signal* leading to acquisition of the desired signal code and synchronization. To conclude, we depict in Figure 3 the output signal-to-interference ratio as a function of the signal-to-threshold power ratio as well as of the signal's relative direction $\theta = \theta_{I_{10}} - \theta_{S_{10}}$. This is done by considering the different signals-to-threshold possibilities from (37).

2. Code Tracking Mode

Due to synchronization, the bandwidth of the desired signal at the input of the reference loop filter is small (and equal to the information bandwidth) and can, therefore, be assumed to be much smaller than the filter bandwidth. Thus, F_s can be approximated by a complex number, $F_s = \gamma e^{j\theta_{s_r}}$ (see (13)). However, the interference signal bandwidth at the input of the filter is assumed to be much larger than the filter's bandwidth as a consequence of the spreading caused by the local code. Thus, $F_I = 0$. Hence, from (33) and (34) we have

* This is so since, if the desired signal were the larger, then the system would have been in synchronization and not in acquisition mode, as it is assumed.

$$\frac{|S|^2_{out}}{|I|^2_{out}} = \frac{|S|^2}{|I|^2} \frac{\left|1+g|I|^2(1-e^{j(\theta_{s_{10}}-\theta_{I_{10}})})\right|^2}{\left|1+g(1-\gamma e^{j\theta_{s_r}})|S|^2(1-e^{j(\theta_{I_{10}}-\theta_{s_{10}})})\right|^2}$$

Using (p-11) of the appendix, this becomes

$$\frac{|S|^2_{out}}{|I|^2_{out}} = \frac{|S|^2}{|I|^2} \frac{[1+2g|I|^2(1+g|I|^2)(1-\cos(\theta_{s_{10}}-\theta_{I_{10}}))]}{1+2g|S|^2f_1+2g^2|S|^4f_2} \tag{40}$$

where

$$f_1 = 1-\gamma\cos\theta_{s_r}-\cos(\theta_{I_{10}}-\theta_{s_{10}}) + \gamma\cos(\theta_{s_r}+\theta_{I_{10}}-\theta_{s_{10}}) \tag{41}$$

$$f_2 = (1+\gamma^2-2\gamma\cos\theta_{s_r})(1-\cos(\theta_{I_{10}}-\theta_{s_{10}})) \tag{42}$$

First we will consider the case of an ideal loop filter; that is, when $\gamma = 1$ and $\theta_{s_r} = 0$. With this, $f_1 = f_2 = 0$ and (40) becomes

$$\frac{|S|^2_{out}}{|I|^2_{out}} = \frac{|S|^2}{|I|^2} [1+2g|I|^2(1+g|I|^2)(1-\cos(\theta_{s_{10}}-\theta_{I_{10}}))] \tag{43}$$

Again, if the angular separation of the two signals is small, or if the interference signal power is small in comparison to the threshold power, then $|S|^2_{out}/|I|^2_{out} = |S|^2/|I|^2$ and the array has no effect on the output signal-to-interference ratio. Notice that this result is true regardless of the desired signal power. If, on the other hand, the angular separation between signals and the interference signal power are such that the second term of (43) is much larger than one, then

$$\frac{|S|^2_{out}}{|I|^2_{out}} = \frac{|S|^2}{|I|^2} 2g^2|I|^4(1-\cos(\theta_{s_{10}}-\theta_{I_{10}})) \tag{44}$$

For this to hold we must have

$$|I|^2 >> 1/2g = Pth/2$$

This is so because if $2g|I|^2 << 1$, then $2g|I|^2(1+g|I|^2) << 1$ in contradiction to our assumption. Notice that the improvement in the desired signal-to-interference ratio depends on the square of the interference-to-threshold power ratio $((g|I|^2)^2 = (|I|^2/Pth)^2)$as well as on the angular separation between the desired signal and interference. In contrast to the case without reference signal (without a loop for extracting the desired signal or when this loop is ineffective as in the acquisition mode discussed previously), this result is independent of the desired signal power. Figure 4 depicts the output signal-to-interference ratio, for the ideal filter case, as a function of the signal-to-threshold, the interference-to-threshold and θ as it is described in (43).

To demonstrate the effect of a nonideal filter in the reference signal loop we reconsider (40). We will assume that $\theta_{s_r} << \theta_{I_{10}} - \theta_{s_{10}}$ so that

$$f_1 = (1-\gamma\cos\theta_{s_r})\ (1-\cos(\theta_{I_{10}} - \theta_{s_{10}})) \tag{46}$$

With this (49) becomes

$$\frac{|S|^2_{out}}{|I|^2_{out}} = \frac{|S|^2}{|I|^2}\ \frac{1+2g|I|^2(1+g|I|^2)(1-\cos(\theta_{s_{10}} - \theta_{I_{10}}))}{1+[2g|S|^2(1-\gamma\cos\theta_{s_r})+2g^2|S|^4(1+\gamma^2-2\gamma\cos\theta_{s_r})](1-\cos(\theta_{I_{10}} - \theta_{s_{10}}))} \tag{47}$$

In order to minimize the effect of the imperfect estimation of the reference signal and to obtain a result approximating (43), it is sufficient to recuire that the ednominator factor in brackets in (47) satisfy

$$2g|S|^2(1-\gamma\cos\theta_{s_r})+2g|S|^4(1+\gamma^2-2\gamma\cos\theta_{s_r}) << 1 \quad * \tag{48}$$

Now, let us further assume that θ_{s_r} is very small: This condition might be met by using a reference loop filter wide enough for the desired signal information bandwidth (but narrow enough to enable the assumption of $F_I \simeq 0$), or by adding (in the reference signal loop) compensation weight that will reduce θs_r [3]. With this condition on θ_{s_r} (48) can be approximated by

$$2g|S|^2(1-\gamma\cos\theta_{s_r})+2g^2|S|^4(1-\gamma\cos\theta_{s_r})^2 < 1/2 \quad *$$

which implies that

$$\frac{2.414}{2} \leq g|S|^2(1-\gamma\cos_{s_r}) \leq \frac{0.414}{2}$$

or, *equivalently*

$$-1.207\,\frac{Pth}{|S|^2} \leq (1-\gamma\cos\theta_{s_r}) \leq 0.207\,\frac{Pth}{|S|^2} \tag{49}$$

Therefore, for larger desired signal-to-threshold power ratio, $\gamma\cos\theta_{s_r}$ must be closer to unity. This is easy to establish since with high SNR a better estimator for γ and θ_{s_r} can be obtained. (For example, with the second compensation scheme of [3] it was shown that $\gamma \to 1$, $\theta_{s_r} \to 0$, and obviously high SNR will be helpful.)

* The inequality condition of (48) is to be understood as searching for the assymptotic behavior of the denominator of (47). Therefore, for 3db point, for example, it is enough to require $\leq 1/2$ instead of $<< 1$ condition.

[3] Y. Bar-Ness, "On the Problem of the Reference Loop Phase Shift in an N-Element Adaptive Array," UP-VFRC-11-80, July 1980.

Equation (49) represents the design requirement on the loop filter response. If this can not be met with a fixed filter design then a compensation scheme is needed. Notice, however, that this condition is only sufficient (but not necessary) to obtain the desired signal-to-interference improvement of (43). Violating this condition may still lead to an improvement, although of smaller value.

If, however, (48) can not be satisfied, for example, because the desired signal power is very large, then we might have instead the condition that

$$g|S|^2(1-\gamma\cos\theta_{s_r})(1-\cos(\theta_{I_{10}}-\theta_{s_{10}})) >> 1 \tag{50}$$

Then (as we show in (P-12) of the appendix B7), the denominator of (47) can be approximated by

$$2g^2|S|^4(1+\gamma^2-2\gamma\cos\theta_{s_r})(1-\cos(\theta_{I_{10}}-\theta_{s_{10}})).$$

Substituting in (47) we get

$$\frac{|S|^2_{out}}{|I|^2_{out}} = \frac{|S|^2}{|I|^2}\ \frac{1+2g|I|^2(1+g|I|^2)}{2g^2|S|^4(1+\gamma^2-s\gamma\cos\theta_{s_r})} \tag{51}$$

If also we have $|I|^2 >> 1/g = Pth$ then, after some easy manipulation, (51) becomes

$$\frac{|S|^2_{out}}{|I|^2_{out}} \simeq \frac{|I|^2}{|S|^2}\ \frac{1}{(1-\gamma\cos\theta_{s_r})^2+\gamma^2(1-\cos\theta_{s_r})} \tag{52}$$

Notice that the term in the denominator of the second fraction is very small ($\gamma\cos\theta_{s_r} \simeq 1$, although it can not be equal to one, since otherwise (50) can not be satisfied). Comparing with (39) we observe that in this case of code tracking mode the power inversion formula, if it is enforced by the signal's

input conditions (both $|I|^2$ and $|S|^2$ are very large), is still favoring the desired signal.

DESIRED SIGNAL-TO-NOISE RATIO AT ARRAY OUTPUT

First, from (35) we can write for the output noise power

$$|V_N(t)|^2 = \sigma_N^2 \left[1 + \frac{g^2|I_0 I_1^*(1-F_I)+S_0 S_1^*(1-F_s)|^2}{|1+g(|S|^2(1-F_s)+|I_1|^2(1-F_I)|^2}\right]$$

where we used the fact that the noise processes at the two inputs are uncorrelated. Using the analysis that led to (P-13) of the appendix, we get

$$|V_N(t)|^2 = \sigma_N^2 \frac{A_1+A_2}{|1+g[|S|^2(1-F_s)+|I|^2(1-F_I)|^2} \tag{53}$$

where

$$A_1+A_2 = 1+2g[|S|^2 Re1(1-F_s)+|I_1|^2 Re1(1-F_I)].$$

$$\left[1+g \frac{|S|^4|1-F_s|^2+|I_1|^4|1-F_I|^2+|I_1|^2|S_1|^2 Re1((1+e^{j(\theta_{I_{10}}-\theta_{S_{10}})})(1-F_s)(1-F_I^*))}{|S|^2 Re1[1-F_s)+|I_1|^2 Re1(1-F_I)}\right] \tag{54}$$

Again we will distinguish between the different modes of the system's operation; that is, the acquisition and the tracking modes.

1. Acquisition Mode

Arguing as before we will assume in this case that both F_I and F_s are approximately zero, so that we can write, using (33) and (53), for the output desired signal-to-noise ratio,

$$\frac{|S|^2_{out}}{N_{out}} =$$

$$\frac{|S|^2}{\sigma_N^2} \frac{1+2g|I|^2(1+g|I|^2)(1-\cos(\theta_{s_{10}}-\theta_{I_{10}}))}{1+2g(|S|^2+|I|^2)[1+g(|S|^4+|I|^4+|I|^2|S|^2(1+\cos(\theta_{I_{10}}-\theta_{s_{10}}))/|S|^2+|I|^2)]}$$

$$\geq \frac{S^2}{\sigma_N^2} \frac{1+2g|I|^2(1+g|I|^2)(1-\cos(\theta_{s_{10}}-\theta_{I_{10}}))}{1+2g(|S|^2+|I|^2)[1+g(|S|^2+|I|^2)]} \qquad (55)$$

Therefore, when the directions of the signals are so close ($\cos\theta_{I_{10}}-\theta_{s_{10}} \simeq 1$) and the signal power is small compared to 1/g, or both signals' powers are small, then the output SNR is bounded below by $|S|^2/\sigma_N^2$ which is the input SNR. When the angular separation between the two signals and their powers are such that the second terms of both the numerator and the denominator of the right hand side of (55) are much larger than unity, then

$$\frac{|S|^2_{out}}{N_{out}} \geq \frac{|S|^2}{\sigma_n^2} \frac{|I|^4}{(|S|^2+|I|^2)^2}$$

$$\simeq \frac{|S|^2}{\sigma_N^2} \qquad \text{for } |I| > |S|$$

$$\simeq \frac{|S|^2}{\sigma_n^2} \cdot \frac{|I|^4}{|S|^4} \qquad \text{for } |S| > |I|$$

That is, when the desired signal is larger than the interference signal at the input then the array will not only null the first to a level below that of the second (see (39)), but it will also degrade the signal-to-noise ratio. In all other cases it is reasonable to expect approximately the same value of SNR at the output of the array as at the input, or even a slight improvement in SNR.

2. Code Tracking Mode

Again, as before, we assume $F_s \simeq \gamma e^{j\theta_{s_r}}$ and $F_I \simeq 0$ so that we can write for this case, using (33) and (53),

$$\frac{|S|^2_{out}}{N_{out}} =$$

$$\frac{|S|^2}{\sigma_N^2} \frac{1+2g|I|^2(1+g|I|^2)(1-\cos(\theta_{s_{10}}-\theta_{I_{10}}))}{1+2g(|I|^2+|S|^2 h_1)+2g^2(|I|^4+|S|^4 h_2+|S|^2|I|^2 h_3)} \tag{57}$$

where
$$h_1 = 1-\gamma\cos\theta_{s_r}$$
$$h_2 = (1+\gamma^2-2\gamma\cos\theta_{s_r}) \tag{58}$$
$$h_3 = 1-\gamma\cos\theta_{s_r}+\cos(\theta_{I_{10}}-\theta_{s_{10}})-\gamma\cos(\theta_{I_{10}}-\theta_{s_{10}}+\theta_{s_r})$$

For the case of an ideal reference loop filter, $\theta_{s_r} = 0$, $\gamma = 1$, so that $h_1 = h_2 = h_3 = 0$, and (57) becomes

$$\frac{|S|^2_{out}}{N_{out}} = \frac{|S|^2}{\sigma_N^2} \frac{1+2g|I|^2(1+g|I|^2)(1-\cos(\theta_{s_{10}}-\theta_{I_{10}}))}{1+2g|I|^2(1+g|I|^2} \tag{59}$$

Therefore, except when the directions of arrival are such that $\cos(\theta_{s_{10}}-\theta_{I_{10}}) \approx 1$, the output SNR is approximately equal to the input SNR regardless of the desired signal power.

To see the effect of a non-ideal filter on the output SNR we first assume (48) is satisfied and write (57) as

$$\frac{S^2_{out}}{N_{out}} \simeq \frac{|S|^2}{\sigma_N^2} \frac{1+2g|I|^2(1+g|I|^2)(1-\cos(\theta_{I_{10}}-\theta_{s_{10}}))}{1+2g|I|^2[1+g(|I|^2+|S|^2 h_3)]} \tag{60}$$

$$\simeq \frac{|S|^2}{\sigma_N^2} \frac{1+2g|I|^2(1+g(|I|^2)(1-\cos(\theta_{I_{10}}-\theta_{s_{10}}))}{1+2g\,I^2(1+g(\,I\,^2+S\,^2(1-\,)\cos(\,_{I_{10}}-\,_{s_{10}}))} \tag{60}$$

where by (48) we have used $g|S|^2(1-\gamma\cos\theta_{s_r}) >> 1$ in h_3 of (58). Comparing with (59) we notice the effect of $\gamma \neq 1$ on the output SNR.

Effect of Non-Zero Interference Residue at the Output of the Reference Loop

In the previous discussion we assumed that in the tracking mode the reference loop filter rejects the interference signal totally: that is, we assumed the $F_I = 0$. In practice this will not be the case, since the filter bandwidth can not be negligibly small (otherwise it will reject the desired signal as well). Thus, even though the filter bandwidth is smaller than the spread interference bandwidth and it will reject a large part of the interference power, nevertheless, there will still remain some residue at the output of the reference loop filter. In this section we estimate the effect of this residue.

We will assume that the filter is ideal in estimating the desired signal, that is $F_s = 1$, F_I, however, is not zero. With these assumptions used in (33) and (34) we get

$$\frac{|S|^2_{out}}{|I|^2_{out}} = \frac{|S|^2}{|I|^2} \left| 1+g(1-F_I)|I|^2(1-e^{j(\theta_{I_{10}}-\theta_{s_{10}})}) \right|^2$$

Using (P-11) of the appendix this becomes

$$\frac{|S|^2_{out}}{|I|^2_{out}} = \frac{|S|^2}{|I|^2} [1+2g|I|^2e_1+2g^2|I|^4e_2] \tag{61}$$

where, analogous to (41) and (42), we define

$$e_1 = 1-\beta\cos\theta_{I_r}-\cos(\theta_{I_{10}}-\theta_{s_{10}})+\beta\cos(\theta_{I_r}+\theta_{I_{10}}-\theta_{s_{10}}) \tag{62}$$

$$e_2 = (1+\beta^2-2\beta\cos\theta_{I_r})(1-\cos(\theta_{I_{10}}-\theta_{s_{10}})) \tag{63}$$

Here we used the relation $I_r(t) = F_I V_i(t) = \beta e^{j\theta_{I_r}} V_I(t)$ where, as before, $I_r(t)$ and $V_I(t)$ are the interference signal at the output and the input, respectively, of the reference loop. Note that $V_I(t)$ is also the array output. Since the interference signal is assumed to be wideband (it is widened by multiplication with the system code), β and θ_{I_r} would obviously be frequency-dependent. As a first approximation we may assume that the reference loop filter has an ideal rectangular shape with zero passband phase shift. That is, we assume $\theta_{I_r} \simeq 0$ and $\beta = 1$ within the passband and $\beta = 0$, and θ_{I_r} is undefined outside the passband.

Define

$$\bar{\beta} = (1/B_I)\int \beta(w)dw$$

$$\simeq \frac{B_f}{B_I} \tag{64}$$

where B_I is the interference signal bandwidth and B_f is the reference loop filter bandwidth. Then (61) together with (62) and (63) becomes

$$\frac{|S|_{out}}{|I|_{out}} = \frac{|S|^2}{|I|^2} [1+2g|I|^2(1-\bar{\beta})(1+g|I|^2(1-\bar{\beta}))(1-\cos(\theta_{I_{10}}-\theta_{s_{10}}))]$$

Comparing with (43) which was obtained with an assumption of an ideal filter ($F_s = 1$), we notice that the effect of the interference residue at the output of the reference loop is equivalent to that of reducing this signal power by $1 - \bar{\beta}$.

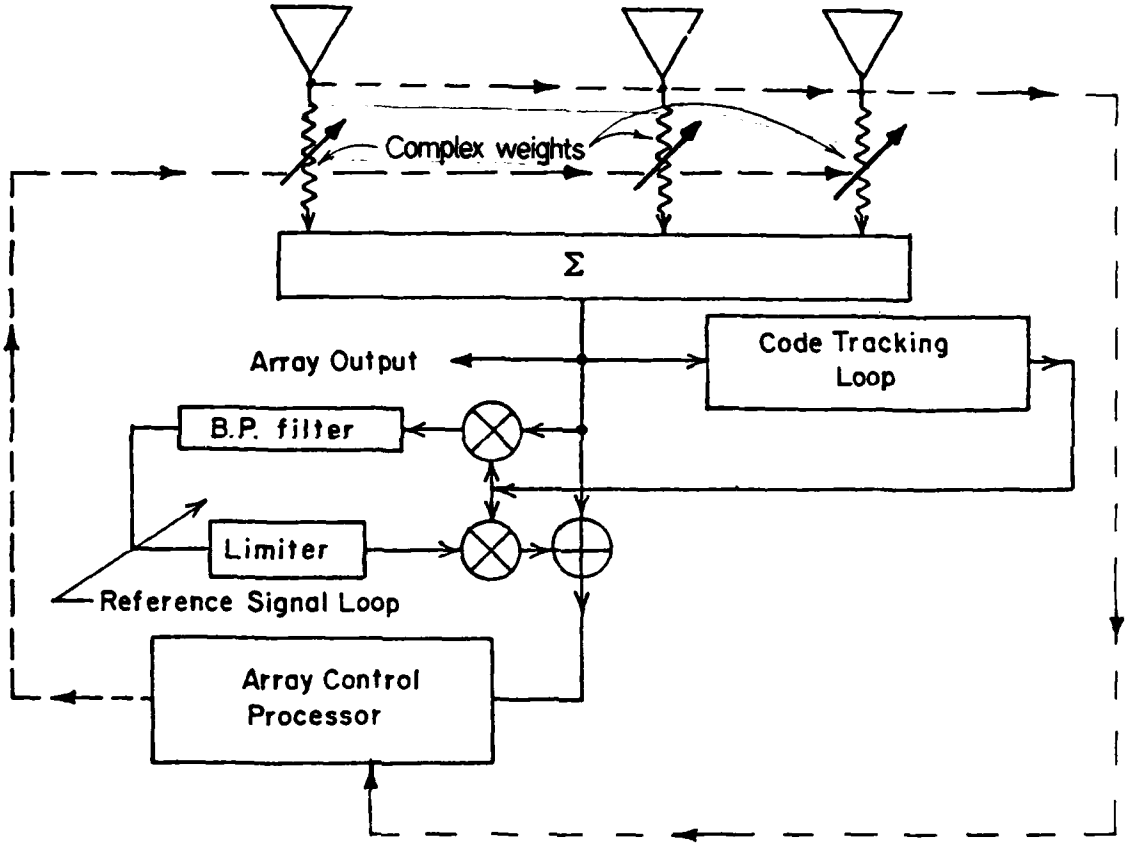

Figure 1 The LMS Adaptive Array with Coded Reference Signal Loop for Spread Spectrum Communication

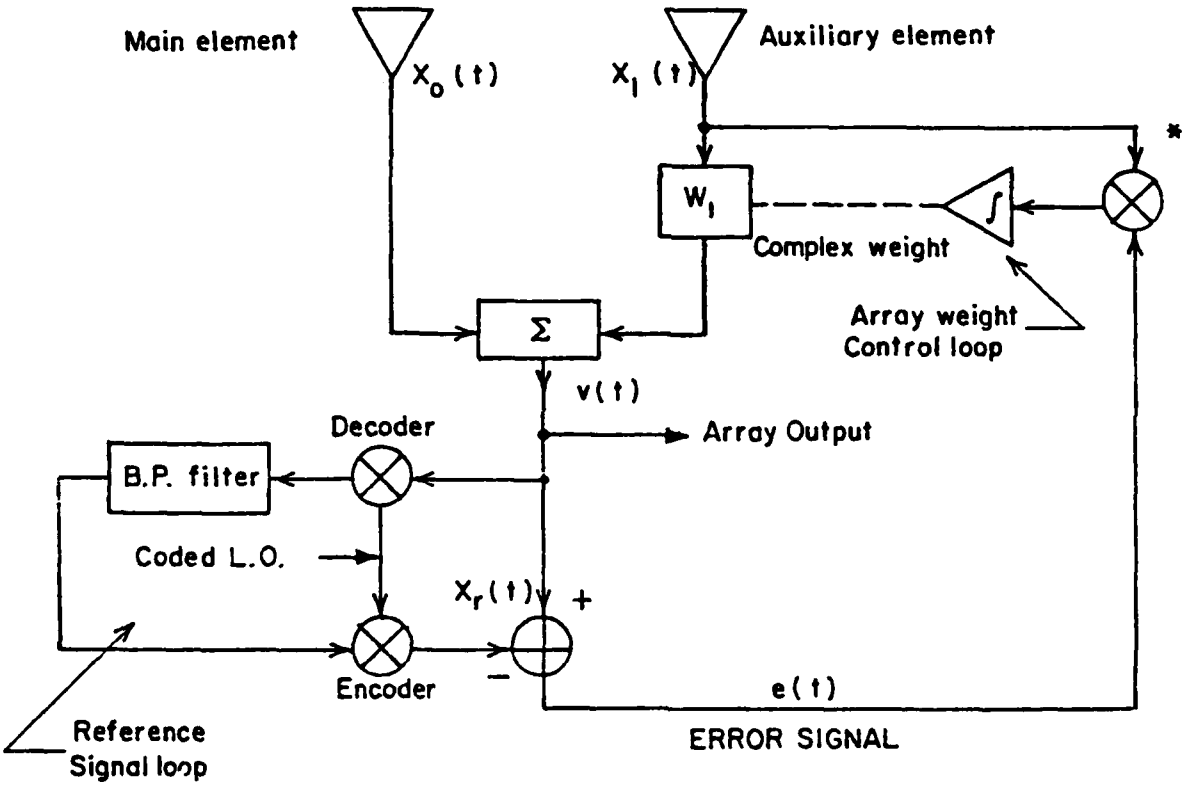

Figure 2 The LMS Interference Canceller with Coded Reference Signal Loop for Spread Spectrum Communication

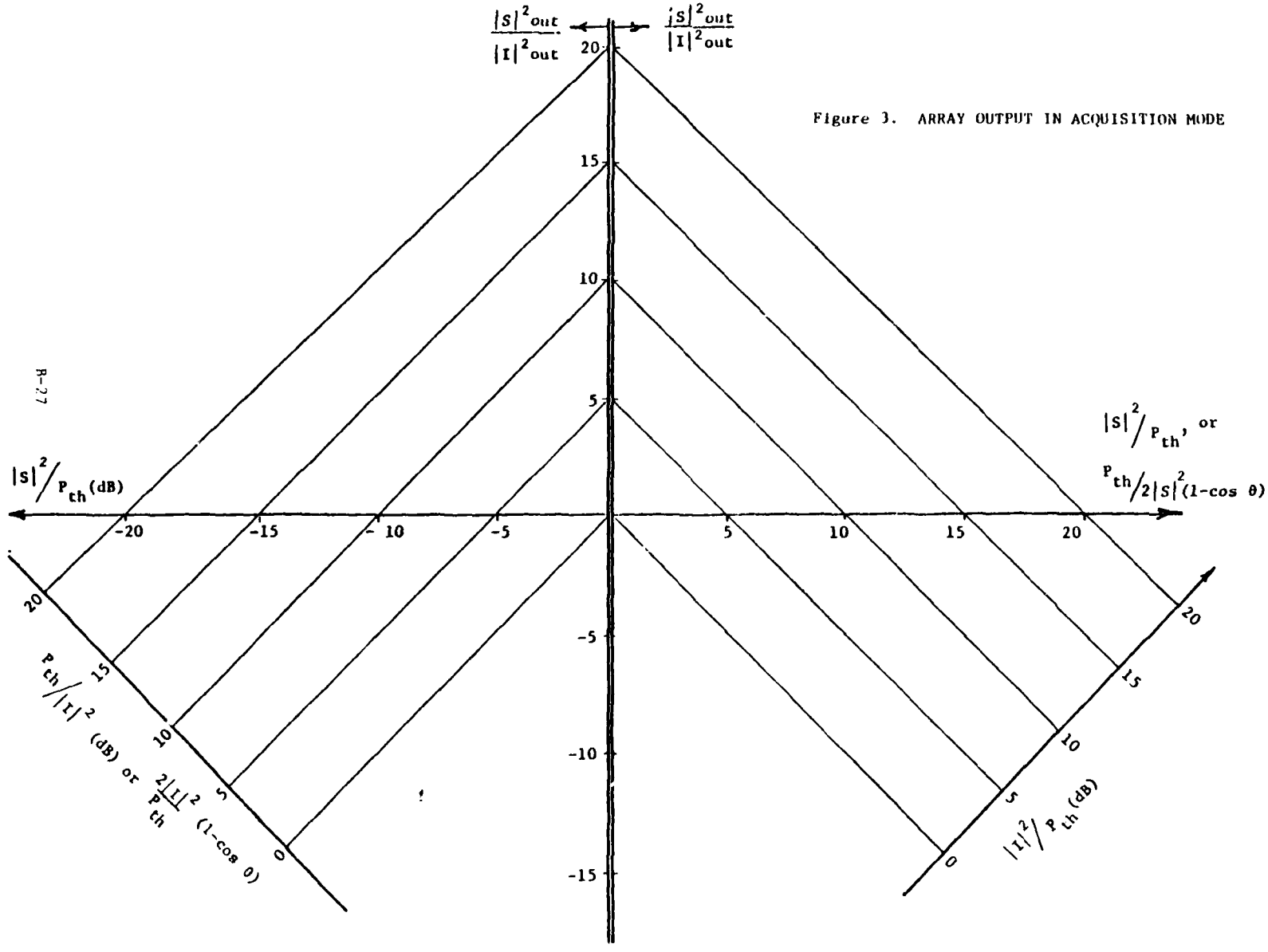

Figure 3. ARRAY OUTPUT IN ACQUISITION MODE

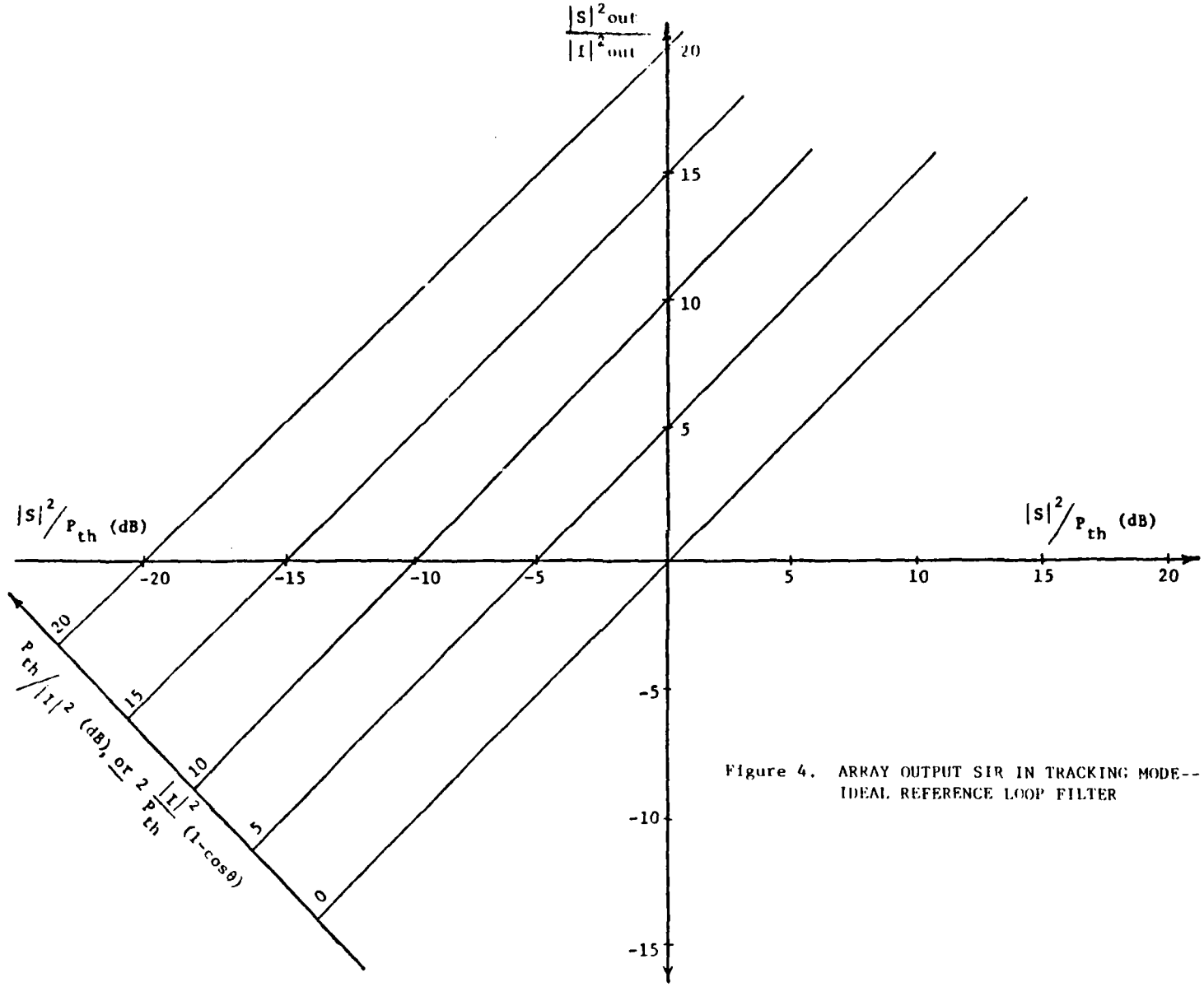

Figure 4. ARRAY OUTPUT SIR IN TRACKING MODE--
IDEAL REFERENCE LOOP FILTER

ACKNOWLEDGEMENTS

The author would like to thank Professor F. Haber for the important discussions which helped to clarify some of the ideas in this work, and Sam Seeleman for editing the manuscript.

APPENDIX

B-1 The array output

$$V(t) = X_0(t)+W_1(t)X_1(t) \qquad (P\text{-}1)$$

Using the definition of $X_i(t)$, i = 0,1 together with $W_1(t)$ from (6) and corresponding terms of (7) and (8), we get

$$V(t) = I_0+S_0+N_0 - \frac{K(I_0I_1^* - I_rI_1^* + S_0S_1^* - S_rS_1^*)}{1+K(|I_1|^2+|S_1|^2+\sigma_N^2)}(I_1+S_1+N_1) \qquad (P\text{-}2)$$

Let

$$(1+K\sigma_N^2)/K = 1/g \triangleq Pth$$

where Pth stands for the system threshold power. Then (P-2) becomes

$$V(t) = (I_0+S_0+N_0) - \frac{g(I_0I_1^* - I_rI_1^* + S_0S_1^* - S_rS_1^*)}{1+g(|I_1|^2+|S_1|^2)}(I_1+S_1+N_1)$$

$$= \frac{(I_0+S_0)[1+g(|I_1|^2+|S_1|^2)]-g(I_1+S_1)[I_0I_1^* - I_rI_1^* + S_0S_1^* - S_rS_1^*}{1+g(|I_1|^2+|S_1|^2)}$$

$$+N_0 - \frac{gN_1(I_0I_1^* - I_rI_1^* + S_0S_1^* - S_rS_1^*)}{1+g(|I_1|^2+|S_1|^2}$$

Thus

$$V(t) = \frac{I_0(1+g|S_1|^2)-gI_1(S_0S_1^*)+g(I_r|I_1|^2+I_1S_rS_1^*}{1+g(|S_1|^2+|I_1|^2)}$$

$$+\frac{S_0(1+g|I_1|^2)-gS_1(I_0I_1^*)+g(S_r|S_1|^2+S_1I_rI_1^*}{1+g(|S_1|^2+|I_1|^2}$$

$$+N_0-\frac{gN_1(I_0I_1^*-I_rI_1^*+S_0S_1^*-S_rS_1^*}{1+g(|S_1|^2+|I_1|^2} \qquad \text{(P-3)}$$

B-2 Using (19) and (20) we can write (16) as

$$\begin{bmatrix} S_r \\ I_r \end{bmatrix} = A^{-1} \left[\begin{array}{c} F_s\ S_{NOR} \\ \hline F_I\ I_{NOR} \end{array}\right] \qquad \text{(P-4)}$$

when

$$A^{-1} = \frac{1}{\Delta} \begin{vmatrix} 1+g(|S_1|^2+|I_1|^2(1-F_I)) & gF_sS_1I_1^* \\ gF_II_1S_1^* & 1+g(|I_1|^2+|S_1|^2(1-F_s)) \end{vmatrix} \qquad \text{(P-5)}$$

and

$$\Delta = [1+g(|I_1|^2+|S_1|^2(1-F_s)][1+g(|S_1|^2+|I_1|^2(1-F_I)]$$

$$- g^2F_IF_s|I_1|^2|S_1|^2$$

$$= [1+g(|I_1|^2+|S_1|^2)](1+g(|S_1|^2+|I_1|^2(1-F_I))$$

$$- gF_s|S_1|^2(1+g(|S_1|^2+|I_1|^2$$

$$\Delta = [1+g(|I_1|^2+|S_1|^2)][1+g(|S_1|^2(1-F_s)+|I_1|^2(1-F_I))] \qquad \text{(P-6)}$$

B-3 Using (18) we have

$$[S_1^* \mid I_1^*]\, A^{-1} = \frac{1}{\Delta} \left[\begin{array}{l|l} S_1^*[1+g(|S_1|^2+|I_1|^2(1-F_I)] & gI_1^* F_s|S_1|^2+ \\ +gS_1^* F_I|I_1|^2 & I_1^*(1+g(|I_1|^2+|S_1|^2(1-F_s) \end{array}\right]$$

$$= \frac{1+g(|S_1|^2+|I_1|^2)}{\Delta}[S_1^* \mid I_1^*] \qquad \text{(P-7)}$$

B-4 From (24) and using (21) we write

$$W_1(t) = -g\left(\frac{I_0 I_1^* + S_0 S_1^*}{1+g(|I_1|^2+|S_1|^2} - \frac{F_s S_1^* S_{NOR} + F_I I_1^* I_{NOR}}{\Delta}\right)$$

Using the definitions of S_{NOR} and I_{NOR} in (19) and (20), respectively, and that of Δ in (22) we can write

$$W_1(t) = \frac{-g}{\Delta}\{(I_0 I_1^* + S_0 S_1^*)[1+g(|S_1|^2(1-F_s)+|I_1|^2(1-F_I))]$$

$$- F_s S_1^*[S_0(1+g|I_1|^2) - gS_1(I_0 I_1^*)]$$

$$- F_I I_1^*[I_0(1+g|S_1|^2 - gI_1(S_0 S_1^*)]\}$$

$$= -\frac{g}{\Delta}\{I_0 I_1^*[1+g(|S_1|^2(1-F_s)+|I_1|^2(1-F_I)) + gF_s|S_1|^2 - F_I(1+g|S_1|^2)]$$

$$S_0 S_1^*[1+g(|S_1|^2(1-F_s)+|I_1|^2(1-F_I)) + gF_I|I_1|^2 - F_s(1+g|I_1|^2)]\}$$

which can be brought, after some simple manipulation and (22), to the form,

$$W_1(t) = \frac{-g[I_0 I_1^*(1-F_I)+S_0 S_1^*(1-F_s)]}{1+g[|S_1|^2(1-F_s)+|I_1|^2(1-F_I)]} \qquad \text{(P-8)}$$

B-5 Substituting (26) in (27) we have

$$V_s(t) = S_0 - \frac{g[I_0 I_1^* (1-F_I)+S_0 S_1^* (1-F_s)]}{1+g(|S_1|^2(1-F_s)+|I_1|^2(1-F_I))} S_1$$

$$= \frac{[1+g(|S_1|^2(1-F_s)+|I_1|^2(1-F_I)]S_0}{1+g(|S_1|^2(1-F_s)+|I_1|^2(1-F_I)}$$

$$- \frac{gS_1(I_0 I_1^* (1-F_I)-g|S_1|^2(1-F_s)S_0}{1+g(|S_1|^2(1-F_s)+|I_1|^2(1-F_I)}$$

$$= \frac{S_0+g(1-F_I)[S_0|I_1|^2-S_1(I_0 I_1^*)]}{1+g(|S_1|^2(1-F_s)+|I_1|^2(1-F_I)} \qquad \text{(P-9)}$$

and, similarly, we obtain by using (26) in (28)

$$V_I(t) = \frac{I_0+g(1-F_I)[I_0|I_1|^2-S_0(I_0 I_1)]}{1+g(|S_1|^2(1-F_s)+|S_1|^2(1-F_I))} \qquad \text{(P-10)}$$

B-6 Let $g(\alpha,F,\theta) = 1+\alpha(1-F)(1-e^{j\theta})$

where F is complex and θ are reals. Then,

$$|g(\alpha,F,\theta)|^2 = [1+ (1-F)(1-e^{j\theta})][1+ (1-F)^* (1-e^{-j\theta})]$$

$$= 1+2\ [1-\mathrm{Re}1(F)-\cos\theta+\mathrm{Re}1(Fe^{j\theta})]$$

$$+2\ ^2(1+|F|^2-2\mathrm{Re}1(F))(1-\cos\theta) \qquad \text{(P-11)}$$

B-7 Condition (50) obviously implies that $g|S|^2(1-\cos\theta_{s_r}) >> 1$.

Now

$$g|S|^2 \frac{(1+\gamma^2-2\gamma\cos\theta_{s_r})}{1-\gamma\cos\theta_{s_r}} = g|S|^2(1-\gamma\cos\theta_{s_r}) \frac{1+\gamma^2-2\gamma\cos\theta_{s_r}}{(1-\gamma\cos\theta_{s_r})^2}$$

$$\geq g|S|^2(1-\gamma\cos\theta_{s_r}) >> 1$$

Therefore, the denominator of (47) can be approximated by

$$1+2g|S|^2(1-\gamma\cos\theta_{s_r})[1+g|S|^2 \frac{(1+\gamma^2-2\gamma\cos\theta_{s_r})}{1-\gamma\cos\theta_{s_r}}](1-\cos(\theta_{I_{10}}-\theta_{s_{10}}))$$

$$\simeq 2g^2|S|^4(1+\gamma^2-2\gamma\cos\theta_{s_r})(1-\cos(\theta_{I_{10}}-\theta_{s_{10}})) \qquad \text{(P-12)}$$

B-8 To derive the noise power at the output of the array we notice, using (35), that

$$|V_N(t)|^2 = \sigma_N^2 \left(1+ \frac{g^2|I_0I_1^*(1-F_I)+S_0S_1^*(1-F_s)|^2}{|1+g(|S_1|^2(1-F_s)+|I_1|^2(1-F_I))|^2}\right)$$

where we used the fact that N_0 and N_1 are uncorrelated.

$$A_1 \triangleq |1+g(|S_1|^2(1-F_s)+|I|^2(1-F_I))|^2$$

$$= 1+g^2[|S_1|^4|1-F_s|^2+|I_1|^4|1-F_I|^2+2|I_1|^2|S_1|^2\mathrm{Re}(1-F_s)(1-F_I)^*]$$

$$+ 2g[|S_1|^2\mathrm{Re}(1-F_s)+|I_1|^2\mathrm{Re}(1-F_I)]$$

$$A_2 \triangleq g^2 \left| I_0 I_1^* (1-F_I) + S_0 S_1^* (1-F_s) \right|^2$$

$$= g^2 (|I|^4 |1-F_I|^2 + |S_1|^4 |1-F_s|^2 + 2|I|^2 \mathrm{Re}[e^{j(\theta_{I10} - \theta_{s10})} (1-F_s)(1-F_I)^*])$$

where we used $|I_0|^2 = |I_1|^2$ and, similarly, for S

$$A_1 + A_2 = 1 + 2g^2 [|S|^4 |1-F_s|^2 + |I|^4 |1-F_I|^2$$

$$+ |I|^2 |S|^2 \mathrm{Re}[(1+e^{j(\theta_{I10} - \theta_{s10})})(1-F_s)(1-F_I)^*]$$

$$+ 2g[|S|^2 \mathrm{Re}(1-F_s) + |I|^2 \mathrm{Re}(1-F_I)]$$

$$= 1 + 2g[|S|^2 \mathrm{Re}(1-F_s) + |I|^2 \mathrm{Re}(1-F_I)]$$

$$[1+g \frac{|S|^4 |1-F_s|^2 + |I|^4 |1-F_I|^2 + |I|^2 |S|^2 \mathrm{Re}[(1+e^{j(\theta_{I10} - \theta_{s10})})(1-F_s)(1-F_I)^*]}{|S|^2 \mathrm{Re}(1-F_s) + |I|^2 \mathrm{Re}(1-F_I)}] \quad \text{(P-13)}$$

APPENDIX C

COMPARING THE PERFORMANCE OF AN INTERFERENCE CANCELER WITH REFERENCE SIGNAL LOOP AND AN INTERFERENCE CANCELER THAT UTILIZES DIRECTIONAL CONSTRAINT

By

Yeheskel Bar-Ness*

Valley Forge Research Center
Moore School of Electrical Engineering
University of Pennsylvania
Philadelphia, Pennsylvania 19104

ABSTRACT

The performances of two kinds of interference cancelers are compared, namely, an interference canceler that utilizes a directional constraint (directionally constrained interference canceler) and an interference canceler with reference signal loop (LMS interference canceler). For simplicity, this is done for a two-element array. In our comparison we use the array output desired signal-to-interference power ratio (SIR) and desired signal-to-noise ratio. These power ratios, obtained with the first canceler when the angle of arrival of the desired signal relative to the constraint direction is sufficiently small, are compared with the corresponding power ratios obtained with the second canceler when it operates in code tracking mode. Similarly, power ratios, obtained with the first canceler when the angle of arrival relative to the constraint direction is not so small, are compared with the corresponding power ratios obtained with the second canceler when it operates in code acquisition mode. Finally, in considering the "accurately constrained" case of the first canceler and the "ideally filtered" case of the second canceler, we establish the condition under which one or the other of these cancelers performs better.

* On leave of absence from the School of Engineering, Tel Aviv University

INTRODUCTION

Adaptive array processors are used more and more as a method for interference cancellation in the design of advanced systems. However, these automatic processors might also cancel the desired signal unless it is somehow protected by the algorithm used: in particular, this is true when the desired signal power is much larger than the interference power. One way of obtaining such protection is by using a cross-coupled processor that implements, in a genuine boot-strapping form, the "power-inversion" property of the interference canceler. This form of "power separator" was reported in [1]. Customarily, some a priori known properties of the desired signal are used--properties which sufficiently distinguish it from other signals (interferences).

An array for spread-spectrum communication system has been described [2,3] using a reference signal loop to process the output of the array and extract a sufficiently clean estimate of the desired signal. This is then used as a reference in the Widrow LMS algorithm [4]. Such an adaptive array processor, as it was proposed by Compton [2], is depicted in Figure 1. In Figure 2 a different approach is presented: The approach is termed "LMS interference canceler," and its performance was studied in [3]. Both approaches use the special spectral property (spread spectrum) of the desired signal to keep the processor from affecting the desired signal regardless of its dynamic range. As a result, the desired-signal-

to-interference ratio (SIR) is substantially improved except when the relative directions of arrival of these two signals are close. The improvement in SIR depends on the signals' relative directions of arrival as well as on the interference-to-threshold power ratio (ITR): (Threshold power approximately equals the system noise power).

The improvement decreases when the estimation of desired signal by the reference signal loop becomes less and less accurate.

An alternative use of a priori information is found in the constrained algorithm [5]. Here, knowledge of the desired signals' direction of arrival is used to prevent the processor from affecting the signal. The canceler of this approach will be called "directionally constrained interference canceler."

In radar, the direction of arrival of the desired signal is assumed accurately known (the direction of the main beam) and, therefore, the second alternative can be used satisfactorily. In point-to-point communication, on the other hand, the direction of arrival of the desired signal might be known with only a modest level of accuracy. Some special spectral property, such as spread-spectrum modulation, might or might not be available. Nevertheless, the questions that the system designer might be faced with are (considering the output SIR) which of these approaches is preferred? How does the preference depend on the dynamic range of the input powers? How does it depend on uncertainty in the desired signal's direction of arrival (used in the second approach). How does it depend on the amount of imperfection of estimating the reference signal (used in the first approach)?

The performances of these two alternatives are to be compared in this

article. We first use the Applebaum approach for a directioanl constraint interference canceler and derive the output desired-signal-to-interference power ratio (SIR) and desired signal-to-noise ratio (SNR). For simplicity this is done for a two-element array. In particular, we notice the change in performance due to change in desired signal direction relative to constraint direction. We then compare the performance of the directional constraint canceler (hereinafter called canceler A) with that of an interference canceler that utilizes a reference signal loop (hereinafter called canceler B). In our comparison we use the array output SIR and SNR. These power ratios, obtained with canceler A when the angle of arrival of the desired signal relative to the constraint direction is sufficiently small, are comapred with the corresponding power ratios obtained with canceler B when it operates in the code tracking mode. Similarly, power ratios obtained with canceler A when the angle of arrival relative to the constraint direction is not so small are comapred with the corresponding power ratios obtained with canceler B when it operates in code acquisition mode. Finally, in considering the "accurately constrained" canceler A and the "ideally filtered" canceler B, we establish the conditions under which one or the other of these cancelers performs better.

DIRECTIONALL CONSTRAINED INTERFERENCE CANCELER

The array arrangement is depicted in Figure 3. In complex envelope notation the inputs to the array elements are denoted by X_1, X_2, ... X_n where n is the number of elements and,

$$X_i(t) = S_i(t)+N_i(t) + \sum_{j=1}^{m} I_{ij}(t) \qquad (1)$$

$I_{ij}(t)$, j=1,2,...m is the jth interference signal at the array's ith element, $S_i(t)$ is the desired signal at the ith element and $N_i(t)$ is the noise term. In vector notation

$$\underset{\sim}{X}(t) = \underset{\sim}{S}(t)+\underset{\sim}{N}(t)+\sum_{j=1}^{m}\underset{\sim}{I}_j(t) \tag{2}$$

For plane wave signals we can write

$$\underset{\sim}{S}(t) = s(t)\underset{\sim}{S} \tag{3}$$

$$\underset{\sim}{I}_j(t) = i_j(t)\underset{\sim}{I}_j \tag{4}$$

where $\underset{\sim}{S}$ and $\underset{\sim}{I}_j$ are the complex magnitude vectors (phase and amplitude) of the desired signal and the interfering signals, respectively. These vectors obviously depend on the direction of arrival of these signals with respect to the array. We will also assume that $\overline{|s(t)|^2}=1$ and $\overline{|i(t)|^2}=1$.

A processor for a directaionally constrained interference canceler is one that derives the weight vector $\underset{\sim}{W}$, such that in the steady state the following statements are satisfied simultaneously;

$$\overline{|V(t)|^2} = \overline{|\underset{\sim}{W}^T\underset{\sim}{X}(t)|^2} = \min \tag{5}$$

and

$$\underset{\sim}{E}^T\underset{\sim}{W} = n \tag{6}$$

where T stands for transpose and the overbar for the mean value. That is, according to (5) the processor will minimize the mean square value of the array output. By (6), any signal s(t) impinging on the array from a direction $\underset{\sim}{E}$ will not be affected by the array (will become s(t)·n at the array output). Therefore, $\underset{\sim}{E}$ is the *direction of constraint*.

For the implementation of this processor we propose to use the "mainbeam constraint" approach of Applebaum and Chapman [5] as it is given in Figure 4. The output of the summer, Y_o, where

$$Y_o(t) = \underset{\sim}{\phi}^T \underset{\sim}{X}(t) \tag{7}$$

($\underset{\sim}{\phi}$ is the beam steering vector), and the outputs of the linear transformation $\underset{\sim}{Y}(t) = \{Y_1(t), \ldots, Y_{n-1}(t)\}$, where

$$\underset{\sim}{Y}(t) = \underset{\sim\sim}{A}\underset{\sim}{X}(t), \tag{8}$$

are the main and auxiliary inputs of an unconstrained interference canceler. The weight vector of this canceler $\underset{\sim}{W}_y = \{W_{y_1}, \ldots, W_{y_{n-1}}\}$ is controlled so that the mean square value of the array output $\overline{|V(t)|^2}$ is minimized. That is, in the steady state $\underset{\sim}{W}_y$ must satisfy

$$\overline{[I + K\underset{\sim}{Y}^*(t)Y^T(t)]}\underset{\sim}{W}_y = -K\overline{\underset{\sim}{Y}^*(t)Y_o(t)} \tag{9}$$

where K is the gain of the control, loop, I is an (n-1) identity matrix and the (*) stands for the complex conjugate.

It is possible to show [5] that if we choose the steering vector

$$\underset{\sim}{\phi} = \underset{\sim}{E}^* \tag{10}$$

the direction of constraint, and choose the transformation $\underset{\sim}{A}$ such that

$$\underset{\sim\sim}{A}\underset{\sim}{E} = \underset{\sim}{0}, \tag{11}$$

then the solution of (9) together with (7) and (8) is the solution of the constraint problem (5) and (6), which we called the "directionally constrained interference canceler." Notice, from Figure 4 and (8), that

$$\underset{\sim}{A} = \underset{\sim}{B}\begin{bmatrix} \phi_1 & & & \\ & \phi_2 & & \\ & & \ddots & \\ & & & \phi_n \end{bmatrix} \tag{12}$$

Hence, by (10) and (11),

$$\underset{\sim}{A}\underset{\sim}{E} = \underset{\sim}{0} \Rightarrow \underset{\sim}{B}\underset{\sim}{1} = \underset{\sim}{0} \tag{13}$$

(where $\underset{\sim}{1} = [1,\ldots,1]$ is the required constraint transformation.

The Two-Element Case

To facilitate a comparison of the performance of the "directionally constrained interference canceler" with that of the "LMS interference canceler," we will restrict ourselves to the case of a two-element array and a single interference signal. That is, in (2) the sum contains only one element and the vectors are two-dimensional. Also, without loss of generality we will assume that the direction of constraint is broadside to the array. That is, from (10) $\underset{\sim}{\phi} = \underset{\sim}{E}^* = \underset{\sim}{1}$, and from (12) $\underset{\sim}{A} = \underset{\sim}{B}$. To satisfy (11) we must use $A = [1,-1]$, and by (7) and (8),

$$Y_o(t) = X_1(t)+X_2(t) \tag{16}$$

and

$$Y_1(t) = X_1(t)-X_2(t) \tag{17}$$

where $X_i(t)$ is defined by (1) with m=1 (one interference). This array arrangement is given in Figure 5. Obviously, for this special case (9) becomes

$$[1+K\overline{Y_1^*(t)Y_1(t)}]W_y = -K\overline{Y_1^*(t)Y_o(t)} \tag{18}$$

Using (16), (17) and (1) in the derivation of $\overline{Y_1^*(t)Y_o(t)}$ and $\overline{Y_1^*(t)Y_1(t)}$ in Appendix A-1, equation (18) can be written as

$$W_y = \frac{-g[(S_1-S_2)^*(S_1+S_2)+(I_1-I_2)^*(I_1+I_2)]}{1+g(|S_1-S_2|^2+|I_1-I_2|^2)} \tag{19}$$

where

$$1/g = \frac{1+2K\sigma_N^2}{K} \triangleq P_{th} \tag{20}$$

P_{th} stands for the system power threshold. S_1 and S_2, I_1 and I_2 are the components of vectors $\underline{S}$ and $\underline{I}$, respectively, as they are defined in (3) and (4).

The Array Output

From Figure 5 we have

$$V(t) = Y_o(t) + Y_1(t)W_y \tag{21}$$

Using (16) and (17) with (1) we show that (see Appendix A-2),

$$V(t) = \frac{S_1(t)[1+2g(|I_2|^2-I_1^*I_2)] + S_2(t)[1+2g(|I_1|^2-I_2^*I_1)]}{1+g(|S_1-S_2|^2 + |I_1-I_2|^2)}$$

$$+ \frac{I_1(t)[1+2g(|S_2|^2-S_1^*S_2)] + I_2(t)[1+2g(|S_1|^2-S_2^*S_1)]}{1+g(|S_1-S_2|^2 + |I_1-I_2|^2)}$$

$$+ \frac{N_1(t)[1+2g(|S_2|^2-S_1^*S_2 + |I_2|^2-I_1^*I_2)] + N_2(t)[1+2g(|S_1|^2-S_2^*S_1 + |I_1|^2-I_2^*I_1)]}{1+g(|S_1-S_2|^2 + |I_1-I_2|^2)} \tag{22}$$

Clearly, the first term is the desired signal at the output, the second term is the interfering signal, and the last term is the noise. We will further assume that the two array elements are sufficiently close so that $|S_1| = |S_2| = |S|$ and $|I_1| = |I_2| = |I|$. Hence,

$$\begin{aligned} S_1 &= |S|e^{j\theta_{s_1}} \\ S_2 &= |S|e^{j\theta_{s_2}} \\ I_1 &= |I|e^{j\theta_{i_1}} \\ I_2 &= |I|e^{j\theta_{i_2}} \end{aligned} \tag{23}$$

where

$$\theta_{si}-\theta_{s2} \triangleq \theta_s = \frac{\omega_s d}{c}\sin\psi_s$$

$$\theta_{i1}-\theta_{i2} \triangleq \theta_i = \frac{\omega_i d}{c}\sin\psi_i \qquad (24)$$

d is the distance between the array elements, ω_s and ω_i are the radian frequencies of the desired and interference signals, respectively, c is the speed of electromagnetic waves and ψ_s and ψ_i are the directions of arrival of these signals with respect to the array broadside direction, respectively. With this, (22) can be rewritten as

$$V(t) = \frac{[S_1(t)+S_2(t)](1+2g|I|^2) - 2g(I_1^*I_2S_1(t) + I_2^*I_1S_2(t))}{1+g(|S_1-S_2|^2 + |I_1-I_2|^2)} \qquad (25)$$

$$+ \frac{[I_1(t) + I_2(t)](1+2g|S|^2) - 2g(S_1^*S_2I_1(t) + S_2^*S_1I_2(t))}{1+g(|S_1-S_2|^2 + |I_1-I_2|^2)}$$

$$+ \frac{N_1(t)[1+2g(|S|^2 - S_1^*S_2+|I|^2-I_1^*I_2)] + N_2(t)[1+2g(|S|^2-S_2^*S_1+|I|^2-I_2^*I_1)]}{1+g(|S_1-S_2|^2 + |I_1-I_2|^2)}$$

Using the derivation in Appendix A-3, we finally write (26)

$$V(t) = \frac{2s(t)|S|e^{j/2(\theta_{s1}+\theta_{s2})}[(1+2g|I|^2)\cos(\theta_s/2) - 2g|I|^2\cos(\theta_i-\theta_s/2)]}{1+2g[|S|^2(1-\cos\theta_s) + |I|^2(1-\cos\theta_i)]}$$

$$+ \frac{2i(t)|I|e^{j/2(\theta_{i1}+\theta_{i2})}[(1+2g|S|^2)\cos(\theta_i/2) - 2g|S|^2\cos(\theta_s-\theta_i/2)]}{1+2g[|S|^2(1-\cos\theta_s) + |I|^2(1-\cos\theta_i)]}$$

$$+ \frac{N_1(t)[1+2g(|S|^2(1-e^{-j\theta_s})+|I|^2(1-e^{-j\theta_i}))]+N_2(t)[1+2g(|S|^2(1-e^{j\theta_s})+|I|^2(1-e^{j\theta_i}))]}{1+2g[|S|^2(1-\cos\theta_s) + |I|^2(1-\cos\theta_i)]}$$

From (26), noting that the three terms are uncorrelated, we obtain

after some trigonometric manipulation

$$\overline{|V(t)|^2} = \overline{|V_s(t)|^2} + \overline{|V_i(t)|^2} + \overline{|V_n(t)|^2}$$

where

$$\overline{|V_s(t)|^2} = \frac{4|S|^2\cos^2(\theta_s/2)[1+2g|I|^2\sin\theta_i(\tan(\theta_i/2)-\tan(\theta_s/2))]^2}{[1+2g(|S|^2(1-\cos\theta_s)+|I|^2(1-\cos\theta_i))]^2} \tag{27}$$

$$|V_i(t)|^2 = \frac{4|I|^2\cos^2(\theta_i/2)[1+2g|S|^2\sin\theta_s(\tan(\theta_s/2)-\tan(\theta_i/2))]^2}{[1+2g(|S|^2(1-\cos\theta_s)+|I|^2(1-\cos\theta_i))]^2} \tag{28}$$

$$|V_n(t)|^2 = \frac{2\sigma_N^2|1+2g(|S|^2(1-e^{j\theta_s})+|I|^2(1-e^{j\theta_i}))|^2}{[1+2g(|S|^2(1-\cos\theta_s)+|I|^2(1-\cos\theta_i))]^2} \tag{29}$$

These are the desired signal, the interference signal and the noise powers, respectively.

The Desired Signal-to-Interference Power Ratio at the Array Output (SIR)

From (27) and (28) we get

$$\frac{|S|^2_{out}}{|I|^2_{out}} = \frac{|S|^2}{|I|^2} \cdot F_d$$

where

$$F_d = \frac{\cos^2(\theta_s/2)[1+2g|I|^2\sin\theta_i(\tan(\theta_i/2)-\tan(\theta_s/2))]^2}{\cos^2(\theta_i/2)[1+2g|S|^2\sin\theta_s(\tan(\theta_s/2)-\tan(\theta_i/2))]^2} \tag{30}$$

is the improvement factor which depends on the desired-signal-to-threshold ($g|S|^2 = |S|^2/Pth$) and the interference-to-threshold power ratios, ($g|I|^2=|I|^2/Pth$) as well as on the directions of these signals relative to the direction of constraint (taken to be the broadside direction). Obviously, if the direction of the desired signal is the same as the direction of constraint ($\theta_s=0$), then the

improvement factor becomes

$$F_{do} = \frac{[1+4g|I|^2\sin^2(\theta_i/2)]^2}{\cos^2(\theta_i/2)} \qquad (31)$$

The Desired Signal-to-Noise Power Ratio at the Array Output (SNR)

From (27) and (29) we get

$$\frac{|S|^2_{out}}{Nout} = 2\frac{|S|^2}{\sigma_N^2}\,\frac{\cos^2(\theta_s/2)[1+2g|I|^2\sin\theta_i(\tan(\theta_i/2)-\tan(\theta_s/2))]^2}{1+4gh_1+8g^2h_2} \qquad (32)$$

$$h_1 = |S|^2(1-\cos\theta_s)+|I|^2(1-\cos\theta_i)$$

$$h_2 = |S|^2|I|^2(1+\cos(\theta_i-\theta_s)-\cos\theta_s-\cos\theta_i)+|S|^4(1-\cos\theta_s)+|I|^4(1-\cos\theta_i)$$

PERFORMANCE COMPARISON

We now intend to compare the performance of the directionally constrained interference canceler with the performance of the canceler which utilizes a reference signal loop. First we compare the desired-signal-to-interference power ratio of these two cancelers and then consider their desired-signal-to-noise power ratio

Comparing the Desired-Signal-to-Interference Power Ratio

In doing so we will distinguish between two cases, where the desired signal angle θ_s (relative to the constraint direction) is either small or not small.

For the second case we may notice the following from (30):

(1) If the relative direction between the desired signal and inter-

ference, and the powers of the two signals, are such that the second terms in brackets of both the numerator and denominator of (30) are much larger than one, then one can easily show that

$$F_{d1} = \frac{|I|^4}{|S|^4} \frac{\sin^2(\theta_i/2)}{\sin^2(\theta_s/2)} \tag{33}$$

and that

$$\frac{|S|^2_{out}}{|I|^2_{out}} = \frac{|I|^2}{|S|^2} \frac{\sin^2(\theta_i/2)}{\sin^2(\theta_s/2)} \tag{34}$$

That is, besides the "power inversion" relation we have further improvement in SIR since one might assume $\theta_s < \theta_i$.

(2) If the signals' directions are close and/or the signal's powers are small, such that the second terms in brackets in both the numerator and the denominator of (30) are much smaller than one, then

$$F_{d2} = \frac{\cos^2(\theta_s/2)}{\cos^2(\theta_i/2)} \tag{35}$$

and that

$$\frac{|S|^2_{out}}{|I|^2_{out}} = \frac{|S|^2}{|I|^2} \frac{\cos^2(\theta_s/2)}{\cos^2(\theta_i/2)} \tag{36}$$

That is, we have some improvement due to the assumption that $\theta_s < \theta_i$.
It is reasonable to compare the performance of the directionally constrained canceler in this case (θ_s is not very small) with the performance of the other canceler only when this other canceler operates in the acquisition mode. That is, when the reference loop generates no reference signal. In so doing we first recall (see [3]) that under the condition of (1) and (2) above, the corresponding output desired-signal-to-interference power ratios

of the interference canceler with reference signal are given by

$$(1) \quad \frac{|S|^2_{out}}{|I|^2_{out}} = \frac{|I|^2}{|S|^2}$$

$$(2) \quad \frac{|S|^2_{out}}{|I|^2_{out}} = \frac{|S|^2}{|I|^2}$$

Thus, this last canceler, when it is in acquisition mode, is inferior to the directionally constrained canceler provided the direction of the desired signal is closer to the constraint direction than the direction of the interference signal.

To consider the case where the desired signal angle of arrival θ_s (relative to the constraint) is small, we first write (30) as

$$F_d = \frac{[1+4g|I|^2\sin^2(\theta_i/2)]^2}{\cos^2(\theta_i/2)} \cdot \frac{[1 - \frac{2g|I|^2\sin\theta_i \tan(\theta_s/2)}{(1+4g|I|^2\sin^2(\theta_i/2))}]^2 \cos^2\theta_s/2}{[1+4g|S|^2\sin^2(\theta_s/2)(1-\tan(\theta_i/2)/\tan(\theta_s/2))]^2} \tag{37}$$

In particular, if $4g|I|^2\sin^2(\theta_i/2)$ is much larger than one, then

$$F_d = F_{do} \cdot \frac{\cos^2(\theta_s/2)[1-\tan(\theta_s/2)/\tan(\theta_i/2)]^2}{[1+4g|S|^2\sin^2(\theta_s/2)(1-\tan(\theta_i/2)/\tan(\theta_s/2))]^2} \tag{38}$$

where F_{do} is the improvement factor when $\theta_s = 0$, and the second term represents the change due to a non-zero θ_s (i.e., a non-accurate constraint).

For $\theta_s < \theta_i$, and if θ_s is sufficiently small so that

$$\sin^2(\theta_s/2) + \frac{1}{2\sqrt{2}} \sin\theta_s < 1/4g|S|^2, \tag{39}$$

then the improvement factor in dB is given by (see Appendix A-4)

$$(F_d)_{dB} = 20\log\left[\frac{1+4g|I|^2\sin^2(\theta_i/2)}{\cos\theta_i/2}\right]$$

$$-10\{(\theta_s/2)^2[1+8g|S|^2]+2(\theta_s/2)[1/\tan(\theta_i/2)-4g|S|^2\tan(\theta_i/2)]\} \quad (40)$$

Notice that $(F_d)_{dB}$ is a quadratic function of $\theta_s/2$ which depends on the location of the interference θ_i and the desired-signal-to-threshold power ratio $(g|S|^2)$, but not on the power of the interference. This function has a maximum

$$([F_d]_{dB})m = 20\log\left[\frac{1+4g|I|^2\sin^2(\theta_i/2)}{\cos(\theta_i/2)}\right]+10\frac{[1/\tan(\theta_i/2)-4g|S|^2\tan(\theta_i/2)]}{1+8g|S|^2} \quad (41)$$

at

$$(\theta_s/2)_m = -\frac{[1/\tan(\theta_i/2)-4g|S|^2\tan(\theta_i/2)]}{1+8g|S|^2} \quad (42)$$

That is, depending on whether $|\tan\theta_i/2|$ is greater or less than $1/2\sqrt{g|S|^2}$, $(\theta_s/2)_m$ has the same, or opposite sign as that of θ_i. $\theta_{sm} = 0$ only when these terms are equal.

It is reasonable to compare the performance of the directionally constrained canceler when θ_s is small with the performance of the other canceler (with reference signal loop) operating in the tracking mode. Recalling [3] that the corresponding improvement factor of the interference canceler with reference signal loop is given by

$$F_R = \frac{1+2g|I|^2(1+g|I|^2)(1-\cos(\theta_s-\theta_i))}{1+2g|S|^2f_1+2g|S|^4f_2} \quad (43)$$

where

$$f_1 = 1-\gamma\cos\theta_{sr}-\cos(\theta_s-\theta_i)+\gamma\cos(\theta_{sr}+\theta_i-\theta_s) \quad (44)$$

$$f_2 = (1+\gamma^2-2\gamma\cos\theta_{sr})(1-\cos(\theta_i-\theta_s)) \quad (45)$$

$\gamma e^{j\theta_{sr}}$ is the reference loop filter complex envelope response to the desired signal. That is, we assumed that the desired signal's complex envelope suffers phase shift θ_{sr} and attenuation γ, while the interference signal residue at the output of the loop is small and can be ignored. We may assume without loss of generality that $\theta_s = 0$. For an ideal loop filter we have

$$F_{RO} = 1+2g|I|^2(1+g|I|^2)(1-\cos\theta_i) \tag{46}$$

Therefore, is $\theta_{sr} << \theta_i-\theta_s = \theta_i$ we can write (43), together with (44) and (45),

$$F_R=F_{RO}\ \frac{1}{1+[2g|S|^2(1-\gamma\cos\theta_{sr})+2g^2|S|^4(1+\gamma^2-2\gamma\cos\theta_{sr})](1-\cos\theta_i)} \tag{47}$$

The second factor represents the change in the improvement factor due to a non-ideal filter. If the term in parenthesis in the denominator is smaller than one, we can write for the improvement factor (in dB),

$$(F_R)_{dB} = 10\log[1+2g|I|^2(1+g|I|^2)(1-\cos\theta_i)]$$

$$- 20([g|S|^2(1-\gamma\cos\theta_{sr})+g^2|S|^4(1+\gamma^2-2\gamma\cos\theta_{sr})](1-\cos\theta_i)]) \tag{48}$$

Notice that $(F_R)_{dB}$ is a decreasing function of $\gamma\cos\theta_{sr}$($\gamma<1$) and has its maximum at $\gamma=1$, $\theta_{sr}=0$ (ideal filter). The degradation in performance is steeper when the desired-signal-to-threshold power ($=g|S|^2$) is larger.

Finally, we compare the performance of the two cancelers in the case when the first is accurately constrained and the second has an ideal filter. The corresponding improvement factors are then given by (31) and (46), respectively. Under these conditions, the first has better desired-signal-to-interference power ratio if and only if

$$\frac{(1+4g|I|^2\sin^2(\theta_i/2))^2}{\cos^2(\theta_i/2)} > 1+2g|I|^2(1+g|I|^2)(1-\cos\theta_i) \qquad (49)$$

In Appendix A-5 we show that for the validation of (49) we might distinguish between two regions of the location of the interference signal's direction;

1) $|\tan(\theta_i/2)| \geq 1/2$ then (49) is satisfied for any interference-to-threshold power ratio; however, it,

2) $|\tan(\theta_i/2)| < 1/2$ then (49) is satisfied, and the "accurately constrained" canceler performs better than the interference canceler with "ideally filtered" reference loop, only if

$$g|I|^2 \leq \frac{2-\cos^2(\theta_i/2)+\sqrt{\cos^2(\theta_i/2)+\cos^4(\theta_i/2)}}{2[5\cos^2(\theta_i/2)-4]} \qquad (50)$$

Now, one can easily show that for $-1/2 \leq \tan(\theta_i/2) \leq 1/2 (1 \geq \cos^2(\theta_i/2) \geq 4/5)$ the left-hand side of (50) is a decreasing function of $\cos^2(\theta_i/2)$. Therefore, the interference-to-threshold power must be bounded above by an increasing function of $|\theta_i|$. In particular, for $\theta_i = 0$, (50) becomes

$$g|I|^2 \leq 1{,}207 \qquad (51)$$

In Figure 6 we sketch the different regions of superiority of each canceler as a function of θ_i.

To see the level of superiority one canceler has relative to the other, we write from (31) and (46)

$$F_{do}/F_{Ro} = \frac{[1+4g|I|^2\sin^2(\theta_i/2)]^2}{\cos^2(\theta_i/2)[1+4g|I|^2(1+g|I|^2)\sin^2(\theta_i/2)]} \qquad (52)$$

$$(F_{do}/F_{Ro})_{dB} = 20\log[1+4g|I|^2\sin^2(\theta_i/2)]$$

$$-10\log[1+4g|I|^2(1+g|I|^2\sin^2(\theta_i/2)]-20\log[\cos(\theta_i/2)] \quad (53)$$

Comparing the Desired Signal-to-Noise Ratio

From (32) and (A-31) we write

$$\frac{|S|^2_{out}}{Nout} \geq 2\frac{|S|^2}{\sigma_N^2}\,\frac{\cos^2(\theta_s/2)[1+2g|I|^2\sin\theta_i(\tan(\theta_i/2)-\tan(\theta_s/2)]^2}{1+4g[(|S|^2(1-\cos\theta_s)+|I|^2(1-\cos\theta_i))(1+2g(|I|^2+|S|^2)]} \quad (54)$$

If the desired signal angle θ_s is not so small, and the relative directions between the desired signal and interference as well as their powers are such that the second terms in the bracket of both the numerator and the denominator of (54) are much less than one, then

$$\frac{|S|^2_{out}}{N_{out}} \geq 2\,\frac{|S|^2}{\sigma_N^2}\cos^2(\theta_s/2) \quad (55)$$

On the other hand, if these terms in the brackets are much greater than one, then

$$\frac{|S|^2_{out}}{N_{out}} \geq 2\,\frac{|S|^2}{\sigma_N^2}\cdot\frac{|I|^4\sin^2(\theta_i/2)\sin^2(\theta_i/2-\theta_s/2)}{[|I|^2+|S|^2][|S|^2\sin^2(\theta_s/2)+|I|^2\sin^2(\theta_i/2)]} \quad (56)$$

$$= \frac{|S|^2}{\sigma_N^2}(1-\cos(\theta_i-\theta_s)) \qquad |I| >> |S|,\ \theta_s<\theta_i$$

$$= \frac{|S|^2}{\sigma_N^2}\frac{|I|^4}{|S|^4}(1-\cos(\theta_i-\theta_s)) \qquad |S| << |I|,\ \theta_i<\theta_s$$

Except for the factor $\cos^2(\theta_s/2)$ in (55), these are the same results as the ones obtained with the interference canceler with reference signal loop when

it operates in the acquisition mode [3].

For the case when θ_s is small, and in particular with $\theta_s=0$, (32) becomes (see also (A-30))

$$\frac{|S|^2_{out}}{N_{out}} = 2\frac{|S|^2}{\sigma_N^2}\frac{[1+4g|I|^2\sin^2(\theta_i/2)]^2}{1+8g|I|^2(1+2g|I|^2)\sin^2(\theta_i/2)} \tag{57}$$

If $2g|I|^2\sin^2(\theta_i/2) >> 1$, then

$$\frac{|S|^2_{out}}{N_{out}} = 2\frac{|S|^2}{\sigma_N^2}\sin^2(\theta_i/2)$$

$$= \frac{|S|^2}{\sigma_N^2}(1-\cos\theta_i) \tag{58}$$

Therefore, when the direction of arrival is such that $|\cos\theta_i|<<1$, the output SNR is approximately equal the input SNR regardless of the desired signal power. It degrades when $\cos\theta_i$ approaches one. This result is the same as the one obtained for the interference canceler with reference signal loop when it operates in the tracking mode [3].

CONCLUSION

For the two-element array directionally constrained canceler we establish the dependence of the SIR and SNR on the STR and the ITR power ratios as well as on the directions of arrival of the desired signal and interference relative to the direction of constraint (assumed zero). From this we obtained the improvement factor in STR and SNR. Two modes of operation were distinguished. Firstly, we took the direction of arrival of the desired signal to be far away from that of the constraint direction (θ_s is sufficiently large) and found the improvement factor in SIR for the

extreme conditions when both signal powers are large or both are small. Secondly, assuming the desired signal's direction of arrival is sufficiently close to the constraint direction (θ_s is small), we establish the sensitivity of the performance of this canceler to the inaccuracy in constraint ($\theta_s \neq 0$). We found that for sufficiently small θ_s the improvement factor (in dB) is quadratic in θ_s with a maximum at a point which might differ from $\theta_s = 0$ (accurately constrained). Depending on the direction of arrival of the interference and on the STR, this maximum may occur when the desired signal's direction, θ_{sm}, has the same or opposite sign (the direc- of constraint is taken to be at zero) as that of the interference direction.

In comparing the performance of the "directionally constrained canceler with that of the "LMS canceler," firstly, in relating the first canceler when θ_s is sufficiently large to the second canceler operating in the acquisition mode, it was shown that in both extreme power conditions (large or small signals powers), the first canceler is superior. Secondly, we related the first canceler when θ_s is small to the second canceler operating in the tracking mode. In particular, special attention was paid to the ideal case of both cancelers; namely, the first canceler accurately constrained and the second canceler having an ideally filtered reference loop. It was found that the directionally constrained canceler performs better with any ITR only if the interference direction of arrival is such that $|\tan\theta_1/2 \geq 1/2$ (off-main-beam interference). If, however, the interference gets closer (in main-beam interference) then the directionally constrained canceler is preferred only if the ITR is smaller than a certain value. This value becomes smaller and smaller when the interference direction of arrival gets closer and closer to the constraint direction.

This behavior suggests complementary properties of the two cancelers, so that still better performance can be obtained if we use both directional (directionally constrained) and spatial (reference loop) information of the desired signal. The SNR performances of both cancelers are found to be quite similar.

APPENDICES

C-1

Using (17) and (1) we have

$$\overline{Y_1^*(t)Y_1(t)} = \overline{|[S_1(t)-S_2(t))+(I_1(t)-I_2(t))+(N_1(t)-N_2(t))]|^2}$$

$$= \overline{|S_1(t)-S_2(t)|^2} + \overline{|I_1(t)-I_2(t)|^2} + \overline{|N_1(t)-N_2(t)|^2}$$

$$= |S_1-S_2|^2 + |I_1-I_2|^2 + 2\sigma_N^2 \qquad \text{(C-1)}$$

where from (3) and (4) we assumed that $\overline{|s(t)|^2} = 1$, $\overline{|i(t)|^2} = 1$; and that the signals and noise processes are mutually uncorrelated.

Similarly, from (16) and (17)

$$\overline{Y_1^*(t)Y_0(t)} = [(S_1(t)-S_2(t)) + (I_1(t)-I_2(t) + N_1(t)-N_2(t))]^*$$

$$\cdot [(S_1(t)+S_2(t)) + (I_1(t)+I_2(t)) + (N_1(t)+N_2(t))]$$

$$= (S_1-S_2)^*(S_1+S_2) + (I_1-I_2)^*(I_1+I_2) \qquad \text{(C-2)}$$

The noise terms cancel out since we assumed $\sigma_{N_1}^2 = \sigma_{N_2}^2$.

C-2

Substituting for $Y_1(t)$ from (16) together with (1), and for W_y from (19) we obtain

$$Y_1(t)W_y = \frac{-g[S_1-S_2)^*(S_1+S_2)+(I_1-I_2)^*(I_1+I_2)]}{1+g(|S_1-S_2|^2+|I_1-I_2|^2)}$$

$$[(S_1(t)-S_2(t)) + (N_1(t)-N_2(t))+ (I_1(t)-I_2(t))]$$

$$= \frac{-g[|S_1-S_2|^2(S_1(t)+S_2(t))+(I_1-I_2)^*(I_1+I_2)(S_1(t)-S_2(t))]}{1+g(|S_1-S_2|^2+|I_1-I_2|^2}$$

$$\frac{-g[|I_1-I_2|^2(I_1(t)+I_2(t))+(S_1-S_2)^*(S_1+S_2)(I_1(t)-I_2(t)]}{1+g(|S_1-S_2|^2+|I_1-I_2|^2}$$

$$\frac{-g[(S_1-S_2)^*(S_1+S_2)+(I_1-I_2)^*(I_1+I_2)](N_1(t)-N_2(t))}{1+g(|S_1-S_2|^2+|I_1-I_2|^2} \quad \text{(C-3)}$$

Together with (17) and (1) we have, after simple algebraic manipulation

$$Y_o(t)+Y_1(t)W_y = \frac{(1+g|I_1-I_2|^2)(S_1(t)+S_2(t))-g(I_1-I_2)^*(I_1+I_2)(S_1(t)-S_2(t))}{1+g(|S_1-S_2|^2+|I_1-I_2|^2)}$$

$$+ \frac{(1+g|S_1-S_2|^2)(I_1(t)+I_2(t))-g(S_1-S_2)^*(S_1+S_2)(I_1(t)-I_2(t))}{1+g(|S_1-S_2|^2+|I_1-I_2|^2)}$$

$$+ N_1(t)+N_2(t)- \frac{g[(S_1-S_2^*)(S_1+S_2)+(I_1-I_2)^*(I_1+I_2)](N_1(t)-N_2(t))}{1+g(|S_1-S_2|^2+|I_1-I_2|^2)}$$

$$= \frac{S_1(t)[1+2g(|I_2|^2-I_1^*I_2)]+S_2(t)[1+2g(|I_1|^2-I_2^*I_1)]}{1+g(|S_1-S_2|^2+|I_1-I_2|^2)}$$

$$+ \frac{I_1(t)[1+2g(|S_2|^2-S_1^*S_2)]+S_2(t)[1+2g(|S_1|^2-S_2^*S_1)]}{1+g(|S_1-S_2|^2+|I_1-I_2|^2)}$$

$$+ \frac{N_1(t)[1+2g(|S_2|^2-S_1^*S_2+|I_2|^2-I_1^*I_2)]+N_2(t)[1+2g(|S_1|^2-S_2^*S_1+|I_1|^2-I_2^*I_1)]}{1+g(|S_1-S_2|^2+|I_1-I_2|^2)} \quad \text{(C-4)}$$

Using (3) and (23)

$$S_1(t)+S_2(t) = s(t)|S|(e^{j\theta_{s_1}} + e^{j\theta_{s_2}})$$

$$= 2s(t)|S|\, e^{\frac{j}{2}(\theta_{s_1}+\theta_{s_2})} \cos(\theta_s/2) \qquad \text{(C-5)}$$

$$I_1^* I_2 S_1(t) = s(t)|S|e^{j\theta_{s_1}}|I|^2 e^{j(\theta_{i_2}-\theta_{i_1})}$$

$$= s(t)|S||I|^2 e^{\frac{j}{2}(\theta_{s_1}+\theta_{s_2})}\, e^{j(\frac{\theta_s}{2} - \theta_i)}$$

where we also used (24). Also

$$I_2^* I_1 S_2(t) = s(t)|S||I|^2 e^{\frac{j}{2}(\theta_{s_1}+\theta_{s_2})}\, e^{j(\theta_i - \frac{\theta_s}{2})}$$

Hence,

$$I_1^* I_2 S_1(t)+I_2^* I_1 S_2(t) = 2s(t)|S||I|^2 e^{\frac{j}{2}(\theta_{s_1}+\theta_{s_2})} \cos(\theta_i-\theta_s/2) \qquad \text{(C-6)}$$

Similarly,

$$I_1(t)+I_2(t) = 2i(t)|I||S|^2 e^{\frac{j}{2}(\theta_{i_1}+\theta_{i_2})} \cos(\theta_i/2) \qquad \text{(C-7)}$$

$$S_1^* S_2 I_1(t)+S_2^* S_1 I_2(t) = 2i(t)|I||S|^2 e^{\frac{j}{2}(\theta_{i_1}+\theta_{i_2})} \cos(\theta_s-\theta_i/2) \qquad \text{(C-8)}$$

Also

$$|S|^2-S_1^* S_2 = |S|^2(1-e^{-j\theta_s}) \qquad \text{(C-9)}$$

$$|I|^2-I_1^* I_2 = |I|^2(1-e^{-j\theta_i}) \qquad \text{(C-10)}$$

$$|S_1-S_2|^2 = 2|S|^2(1-\cos\theta_s) \qquad \text{(C-11)}$$

$$|I_1-I_2|^2 = 2|I|^2(1-\cos\theta_i)$$

Equation (38) can be written in the form

$$F_d = F_{do} \cdot L_d \qquad \text{(C-13)}$$

where L_d represents the change in the improvement factor due to a non-zero θ_s (i.e., non-accurate constraint). This change in improvement factor can be written (in dB) as

$$(L_d)_{dB} = 20\log\cos(\theta_s/2)+20\log(1-a_1)-20\log(1+a_2) \qquad \text{(C-14)}$$

where

$$a_1 = \frac{\tan(\theta_s/2)}{\tan(\theta_i/2)} \qquad \text{(C-15)}$$

$$a_2 = 4g|S|^2\sin^2(\theta_s/2)(1-\tan(\theta_i/2)/\tan(\theta_s/2)) \qquad \text{(C-16)}$$

For $|\theta_s| < |\theta_i|$ $|a_1| < 1$. Also, one can easily show that for $|a_2| < 1$ it is sufficient to require that θ_s be small enough to satisfy

$$\sin^2(\theta_s/2) + \frac{1}{2\sqrt{2}}\sin\theta_s < 1/4g|S|^2 \qquad \text{(C-17)}$$

where we took $|\theta_i| < \pi/2$.

Under these conditions we can use the series representation of $\log(1-a_1)$, $\log(1+a_2)$, and $\log\cos(\theta_s/2)$ and write

$$(L_d)_{dB} = -20[\frac{(\theta_s/2)^2}{2} + \frac{(\theta_s/2)^4}{12} + \ldots] -20[\frac{\tan\theta_s/2}{\tan\theta_i/2} + \frac{\tan^2\theta_s/2}{\tan^2\theta_i/2} + \cdots]$$
$$-20[a_2 - \frac{a_2^2}{2} + \ldots] \qquad \text{(C-18)}$$

To a first approximation the change in improvement as a result of a non-accurate constraint is given by

$$(L_d)_{dB} \approx -20[\frac{(\theta_s/2)^2}{2} + \frac{\tan\theta_s/2}{\tan\theta_i/2} + 4g|S|^2\sin^2(\theta_s/2)(1-\tan(\theta_i/2)/\tan(\theta_s/2))] \quad \text{(C-18)}$$

Since θ_s is small, $\sin(\theta_s/2) \approx \tan(\theta_s/2) \approx \theta_s/2$, (A-18) can be written as

$$[L_d]_{dB}/-10 = (\theta_s/2)^2[1+8g|S|^2]+2(\theta_s/2)[1/\tan(\theta_i/2)-4g|S|^2\tan(\theta_i/2)] \quad \text{(C-19)}$$

The left-hand term of (A-19) has a minimum at

$$\theta_{sm}/2 = -\frac{[1/\tan(\theta_i/2)-4g|S|^2\tan(\theta_i/2)]}{1+8g|S|^2} \quad \text{(C-20)}$$

The value of this minimum is

$$([L]_{dB}/-10)_m = -\frac{[1/\tan(\theta_i/2)-4g|S|^2\tan(\theta_i/2)]^2}{1+8g|S|^2} \quad \text{(C-21)}$$

C-5

Using trigonometric relations we write (49) as

$$\frac{[1+2g|I|^2(1-\cos\theta_i)]^2}{(1+\cos\theta_i)/2} > 1+2g|I|^2(1+g|I|^2)(1-\cos\theta_i)$$

$$1+4g|I|^2(1-\cos\theta_i)+4g^2|I|^4(1-\cos\theta_i)^2 > \frac{1+\cos\theta_i}{2}[1+2g|I|^2(1+g|I|^2)(1-\cos\theta_i)] \quad \text{(C-22)}$$

Arranging terms we get

$$g^2|I|^4(1-\cos\theta_i)^2[4-\frac{1-\cos^2\theta_i}{(1-\cos\theta_i)^2}]+2g|I|^2(1-\cos\theta_i)[2-\frac{1+\cos\theta_i}{2}]$$

$$+\frac{1}{2}(1-\cos\theta_i) > 0$$

Or

$$ax^2 + bx + c > 0 \quad \text{(C-23)}$$

where

$$x = g|I|^2(1-\cos\theta_i) \geq 0 \quad \text{(C-24)}$$

$$a = 4 - \frac{1+\cos\theta_i}{1-\cos\theta_i} = 4 - \cot n^2(\theta_i/2) \qquad \text{(C-25)}$$

$$b = 2[2 - \frac{1+\cos\theta_i}{2}] = 2(2-\cos^2(\theta_i/2)) \qquad \text{(C-26)}$$

$$c = \frac{1}{2}(1-\cos\theta_i) = \sin^2(\theta_i/2) \qquad \text{(C-27)}$$

Thus,

$$(\frac{b}{2})^2 - ac = (2-\cos^2(\theta_i/2))^2 - \sin^2(\theta_i/2)[4-\cot n^2\ \frac{\theta_i}{2}]$$

$$= \cos^4(\theta_i/2) + \cos^2(\theta_i/2) \qquad \text{(C-28)}$$

We are looking for a positive solution x of (A-23). Notice that $c \geq 0$; therefore,

1) if $a \geq 0$ or $|\tan(\theta_i/2)| \geq 1/2$, then every $x \geq 0$. (C-23) is satisfied, however,

2) if $a \leq 0$ or $\tan(\theta_i/2) \leq 1/2$, then it is easy to show that only when

$$x = g|I|^2(1-\cos\theta_i) \leq \frac{-(2-\cos^2(\theta_i/2) - \sqrt{\cos^4(\theta_i/2)+\cos^2(\theta_i/2)})}{4-\cot n^2(\theta_i/2)}$$

(C-23) is satisfied. Or, equivalently, if

$$g|I|^2 < \frac{2-\cos^2(\theta_i/2) + \sqrt{\cos^2(\theta_i/2)+\cos^4(\theta_i/2)}}{2(5\cos^2(\theta_i/2) - 4)} \qquad \text{(C-29)}$$

C-6

From (32)

$$|1+2g|S|^2(1-e^{j\theta_s})+|I|^2(1-e^{j\theta_i}))|^2$$

$$= 1+4g(|S|^2(1-\cos\theta_s)+|I|^2(1-\cos\theta_i))+8g^2[|S|^2|I|^2(1+\cos(\theta_s-\theta_i)-\cos\theta_i-\cos\theta_s)$$

$$+ |S|^4(1-\cos\theta_s)+|I|^4(1-\cos\theta_i)] \qquad \text{(C-30)}$$

$$= 1+4g(|S|^2(1-\cos\theta_s)+|I|^2(1-\cos\theta_i)$$

$$[1+2g\ \frac{|S|^2|I|^2(1+\cos(\theta_s-\theta_i)-\cos\theta_i-\cos\theta_s)+|S|^4(1-\cos\theta_s)+|I|^4(1-\cos\theta_i)}{|S|^2(1-\cos\theta_s)+|I|^2(1-\cos\theta_i)}$$

$$\leq 1+4g(|S|^2(1-\cos\theta_s)+|I|^2(1-\cos\theta_i))[1+2g(|S|^2+|I|^2] \quad \text{(C-31)}$$

REFERENCES

[1] Y. Bar-Ness and J. Rokach, Cross-Coupled Boot-Strapped Interference Canceler," UP-VFRC-14-80, July 1980.

[2] R.T. Compton, "An Adaptive Array in Spread-Spectrum Communication," Proc. IEEE, Vol. 66, March 1978, p. 289.

[3] Y. Bar-Ness, "Performance Analysis of Interference Canceler with Reference Signal Loop," UP-VFRC-21-80, October 1980.

[4] B. Widrow, J. McCool and J. Ball, "The Complex LMS Algorithm," Proc. IEEE, Vol. 63, April 1975, pp. 719-720.

[5] S.P. Applebaum and D.J. Chapman, "Adaptive Array with Main Beam Constraints," IEEE Trans. Antennas and Propagation, Vol. AP-24, No. 5, September 1976.

[6] Y. Bar-Ness, "Multi-Element, Multi-Signal Widrow Based Power Inversion Processor;" In preparation.

[7] Y. Bar-Ness, "The Ripple Minimization Problems in Sampled Data Systems," Int. J. Control, Vol. 22, 1975, pp. 49-56.

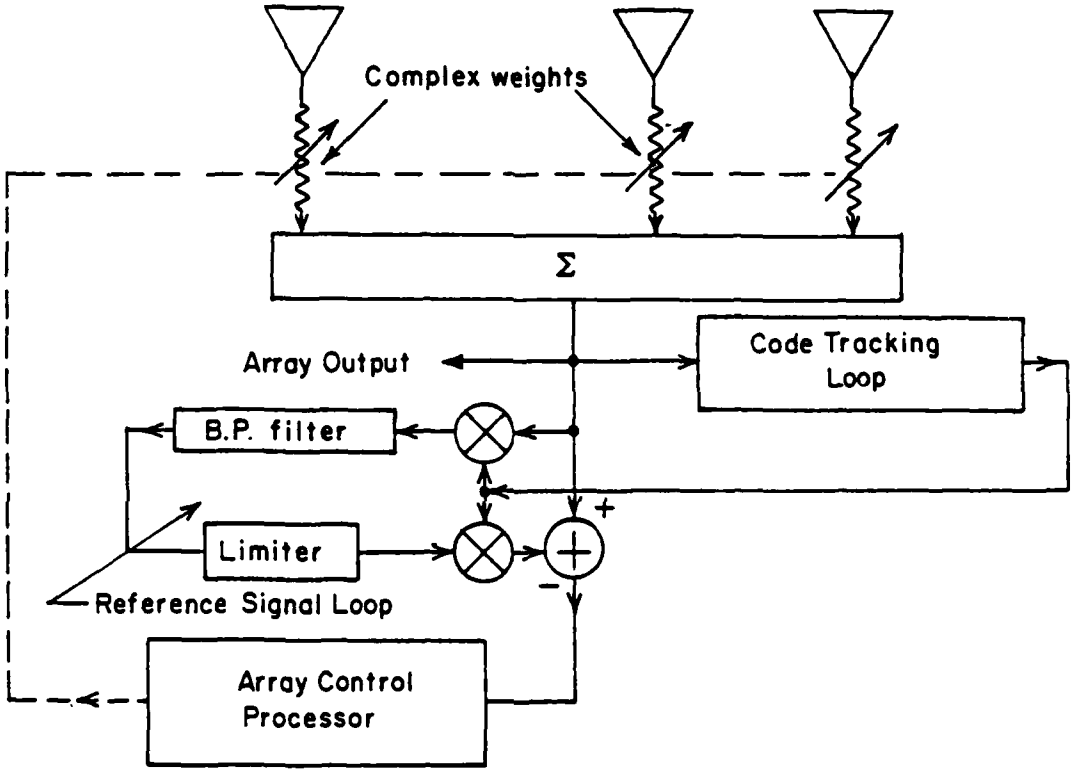

Figure 1 The LMS Adaptive Array with Coded Reference Signal Loop for Spread Spectrum Communication

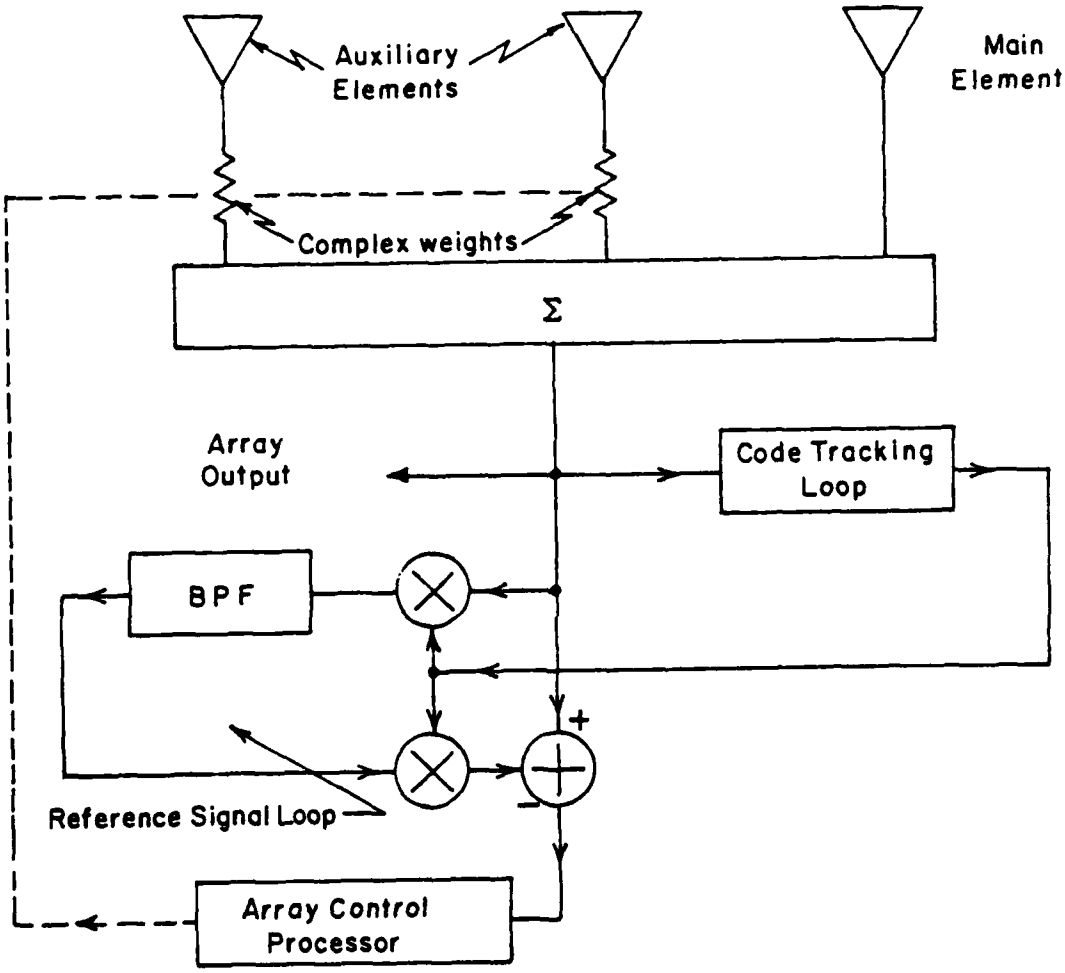

Figure 2 The LMS Interference Canceler With Coded Reference Signal Loop for Spread Spectrum Communications

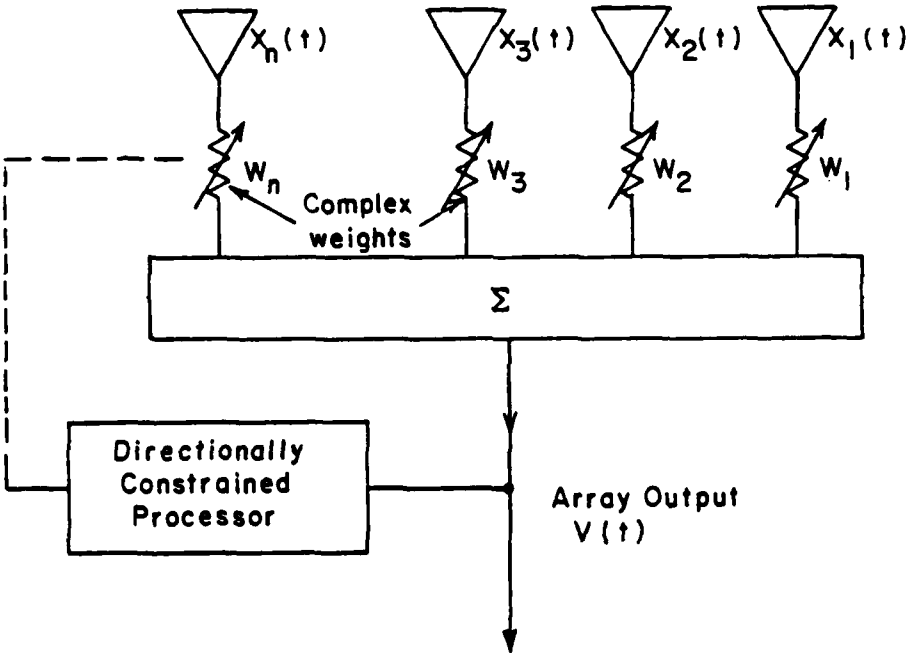

Figure 3 Directionally Constrained Interference Canceler

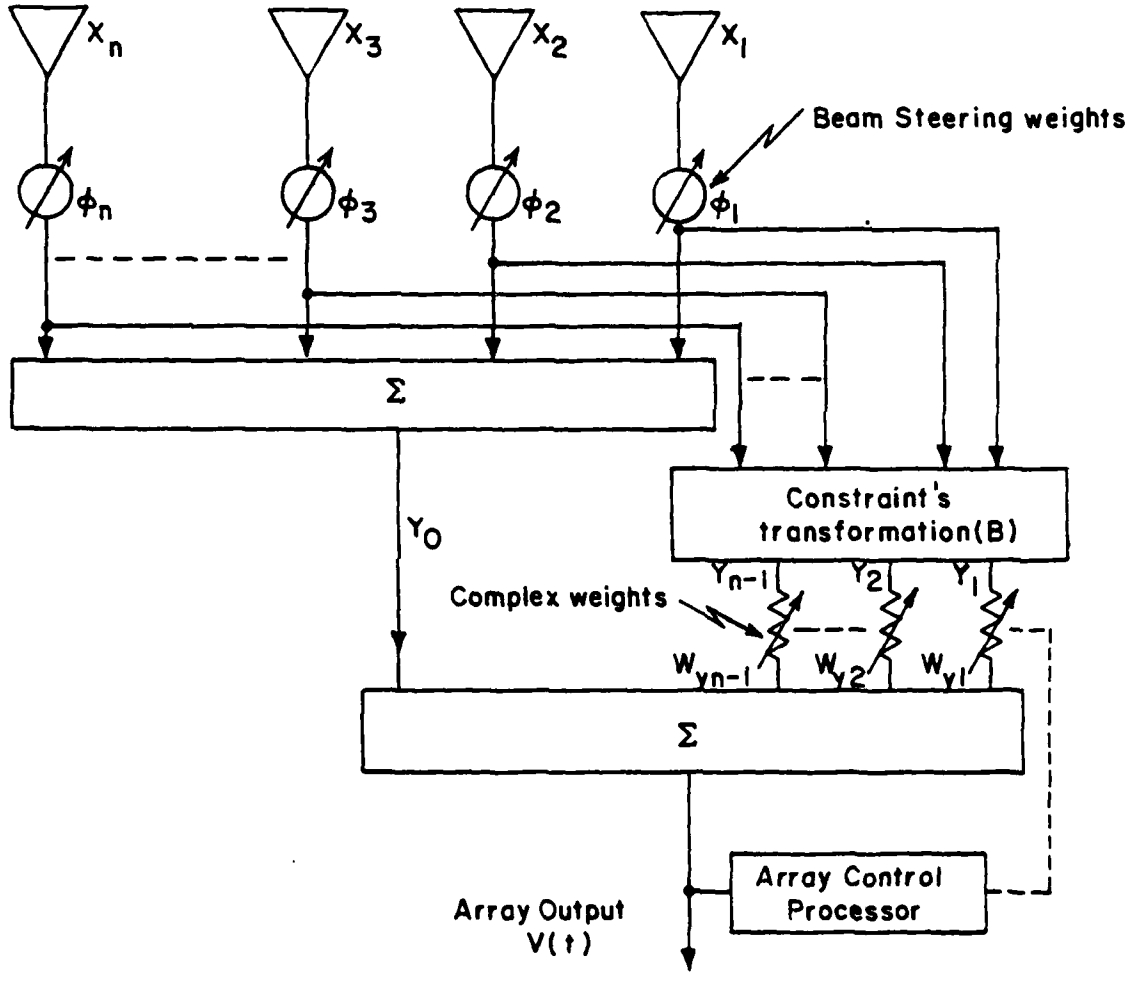

Figure 4 Adaptive Array with Directional Constraint

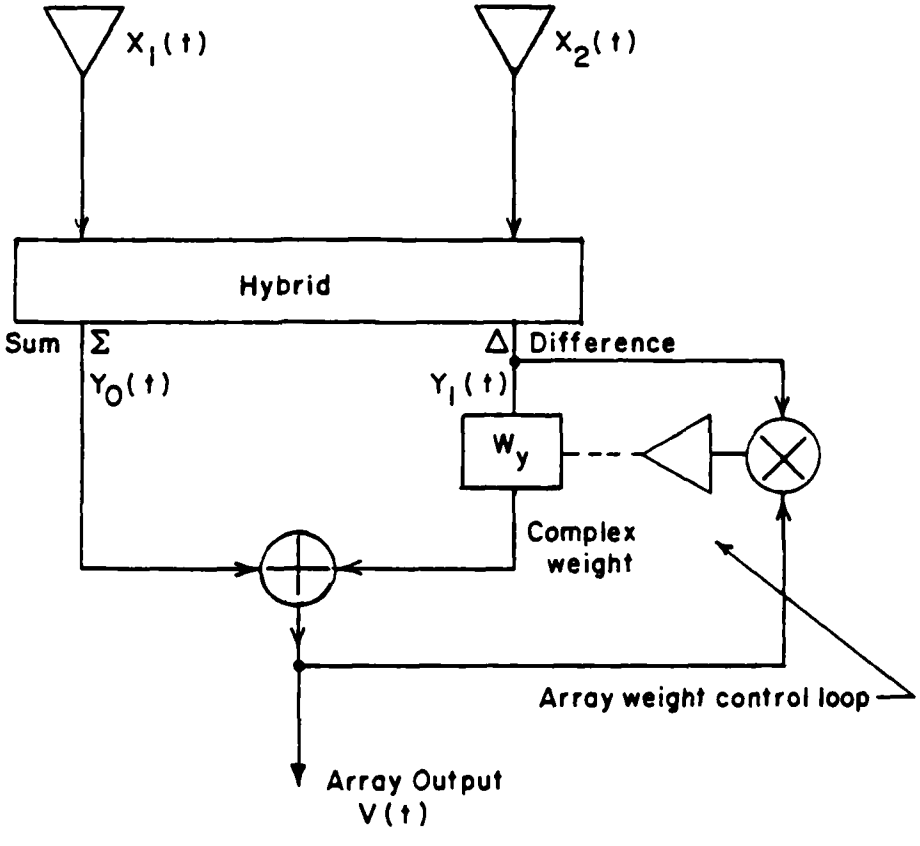

Figure 5 Two-element Interference Canceler With Directional Constraint

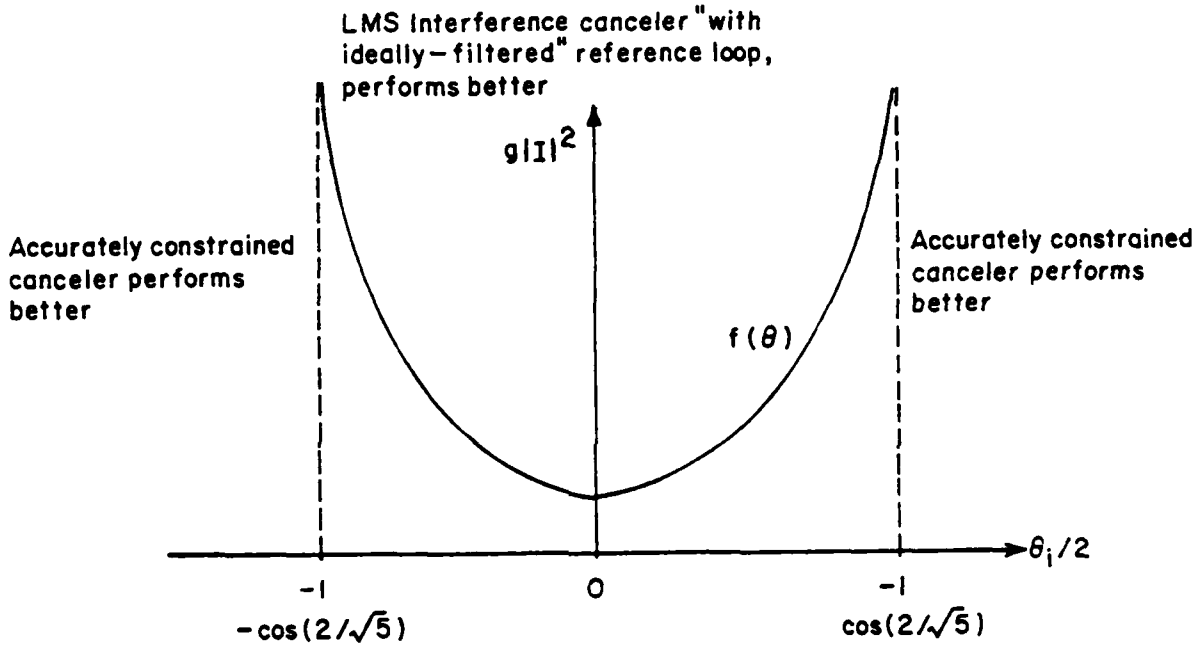

Figure 6 Regions of Superiority of Performance

APPENDIX D

EFFECT OF POINTING ERROR ON A DIRECTIONALLY-CONSTRAINED ADAPTIVE ARRAY

Fred Haber, Paul Yeh

Valley Forge Research Center
The Moore School of Electrical Engineering
University of Pennsylvania
Philadelphia, Pennsylvnaia

EFFECT OF POINTING ERROR ON A DIRECTIONALLY-CONSTRAINED ADAPTIVE ARRAY

We are here concerned with a satellite-borne adaptive array for the uplink of a communication satellite serving widely scattered multiple users. Ground positions will be known, at least approximately, making it reasonable to consider a directionally constrained adaptive algorithm such as that described by Applebaum and Chapman [1]. Of concern, however, is the effect of pointing error, which may arise because of imperfect knowledge of ground position, or because of error in determining satellite orientation, or because of diffraction effects. An investigation of the sensitivity of the signal-to-interference-plus-noise ratio (SINR) to error of this kind in the case of the Applebaum array with zero-order directional constraint, was carried out and is here reported.

The analysis was based on a linear array with randomly deployed elements. For numerical results a 10-wavelength array was used, both filled and sparse. The array structure apt to be used in the final application is likely to be different both in form and size, but the phenomena under study is expected to follow a similar pattern.

The array processor is shown in one of its forms in Figure 1. If the array were linear, as shown in Figure 2, and if a desired signal were arriving from direction θ_d, the induced voltage in the ith element would be the real part of

$$v_i(t) = \alpha(t+\tau_i)e^{j[\omega_c(t+\tau_i) + \phi]} \qquad (1)$$

where $\tau_i = x_i\cos\theta_d/c$, c is the propagation speed along the ray path, $\alpha(t)$

[1] S.P. Applebaum and D.J. Chapman, "Adaptive Array with Main Beam Constraints," IEEE Trans. Anntenas and Propag., Vol. AP-26, September 1976.

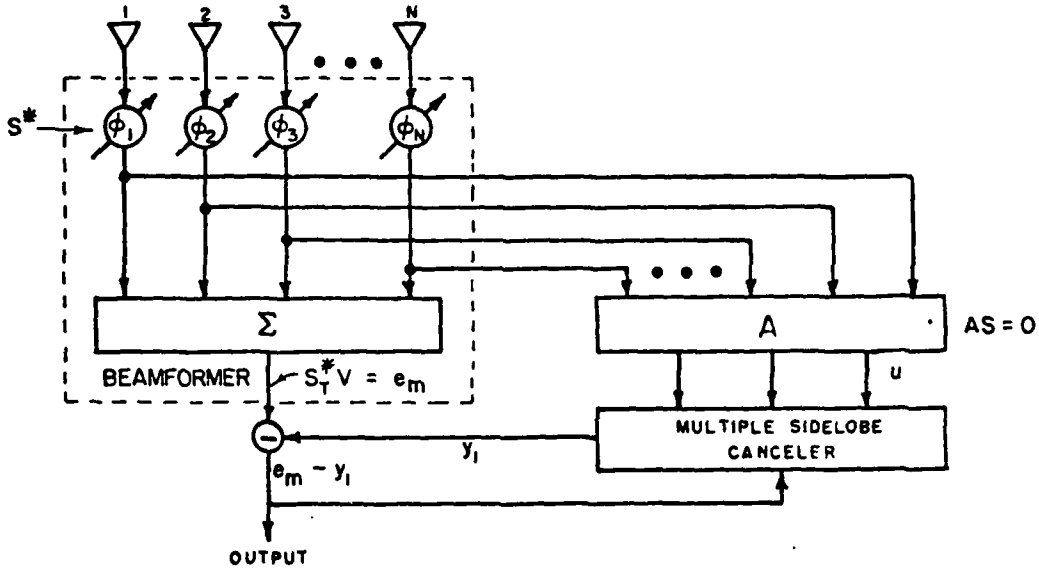

FIGURE 1 DIRECTIONALLY CONSTRAINED ARRAY PROCESSOR

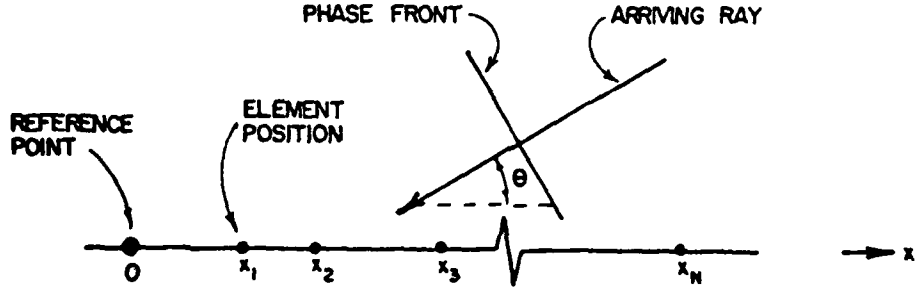

FIGURE 2 LINEAR ARRAY GEOMETRY

is the complex baseband signal, ω_c is the radian carrier frequency, ϕ is the carrier phase at the reference point, and x_i is the position of the ith element relative to a reference point (origin).

The signal at the reference point itself is taken to be

$$v_o(t) = \alpha(t) e^{j(\omega_c t + \phi)} \tag{2}$$

In this work the baseband signal $\alpha(t)$ is assumed to be of narrow bandwidth, changing only slightly in the interval τ_i for all i = 1,2,...N. Thus, we assume $\alpha(t+\tau_i) = \alpha(t)$ and

$$v_i(t) = \alpha(t) e^{jkx_i\cos\theta_d} e^{j(\omega_c t+\phi)}$$

$$= v_i(t) e^{j(\omega_c t+\phi)} \quad , \; i = 1,2,...N \tag{3}$$

where $k = 2\pi/\lambda = \omega_c/c$.

In the following we work explicitly with the complex coefficient $v_i(t)$, suppressing the carrier factor $e^{j(\omega_c t+\phi)}$. Furthermore, these N complex quantifiers are represented by the vector $\underline{v} = (v_1(t), v_2(t), \ldots v_N(t))$. Noise and interference are similarly treated.

The beamformer part of the processes is comprised of a set of phase shifters and an adder which acts to form $e_m = \underline{S}^{T*}\underline{v}$ where S is a pointing vector (T^* signifies transpose conjugate) given by

$$\underline{S} = \begin{bmatrix} e^{jkx_1\cos\theta} \\ e^{jkx_2\cos\theta} \\ \vdots \\ e^{jkx_N\cos\theta} \end{bmatrix} \tag{4}$$

θ is the beam pointing direction. If $\theta = \theta_d$, the direction of the desired signal arrival $e_m = N\alpha(t)$.

Simultaneously, the phase shifted signals are applied through an Nx(N-1) matrix transformer A, chosen such that $A\underline{S} = \underline{0}$, to a multiple side-lobe canceler. The matrix transformer forms a set of (N-1) outputs which contain no signal from the pointing direction. If the signal magnitude is the same at each element, this device only needs to form

$$v_i S_i^* - v_{i+1} S_{i+1}^* \quad , \quad i = 1, 2 \ldots (N-1) \tag{5}$$

The multiple sidelobe canceler (see Applebaum [1], Figure 1) acts to form cancelling signals to those inputs arriving from directions other than the pointing direction θ. Applebaum points out that the scheme approaches the maximum SINR combiner defined by

$$v_o = \underline{v}^T \underline{W} \tag{6}$$

where

$$W = \frac{M^{-1} \underline{S}^*}{\underline{S}^T M^{-1} S^*} \tag{7}$$

and M is the covariance matrix of the complex signals arriving at each element; that is,

$$M = < v^* \; v^T > \tag{8}$$

The SINR at the array processor output is

$$SINR = <|\alpha^2|> \underline{S}^T \, M^{-1} \, \underline{S}^* \tag{9}$$

where $|\alpha^2|$ is the mean square power at each sensor, provided the desired signal arrives from the pointing direction.

Now, if the pointing direction is different from the arrival direction of the desired signal the SINR will be less than that given by (9). An expression for the SINR in this case is now obtained. With $\theta = \theta_d$, the desired signal arrival direction, and $\theta = \theta_{Ik}$, the k^{th} undesired signal direction we define direction vectors $\underline{S}_d$ and $\underline{S}_{Ik}$. Also defining a noise vector $\underline{\eta}$ of independent components, we have

$$M = <|\{[\alpha S_d + \sum_{k=1}^{K} \beta_k \underline{S}_{Ik} + \underline{\eta}]^* \, [\alpha \underline{S}_d + \sum_{k=1}^{K} \beta_k \underline{S}_{Ik} + \underline{\eta}]^T\}>$$

$$= <|\alpha^2|> \, M_d + \sum_{k=1}^{K} <|\beta_k|^2> \, M_{Ik} + \sigma^2 \, I \tag{10}$$

where $Md = \underline{S}_d^* \, \underline{S}_d^T$

$$M_{Ik} = \underline{S}_{Ik}^* \, \underline{S}_{Ik}^T$$

AD-A113 381 INTERSPEC INC PHILADELPHIA PA F/G 20/14
APPLICATION OF SELF-ORGANIZING RANDOM ARRAYS TO COMMUNICATION S--ETC(U)
FEB 82 F HABER, Y BAR-NESS, B D STEINBERG F30602-80-C-0230
UNCLASSIFIED RADC-TR-81-248 NL

END
DATE FILMED
04-82
DTIC

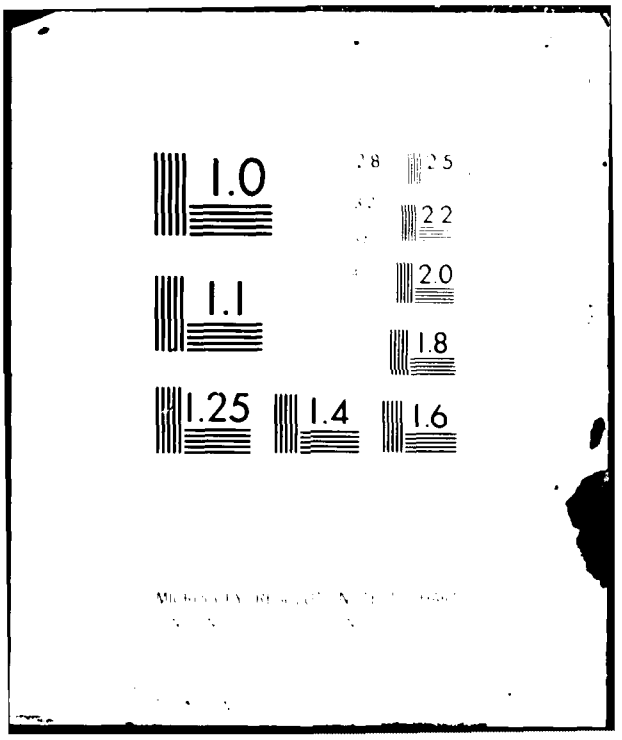
1.0
1.1
1.25
1.4
1.6
2.0
1.8
2.2
2.5

$\langle|\beta_k^2|\rangle$ = mean interference power of the k^{th} interferer at each sensor

σ^2 = noise power at each sensor

and the β_k for the K interferers are independent complex random processes.

θ and the corresponding pointing vector $\underline{S}$ (without subscript) will refer to an arbitrary pointing direction and

$$W = C\, M^{-1} S^* \quad \text{(restatement of (7))}$$

will represent the equivalent weights generated by the processor when pointing in the direction θ. $C = (S^T M^{-1} S^*)^{-1}$ is a constant for a given pointing angle. The output power of a desired signal arriving from direction θ_d is

$$P_d = \langle(\underline{W}^T \alpha \underline{S}_d)^* (\alpha \underline{S}_d^T \underline{W})\rangle = \langle\alpha^2\rangle C^2 \underline{S}^T M^{-1} M_d M^{-1} \underline{S}^* \tag{11}$$

Similarly the output interference power of the k^{th} interferer is

$$P_{Ik} = \langle\beta_k^2\rangle C^2 \underline{S}^T M^{-1} M_{Ik} M^{-1} S^* \tag{12}$$

and the output noise power is

$$P_N = \sigma^2 C^2 \underline{S}^T M^{-1} IM^{-1} S^* \tag{13}$$

the output SINR is

$$\text{SINR} = \frac{\langle\alpha^2\rangle \underline{S}^T M^{-1} M_d M^{-1} \underline{S}^*}{\sum_{k=1}^{K} \langle\beta_k^2\rangle \underline{S}^T M^{-1} M_{Ik} M^{-1} \underline{S}^* + \sigma^2 S^T (M^{-1})^2 S^*} \tag{14}$$

Equation (14) has been used to calculate the SINR for a number of specific cases as described below.

(a) Filled Array.

An equally-spaced-element linear array was assumed; the interspace between elements is $\frac{\lambda}{2}$ and the beamwidth of this array is approximately $\frac{\lambda}{L} = \frac{1}{10}$ rad $\approx 5.7°$. The desired signal is assumed to arrive from $\theta_d = 90°$ and a single interference signal is assumed to arrive from $\theta_I = 85°$. The signal power is chosen to be 10 dB. The noise power is 0 dB, and the interference power is chosen as 10 db, 5 db, 20 db. By varying the pointing angle θ (the angle to which the

array is focused), the results shown in Figures 3, 4, 5 are obtained. At $\theta = 90^{\circ}$, meaning that the array is focused exactly toward the arriving desired signal, the values of SINR for the three levels of interference are about equal. This means the array nulling is proportional to the interference power. In fact, the curves of Figures 3, 4, 5 are about the same except near $\theta = 85°$, the direction of interference arrival. When the array is pointed at this angle the interference power is constrained to be constant while the signal power is minimized. (SEE NOTE BELOW)

(b) Sparse Array.

A seven-element sparse array of length 10λ was simulated as follows. A uniformly distributed random number generator was used to select seven numbers. These numbers were then linearly scaled to fill the range $(-5\lambda, 5\lambda)$ so that one element would appear at $x = -5\lambda$ and another element would appear at $x = 5\lambda$. One such array was simulated with positions which turned out to be -5.0λ, -3.47λ, -1.55λ, -1.17λ, 0.24λ, 4.33λ, 5.0λ. The beamwidth of this thinned array is about the same as that of the 21-element equal-spaced array. Numerical results were obtained as described below. Signal is always assumed to arrive from $\theta_d = 90^{\circ}$. (SEE NOTE BELOW).

I. One interferer at $\theta_I = 85^{\circ}$ gave the result shown in Figure 6. Compared with Figure 3. the SINR is 5dB less at $\theta = 90^{\circ}$, but it is not so sensitive in the neighborhood of $\theta = 90^{\circ}$. The loss in gain is a direct result of the use of fewer elements here than in the case of the filled array.

II. Figure 7 is the result of two interferers at $\theta_{I1} = 85^{\circ}$ and $\theta_{I2} = 95^{\circ}$. The SINR at 90° is about the same as that in Figure 6, but it is less sensitive around 90° than Figure 6.

III. To see the effect of the nulling in the main beam, we assumed one interferer coming in from $\theta_I = 89^{\circ}$. The result is shown in Figure 8. At 90° the SINR is 10dB, a loss of about 8dB in SINR with no pointing error, but the array is much less sensitive than in Figures 3 - 7. We then assumed that there are four interferers (at 85°, 89°, 91°, 95°). Two of them (89°, 91°) are in the main beam when pointing angle is 90°. The result (Figure 9) shows

---

NOTE: Figures 3 through 18, following, are plots of S/N+I as a function of pointing angle. Figures 3 through 5 are derived from a simulated, 21-element-equal-spaced, linear, filled array of length 10λ. Figures 6 through 18 are derived from a simulated, 7-element-non-uniformly-spaced, sparse array of length 10λ. Opposite the figures, only the respective measurement conditions are indicated. In all figures, the desired signal is assumed to arrive from 90°, the signal's power is 10dB, and noise power is 0dB.

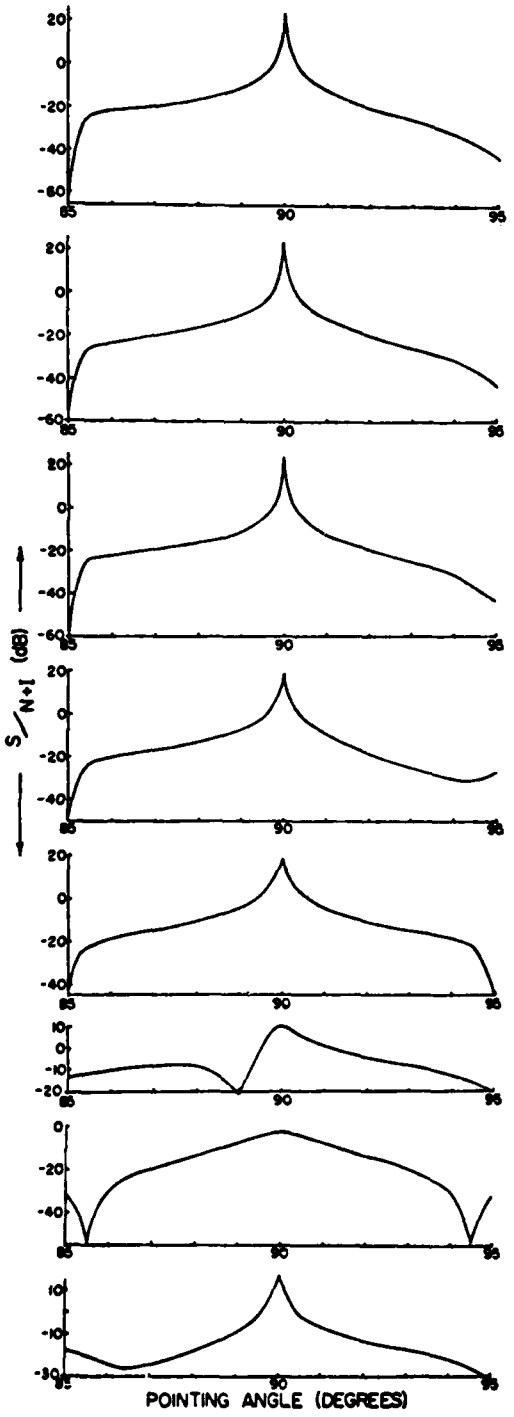

FIGURE 3. 1 INTERFERER, POWER 10dB, AT 85°

FIGURE 4. 1 INTERFERER, POWER 5dB, AT 85°

FIGURE 5. 1 INTERFERER, POWER 20dB, AT 85°

FIGURE 6. 1 INTERFERER, POWER 10dB, AT 85°

FIGURE 7. 2 INTERFERERS, POWER 10dB EACH, AT 85°, 95°

FIGURE 8. 1 INTERFERER, POWER 10dB, AT 89°

FIGURE 9. 4 INTERFERERS, POWER 10dB AT 85°, 89°, 91°, 95°

FIGURE 10. 4 INTERFERERS, POWER 10dB EACH, AT 37°, 127°, 190°, 253°

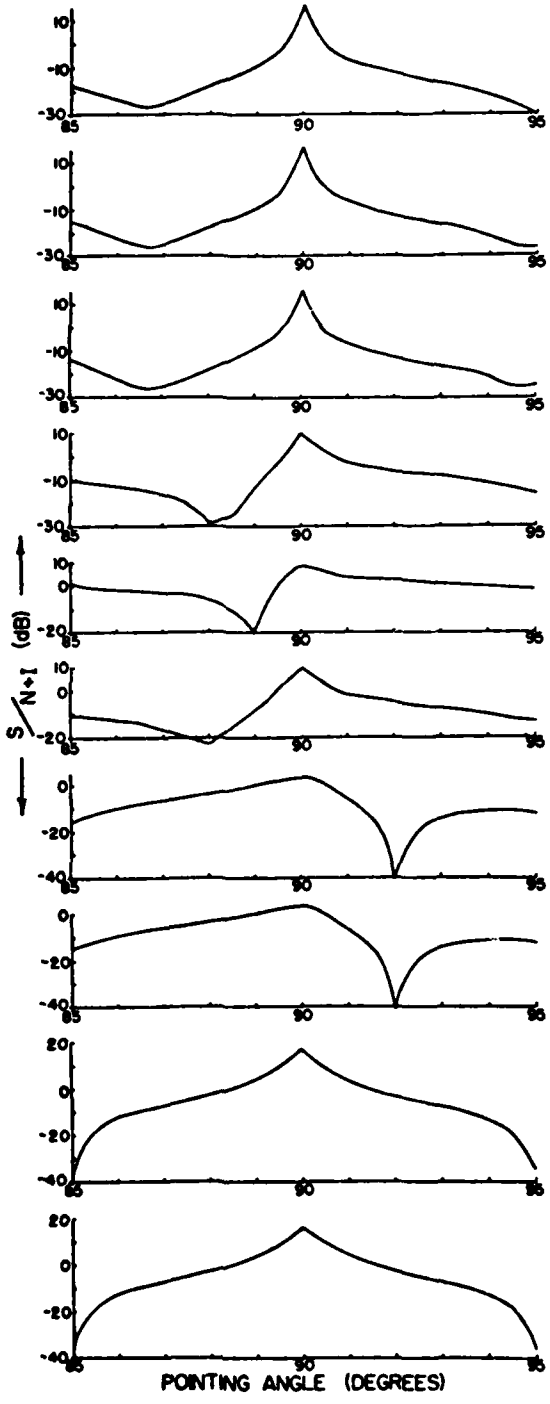

FIGURE 11 4 INTERFERERS, POWER 20dB EACH, AT 37°, 127°, 190°, 253°

FIGURE 11a 5 INTERFERERS, POWER 10dB EACH, AT 37°, 65°, 127°, 190°, 253°

FIGURE 11b 5 INTERFERERS, POWER 20dB EACH, AT 37°, 65°, 127°, 190°, 253°

FIGURE 12 6 INTERFERERS, POWER 10dB EACH, AT 37°, 65°, 127°, 190°, 253°, 335°

FIGURE 13 6 INTERFERERS, POWER 20dB EACH, AT 37°, 65°, 127°, 190°, 253°, 335°

FIGURE 14 7 INTERFERERS, POWER 10dB EACH, AT 0,37,65,127,190,253,335 (DEG)

FIGURE 15 7 INTERFERERS, POWER 10dB EACH,AT 37,65,127,190,253,268.5,335(DEG)

FIGURE 16 7 INTERFERERS, POWER 10dB EACH,AT 37,65,127,190,253,268.5,335(DEG)

FIGURE 17 5 INTERFERERS, POWER 10dB EACH, AT 65°, 75°, 85°, 95°, 105°

FIGURE 18 6 INTERFERERS, POWER 10dB EACH, AT 65°, 76°, 85°, 95°, 105°, 115°

the array is not able to handle this case. The sensitivity to pointing error is small but the SINR has fallen below 0dB even with no pointing error.

IV. We arbitrarily picked four angles, 37°, 127°, 190°, 253° as interference arrival angles to simulate widely spaced interferers, not in the main beam. The results are shown in Figures 10 and 11. In Figure 10 the signal power is 10dB. Interference powers are also 10dB. In Figure 11 signal power is 10dB and interference powers are 20dB. The results as indicated by Figures 10 and 11 are about the same. The SINR at 90° is 16.7dB and the difference between this and the result in Figure 6 is less than 2dB.

V. Five interferers at 37°, 65°, 127°, 190°, 253° were simulated. The results are in Figures 11a and 11b. Again, 10dB and 20dB interference powers were used. The results are about the same, and the SINR at 90° is very close to that in Figures 10 and 11.

VI. Six interferers were then assumed at 37°, 65°, 127°, 190°, 253°, 336° with results shown in Figures 12 and 13 for interference powers of 10 and 20dB respectively. The results are much different from those of four and five interferers. The three major differences are: (1) the SINR at 90° is about 6dB less, (2) the pointing error sensitivity is less, (3) the curves for different interference powers are quite different. For most angles the SINR for 20dB interference power is larger than the SINR for 10dB interference power. The following may explain these phenomena. Since the array consists of seven elements, it can null six inputs. For the six-interferer case, if we point the array at an angle from which no signal or interference comes, the array will try to null all the signal and interferers. However, the array can handle at most six inputs and there are seven signal and interferers together. The larger the interference powers are, the less attention the array will pay to the signal. It is similar to the power inversion array.

VII. For the six-interferer situation, if we point the array exactly at 90° it only needs to null these six interferers, and should be able to handle that. If there are seven interferers, when pointing at 90°,

the array is not going to work well, and we expect the SINR at 90° to be poor. To see this we added another interferer coming from $\theta_I = 0°$ to the six interferers in VI. However, the simulation result shows that the SINR at 90° for these seven interferers is only 1 db less than that of six interferers (compare Figures 14 and 12). In order to explain this phenomenon, we calculated the power pattern for some of the cases treated above, believing that the array with 6 interferers may have a natural null at 0° when it is focused at $\theta = 90°$. The power pattern of the array is $P(\theta) = |\underline{W}^T\underline{S}|^2$, where W^T is the weight vector when signal arrives from 90° and S is the steering vector which we vary from 0° to 360°. By the constraint we have $P(90°) = 1$. The power patterns are given in Table 1.

Direction	5 Interferences (37°, 65°, 127°, 190°, 253°)	6 Interferences (37°, 65°, 127° 190°, 253°, 335°)	7 Interferences (0, 37°, 65°, 127°, 190°, 253°, 335°
0°	* -8.29 dB	* -9.97 dB	-23.33 dB
37°	-38.7 dB	-28.40 dB	-32.34
65°	-46.12	-24.64	-24.63
127°	-41.55	-19.69	-18.30
190°	-39.88	-27.78	-26.14
253°	-43.75	-27.43	-21.20
335	* -6.21	-18.45	-15.90

TABLE 1 Power Pattern when Weights are Fixed for Signal Arriving from $\theta_d = 90°$, and 5, 6, and 7 Interferers Arrive as Specified.

The patterns above are based on signal and interference powers of 10 dB each, and noise power is 0 dB. The numbers with an asterisk (*) in front mean that there is no interference coming from those directions.

From Table 5.1 we can see that even for 6 interferers, the array has a fairly good null at 0°, so that when another interferer arrived from 0°, the array naturally suppressed it. We therefore chose two other angles, 280° and 268.5°, where the values of the power pattern with 6 interferers at these angles are -3.91 dB and 2.94 dB respectively. With the seventh interferer coming in from

these angles, the SINR at 90° is 8.82dB, or 3.75dB. Thus, the array does not handle these cases as well as the one in which the seventh interferer arrives from 0°. But the results are still not decisive. We may argue that in the case of seven or even more interferers the array processor still seeks to minimize the array output to all inputs except for the one in the constraint direction. If it can only null in a smaller number of directions it places them in such a way that the larger number of unwanted inputs is minimized; thus the result observed for 7 interferers should not be surprising. What is perhaps less obvious is why the SINR is not better with 6 interferers. For one to five interferers, the SINR when pointing toward the desired signal is always within about 2dB of the best obtainable. For the 6-interferer case, it falls 8 to 10dB lower. However, this may be a fortuitous result of the particular choice of array element layout; the next article, where we try different layouts, shows that interference-cancelling for some layouts may be poorer than for others.

VIII. In III we simulated a case of main beam nulling, and it showed that the array did not work. In IV-VII, we therefore spread out the interferers and saw acceptable results. It is interesting to see what happens when multiple interferers are compact but still not in the main beam. Therefore we chose interference arrival angles of 65°, 75°, 85°, 95°, 105° for 5 interferers and 65°, 75°, 85°, 95°, 105°, 115° for 6 interferers. The results plotted in Figures 17 and 18 are about the same. The SINR is at least as good at 90° as for the scattered interferer case (it is much better for 6 interferers) and the sensitivity to pointing error is better.

The results of this analysis and computation indicate that pointing sensitivity is such that pointing error of the order of 0.1° may significantly reduce the output SINR. Accurate control of pointing is therefore viewed as being essential. It also confirms the importance of making the array large enough to put potential interferers outside the beamwidth of the array beamformer in Figure 1. Very likely, the sensitivity to pointing error will increase with increasing array size, making it even more necessary to incorporate some mechanism for accurate pointing.

APPENDIX E

EFFECT OF ARRAY ELEMENT LAYOUT ON

OUTPUT-SIGNAL-TO-INTERFERENCE-PLUS-NOISE RATIO (SINR)

Fred Haber, Judy Herman

Valley Forge Research Center
Moore School of Electrical Engineering
University of Pennsylvania
Philadelphia, Pennsylvania

In an earlier section of this report ("Effect of Pointing Error on a Directionally-Constrained Adaptive Array, Appendix D), computational work reported on SINR sensitivity to pointing error was based on a single random deployment of array elements. As part of our study of the effect of array structure we have continued the investigation reported above, determining the SINR for various random element deployments. The array was linear and comprised of seven elements; the powers of signal, a single interferer, and noise were taken to be 10dB, 10dB, and 0dB, respectively. Signal was assumed to arrive broadside ($\theta_d = 90^o$) and interference was assumed to arrive from various angles θ_I. The pointing vector was set to look in the direction of the signal.

Fifty different layouts were selected using a random number generator. Two different cases were treated. In the first, element locations were based purely on a uniform distribution over $(-5\lambda, 5\lambda)$. In the second case the same random dispersion of elements was scaled to fully cover the interval $(-5\lambda, 5\lambda)$. The results are presented in Figures 1 and 2 for unscaled and scaled arrays, respectively. The 4 situations shown in Figure 1 are for interference arriving from directions 10^o, 5^o, 2^o, and 0.1^o from the signal direction. The first two simulate interferers at or beyond the beamwidth of the largest arrays in the 50 samples, the other two simulate interference generally inside the beamwidth. We draw the following conclusions from these results. For interference adequately spaced away from the desired signal the values of SINR are largely concentrated near 18.45dB, the maximum SINR obtainable. Though some cases are found in which the SINR is poorer by about 3dB, these cases are rare. The loss in SINR must be associated with imperfect nulling arising perhaps from poor element placement. When interference is within the beamwidth of the array, the values of SINR are more uniformly spread and almost always lower than it is for interference outside the

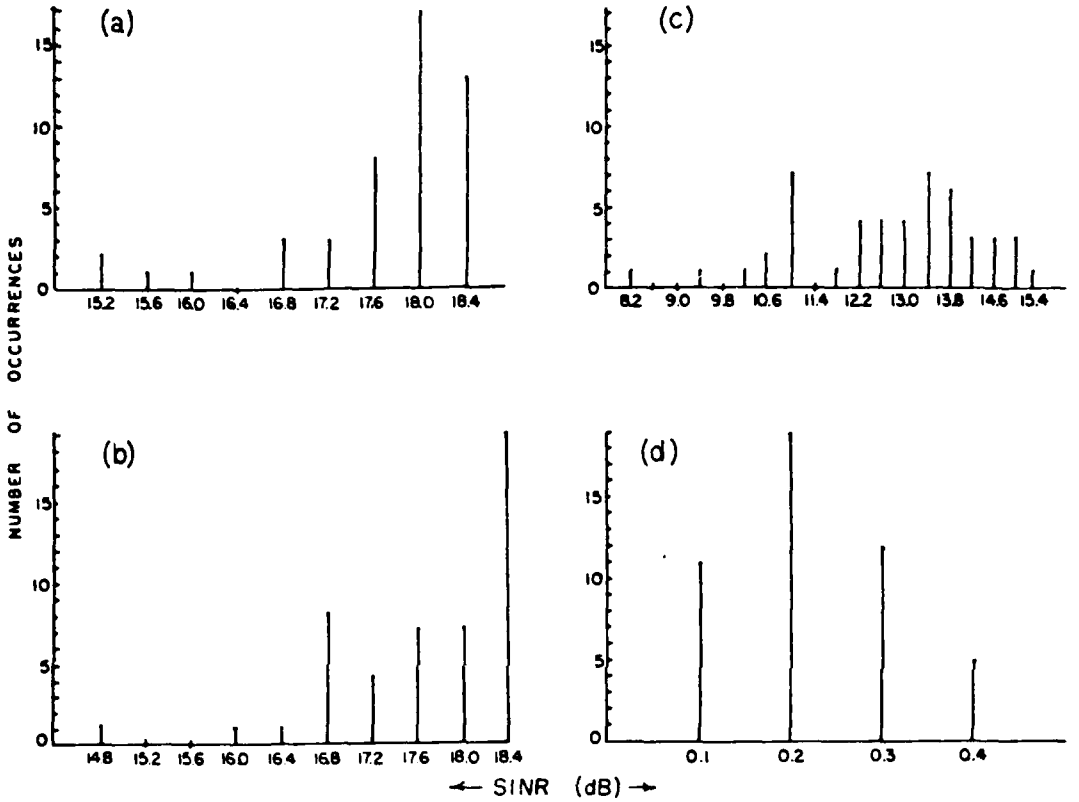

FIGURE 1 HISTOGRAM SHOWING EFFECT OF ELEMENT LAYOUT ON ARRAY SINR (UNSCALED ARRAY)

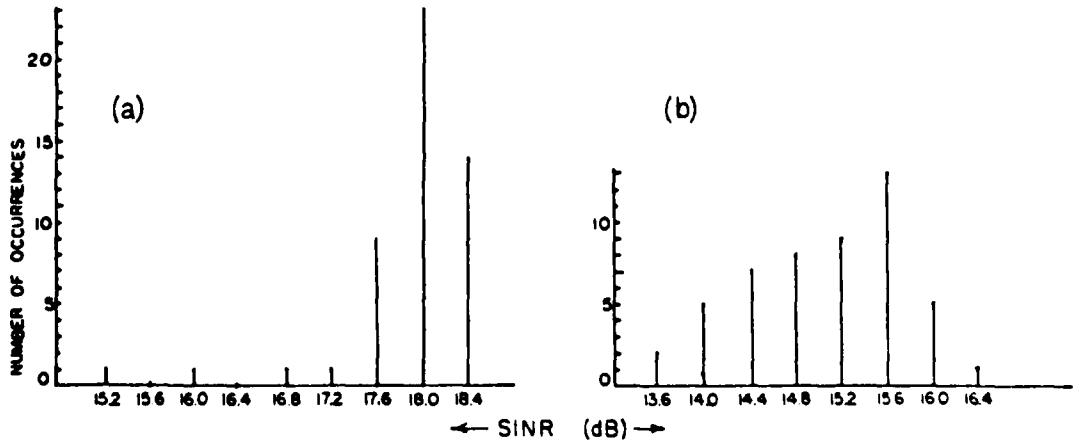

FIGURE 2 HISTOGRAM SHOWING EFFECT OF ELEMENT LAYOUT ON ARRAY SINR (SCALED ARRAY)

beamwidth. The constraint on the main beam gain makes it virtually impossible to get a good null on the interference. One should note that interference about halfway into the beamwidth (2^{o} from the desired signal) produces a median SINR about 5dB poorer than the best obtainable. For interference very close to the desired signal (the 0.1^{o} case) the SINR hovers around 0.2dB,or more than 18dB poorer than the best obtainable.

Because some sample arrays will not span 10λ when element positions are randomly chosen,we scaled the arrays, stretching them to fill the 10λ space. Two cases of interference arrival were simulated, 10° and 2° from the desired signal. For the 10° case the values of SINR generally tended to be nearer the best obtainable value but there still were cases about 3dB poorer. The 2° case was not significantly different than the unscaled case.

APPENDIX F

SELF-CORRECTING INTERFERENCE CANCELLING PROCESSOR FOR POINT-TO-POINT COMMUNICATION

By

Yeheskel Bar-Ness *

And

Fred Haber

Valley Forge Research Center
Moore School of Electrical Engineering
University of Pennsylvania
Philadelphia, Pennsylvania 19104

* On leave of absence from the School of Engineering, Tel Aviv University.

Adaptive interference cancelling arrays utilizing either known direction of signal arrival or known signal waveform structure have been analyzed extensively in the past [1,2]. The former, called here the directionally constrained array, is the more natural one to use in point-to-point communication though the sensitivity to pointing error is substantial [3,4]. Variants of the latter canceller, in which the waveform reference is generated in the receiver using some known signal characteristic such as the code used in spread spectrum modulation has also been advanced for communications applications. We refer to these as LMS interference canceler arrays.

Recently, a study comparing the two approaches has been reported showing each of these to have its area of superiority [3]. Using as improvement factor the ratio

$$F = (SIR)_o/(SIR)_e$$

where $(SIR)_o$ is the output signal-to-interference ratio at the array output and where $(SIR)_e$ is the same ratio at each element output, we find that under ideal conditions--the directionally constrained array is accurately pointed and the LMS canceler array is equipped with a perfect signal reference generator-- the former is superior when

$$\left|\tan \frac{\theta_i}{2}\right| \geq \frac{1}{2}$$

where θ_i is interference arrival angle relative to that of the desired signal. It is also superior when the inequality is reversed if, also,

the interference-to-threshold ratio (ITR) is below some value which decreases as θ_i decreases. (The threshold power approximately equals the noise power σ_N^2.) Both cancellers suffer under conditions of inaccurate constraints; that is, when pointing is in error in one and when the reference is imperfect in the other.

An alternative which suggests itself to overcome the effects of imperfections of these kinds is a hybrid utilizing both types of constraints. One can be expected to compensate for the inadequacy of the other. To this end we propose the scheme shown in Figure 1. The figure shows a two-element array and the results below are for this case; we see no barrier to extending the scheme to multiple elements. The two loops in the figure, opearting on the two array ports Σ and Δ, function as a least mean square (LMS) system with a reference signal extracted from the array output. ϕ is a beam steering weight which, when properly set, generates phase coherent signals at point 1 and 2 for an EM wave arriving from a prescribed direction representing the desired source. Therefore, ϕ sets the directional constraint and Figure 1 becomes a combined canceler.

The improvement in SIR of this combined canceler can be shown to be

$$F = \frac{\cos^2(\theta_s/2)|1+2g(1-F_I)|I|^2\sin\theta_i(\tan(\theta_i/2)-\tan(\theta_s/2))^2}{\cos^2(\theta_i/2)|1+2g(1-F_s)|s|^2\sin\theta_s(\tan(\theta_s/2)-\tan(\theta_i/2))^2} \qquad (1)$$

where F_s and F_I are linear operators that represent the effect of the reference loop filter on the desired signal and on the interference spectral contents, respectively. $1/g = (1+2\sigma_N^2)/K \doteq Pth$. Pth stands for

the system's power threshold, and K is the main loop d.c. gain.

$\theta_s \triangleq \theta_{s1}-\theta_{s2} = \frac{\omega_s d}{c}\sin\psi_s$ and $\theta_i \triangleq \theta_{i1}-\theta_{i2} = \frac{\omega_i d}{c}\sin\psi_i$, where d is the distance between the array elements, ω_s and ω_i are the radian frequencies of the desired and interference signals, respectively. c is the speed of electromagnetic wave and ψ_s and ψ_i are the directions of arrival of these signals with respect to the array broadside.

If the system is in an acquisition mode, the reference signal loop generates no output which is in correlation with the desired signal. In this case $F_I = F_S = 0$ (see [5]) and (1) becomes exactly the improvement factor of the directionally constrained interference canceler. With ϕ at a value close to that needed for accurately constraining the array toward the desired signal we can expect the SIR to be good enough to result in code synchronization, turning the system to a code tracking mode. (The code acquisition circuit is not shown in the diagram.) As a result, F_I remains approximately zero, but F_S becomes close to one ($F_S = \gamma e^{j\theta_{sr}}$ where γ and θ_{sr} are the amplitude and phase of the filter's response). For the ideally filtered case; $F_S = 1$, (1) then becomes

$$F = \cos^2(\theta_s/2)\left[\frac{1+2g|I|^2\sin\theta_i(\tan(\theta_i/2)-\tan(\theta_s/2)))^2}{\cos^2(\theta_i/2)}\right] \qquad (2)$$

$$= F_o\cos^2(\theta_s/2)$$

We have found in other studies [4] that the sensitivity to an inaccurate spatial constraint may result in loss of SIR in the order of 3 dB for 0.1 degree pointing error. This result shows, however, that with perfect reconstruction of the reference signal the imperfect reference mainly affects the improvement in the factor $\cos^2(\theta_s/2)$, θ_s being

the pointing error. This effect is virtually trivial compared to that obtained in a conventional spatially constrained array.

Another potentially useful step is the direct correction of the pointing error via the processor shown in Figure 2. This processor contains the following control loops:

1. The main weight control loop,
2. The reference signal loop,
3. The beam steering weight control loop
4. Reference loop phase compensation

The first and second loops were included in the hybrid scheme of Figure 1. The hybrid which generates sum (Σ) and difference (Δ) signals eliminates the desired signal at the Δ terminal if, indeed, pointing is accurate. With pointing error, this will not be the case.

The purpose of the third loop (the beam steering weight control loop) is to adaptively control the weight ϕ, so that the desired signal residue at the output Δ is minimized. This is done by correlating (in correlator #2) the output of the reference signal loop with the output Δ, of the hybrid.

In tracking, the output of the reference signal loop is a sufficiently clean replica of the desired signal. Ideally, the output of correlator number (2) will settle on the zero value (due to the succeeding integrator) only when the output Δ, contains no power that is correlated with the desired signal. In a practical sense, the desired signal power at the output of hybrid Δ is not totally eliminated, but rather minimized by the beam steering loop which acts in the LMS fashion.

In the acquisition mode the output of the reference signal is very small (due to the filtering of both the spread desired signal and the interference). To prevent output of correlator number 2 from incorrectly

affecting the steering weight, a code tracking inhibit circuit is used. That is, whenever the system is not in code synchronism, the input to integrator number 2 is inhibited, disabling the automatic beam steering. In such a case (acquisition mode with very high interference-to-signal ratio) we have shown (see [3]) that the constrained interference canceler performs as a power-inversion device, resulting in a high SIR, and leading back to code synchronization.

The fourth loop corrects for any phase shift and attenuation caused by the BPF [6].

REFERENCES

[1] S. P. Applebaum and D. J. Chapman, "Adaptive Array with Main Beam Constraints," IEEE Trans. AP, Vol. AP-26, No. 5, September 1976

[2] B. Widrow, J. McCool, J. Ball, "The Complex LMS Algorithm," Proc. IEEE Vol. 63, April 1975, pp. 719-720.

[3] R.T. Compton, Jr., "An Adaptive Array in Spread-Spectrum Communication," Proc. IEEE, Vol 66, March 1978, p. 289.

[4] Y. Bar-Ness, "Comparing the Performance of Interference Canceler with Reference Signal Loop, With Interference Canceler that Utilizes Directional Constraint," UP-VFRC-8-81, Univ. of Pa., Jan. 1981.

[5] F. Haber and P. Yeh, "Effect of Error in Pointing Vector on the Constrained Applebaum Array;" In preparation.

[6] Y. Bar-Ness, "Performance Analysis of Interference Canceler with Reference Signal Loop," UP-VFRC-21-80, Univ. of Pa., October 1980.

[7] Y. Bar-Ness, "On the Problem of Reference Loop Phase Shift in an N-Element Adaptive Array," UP-VFRC-11-80, July 1980. Submitted for publication.

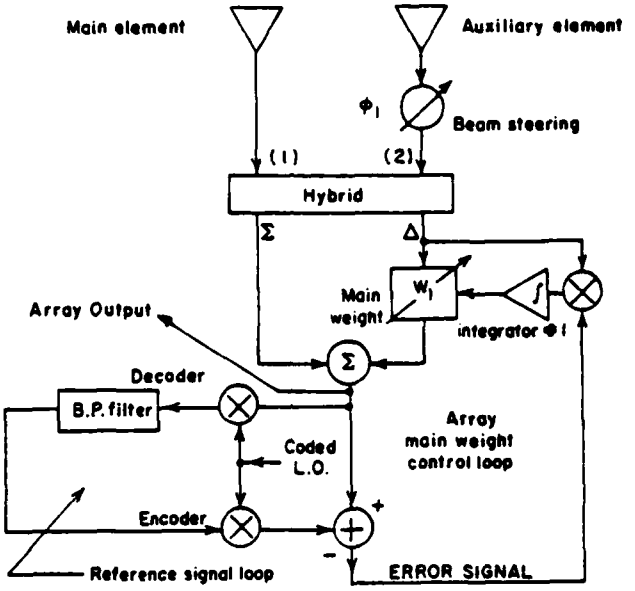

FIGURE 1. HYBRID INTERFERENCE CANCELER

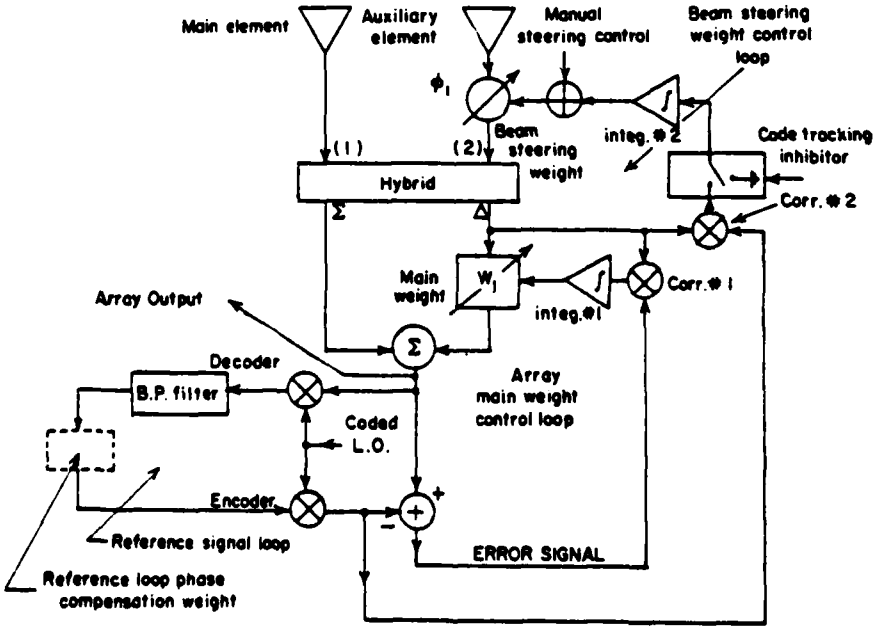

FIGURE 2. SELF-CORRECTING HYBRID INTERFERENCE CANCELER

APPENDIX G

AN APPROACH TO SELF-ORGANIZATION

Fred Haber

Valley Forge Research Center
The Moore School of Electrical Engineering
University of Pennsylvania
Philadelphia, Pennsylvania

The technique of beamforming on a beacon to organize an array of arbitrarily placed sensors is described in the literature [1]. Essentially these methods involve maximizing the array output to the signal by observing the phase of the arrivals at the various elements, and phase shifting to coherently combine them. It has also been shown that once the array is focused, the beam can be steered toward another source by open loop phase correction using the steering angle and nominal array element position information. The angle through which it may be steered with a loss of response of less than 1 dB is

$$\Delta\theta = \frac{\lambda}{4\pi\sigma}$$

where λ is the received signal wavelength and σ is the rms error in the knowledge of the element positions. Typically, at $\lambda = 1$ cm, a 1 cm uncertainty in element position will allow

$$\Delta\theta = 0.08 \text{ radian}$$

steering, which translates to about 1800 miles on the ground.

We propose the following approach here where the initial focusing may have to be carried out in the presence of high amplitude interferers arbitrarily located. See Figure 1. The beacon will be assumed adequately separated from potential interferers so that they will not influence the beam toward the beacon when it is formed. The beacon is assumed to be of strength

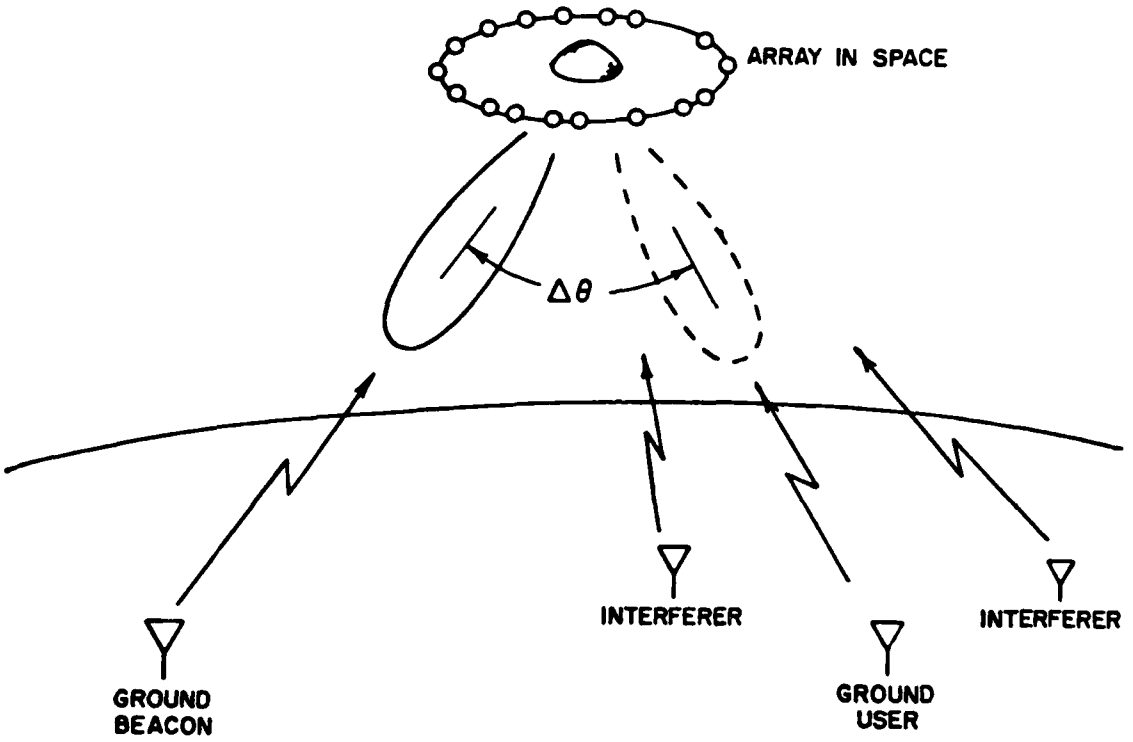

FIGURE 1. BEAMFORMING AND SCANNING IN THE PRESENCE OF INTERFERERS

comparable to that of the interferers and modulated in a manner recognizable by the satellite array. We will assume that the beacon's signal is received separately at the satellite perhaps via a conventional, relatively low gain, mechanically steered antenna. (This link may also be used to convey information to the array concerning spread spectrum codes, timing, control signals, etc.) We imagine the array deployed on a large ring or on crossed arms with the antenna centered. The signal so received will be used as reference input to the array operated initially as a Widrow LMS processing array. The steady state weights generated in this mode are given closely by*

*This result is based on an LMS loop with large open loop gain. The weights are more accurately given by $W = g(I+gM)^{-1}\,\overline{\underline{V}^{*}e_r}$ where g is the open-loop gain and I is the unit matrix.

$$W = M^{-1}\,\overline{\underline{V}^{*}e_r}$$

where $\underline{W}$ is the weight vector

M^{-1} is the inverse of the covariance matrix of array element outputs

$\underline{V}$ is the vector of signal inputs

e_r is the reference signal

The bar represents time averaging over an interval of duration T. The signal vector is comprised of components.

$$v_i(t) = \sigma(t)e^{j\phi}\,S_i' + \sigma_{qi}(t)$$

where $\sigma(t)$ is the signal modulation on the desired carrier arriving from the beacon

ϕ is the carrier phase relative to some reference

S_i' is a complex unit amplitude phasor depending on the arrival direction of the signal and the element position

$\sigma_{qi}(t)$ is noise and interference

The reference signal will have the form

$$e_r = a\sigma(t)e^{j\phi}$$

where a is an arbitrary real constant. Thus the vector $\overline{\underline{V}^{*}e_r}$ will have components

$$\overline{v_i^{*}e_r} = \frac{1}{T}\int_T a|\sigma^2(t)|S_i'^{*}dt + \frac{1}{T}\int_T a\sigma^{*}(t)e^{-j\phi}\,\sigma_{qi}(t)dt$$

Assuming $\sigma(t)$ uncorrelated with the noise and interference, the second integral will be zero if T is made large enough and the first integral will be $a\,P\,S_i'^{*}$ where P is a measure of the power of the beacon signal. Thus

$$\underline{W} = a\,P\,M^{-1}\underline{S}'^{*}$$

where $\underline{S}'^{*}$ is the steering vector to the beacon. If the receiver simultaneouslv

derives the covariance matrix M then forming the matrix product $\underline{MW}$ one has

$$\underline{MW} = a\ P\ \underline{S}'^{*}$$

and the steering vector is isolated. Having the steering vector to the beacon, the altered vector, $\underline{S}$, which will point the array toward the desired source is obtained as described in [1]. The entire system is represented by the block diagram, Figure 2.

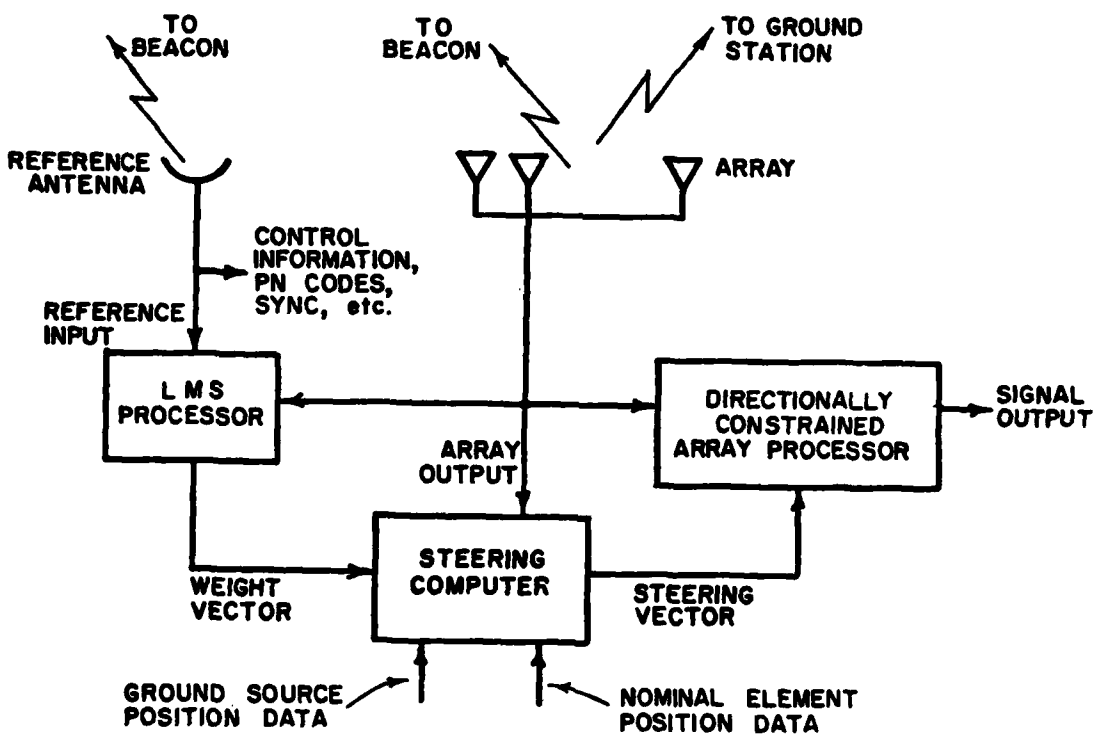

FIGURE 2. BLOCK DIAGRAM OF SELF-ORGANIZING SYSTEM

To summarize, the array initially functions as an adaptive spatial filter selecting a beacon signal from a multitude of signal arrivals. The steering vector inherent in the adaptively-formed element weights is isolated and altered for pointing the array toward a desired ground user. Pointing information is thus generated even in the presence of unwanted signal arrivals. Questions concerning practical implementation and the error in determining the pointing vector in this manner remain to be dealt with.

REFERENCES

[1] Bernard D. Steinberg, Principles of Aperture and Array System Design, John Wiley & Sons, Inc., New York, 1976, Chapter 11.

MISSION
of
Rome Air Development Center

RADC plans and executes research, development, test and selected acquisition programs in support of Command, Control Communications and Intelligence (C^3I) activities. Technical and engineering support within areas of technical competence is provided to ESD Program Offices (POs) and other ESD elements. The principal technical mission areas are communications, electromagnetic guidance and control, surveillance of ground and aerospace objects, intelligence data collection and handling, information system technology, ionospheric propagation, solid state sciences, microwave physics and electronic reliability, maintainability and compatibility.

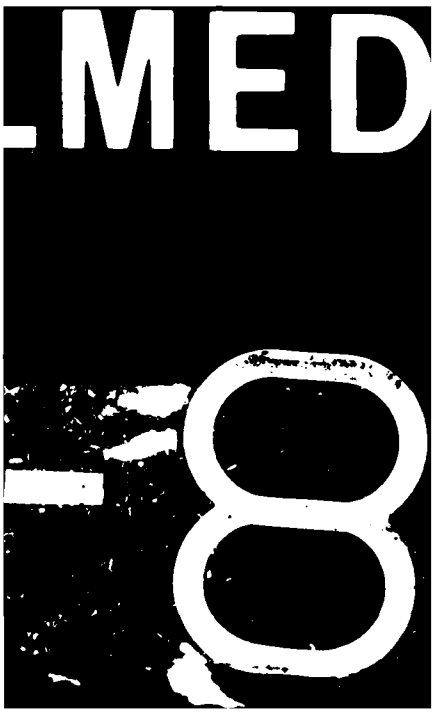
LMED
8